

Efforts Towards the Synthesis of Silanes for Their Use in Catalysis and as Molecular Wires

Noushad Mohd

Submitted in partial fulfillment of the
requirements for the degree of
Doctor of Philosophy
in the Graduate School of Arts and Sciences

COLUMBIA UNIVERSITY

2020

© 2020
Noushad Mohd
All Rights Reserved

Abstract

Efforts Towards the Synthesis of Silanes for Their Use in Catalysis and as Molecular Wires

Noushad Mohd

The Leighton group has long been interested in developing strained silanes for their use in polyketide synthesis. Recently, our interests have led us to develop a new type of silicon Lewis acid and catalyst with high levels of reactivity. Upon activation with a thiourea, a stabilized silylium ion is formed allowing for the facile allylation of aldehydes and ketones, in addition to Diels-Alder catalysis. This represents one of the first examples of the merger between anion-binding catalysis and silylium ion catalysis. Our group's interest in strained silanes has also led us to investigate their conductance properties in molecular break junctions. To further understand the nature of the bond-ruptured species we have proposed new synthetic targets and have described herein our progress towards synthesizing these targets.

Table of Contents

List of Figures	iii
List of Schemes	vi
List of Tables	vii
List of Abbreviations	viii
Acknowledgments	ix
Dedication	xi
Chapter 1: Introduction to Silicon Lewis Acidity and Silylium Ion Catalysis	1
1.1. Introduction to silicon Lewis acidity	1
1.2. Overview of the Leighton Lab's efforts in harnessing silicon Lewis acidity	3
1.3. Overview of silylium ions and their potential in silicon Lewis acid catalysis	5
1.4. Preparation of silylium ions	7
1.5. Previous examples of silylium ions used as catalysts	8
1.6. Summary and outlook	10
1.7. References	11
Chapter 2: The Development of a Novel Cationic Silicon Lewis Acid and Catalyst	12
2.1. Introduction	12
2.2. Initial efforts to synthesize the silane	13
2.3. Initial reactivity	16
2.4. Thiourea Catalysis	19
2.5. A more general silicon Lewis acid catalyst	23
2.6. Reactivity of the new catalyst	24
2.7. Investigating the inability to use lower catalyst loadings	25

2.8. Efforts to develop enantioselectivity	30
2.9. Summary and Conclusion	33
2.10. Experimental procedures	34
2.11. References	51
Chapter 3: Efforts Towards the Synthesis of New Silanes for High Bias-induced Bond	
Rupture Experiments	52
3.1. Introduction	52
3.2. Strained silanes as molecular junctions	53
3.3. New motifs for high bias-induced bond rupture experiments.....	59
3.4. Initial synthesis efforts to form the chloromethyl silanes	61
3.5. Attaching a protected thiol as a chloromethyl alternative	63
3.6. Other routes to access 3.1 and 3.2	67
3.7. Summary and conclusion	68
3.8. Experimental procedures	69
3.9. References	76

List of Figures

Figure 1.1: Hosomi and Sakurai's Lewis base activation of allylsilanes	1
Figure 1.2: Utimoto's strained silane experiments	2
Figure 1.3: Denmark's Strain-release Lewis Acidity rationalization	2
Figure 1.4: The Leighton Group's initial results in developing strained silicon Lewis acids	3
Figure 1.5: Highly enantioselective chiral diamine- based reagents for crotylation	4
Figure 1.6: One-pot crotylation of aldehydes using the tridentate ligand	4
Figure 1.7: Silicon Lewis acid catalyzed Diels-Alder reaction reported by the Leighton group ..	5
Figure 1.8: a) Crystal structure of solvent coordination to a silylium ion. b) Crystal structure of a free silylium ion	6
Figure 1.9: Stabilized silylium ions	7
Figure 1.10: Preparation of silylium ions. a) Corey hydride abstraction. b) alkyl abstraction.....	8
Figure 1.11: Silylium ions used in catalysis	9
Figure 1.12: Oestreich's chiral silylium ion catalysts	9
Figure 2.1: General structure of silatrane and quasisilatrane	12
Figure 2.2: Crystal structure of allyl quasisilatrane 2.3.....	14
Figure 2.3: More crystalline silanes	14
Figure 2.4: Crystal structure of 2.11.	15
Figure 2.5: Allylation of an aromatic and aliphatic aldehyde with 2.11.....	16
Figure 2.6: Allylation of a ketone with 2.11.....	17
Figure 2.7: Allylation of a ketone with 2.11 and Schreiner's thiourea 2.12.	17
Figure 2.8: Pathways for reactivity. a) Hexacoordinate pathway. b) Chloride displacement pathway. c) Silylium ion-generation by adding a thiourea.....	18

Figure 2.9: a) No catalysis with sub-stoichiometric loading of thiourea. b) Preference of the thiourea-chloride-bound species.....	19
Figure 2.10: Thiourea screen in allylation reactions.	20
Figure 2.11: Control reaction with only acetonitrile and no thiourea.....	21
Figure 2.12: Proposed acetonitrile stabilization of silylium ion and solvation sphere around chloride.	22
Figure 2.13: Allylation of an aliphatic aldehyde using a catalytic amount of thiourea	22
Figure 2.14: Crystal structure of 2.15.....	23
Figure 2.15: Diels-Alder reaction. a) No observed catalysis with 2.15. b) Catalysis after adding thiourea 2.12.....	24
Figure 2.16: Proposed stabilization via internal tether	25
Figure 2.17: pKas of selected thioureas	27
Figure 2.18: Electronic effects of different silanes	30
Figure 2.19: Chiral silane catalysis. a) No catalysis at 0 °C. b) Catalysis at room temperature..	31
Figure 2.20: Chiral thiourea scope	32
Figure 3.1: Conductance of a strained silacyclobutane. a) A high and low G pathway. b) Conductance histogram. c) Conductance in similar molecules	54
Figure 3.2: Conductance histograms for cis and trans 1,2-disilaacenaphthenes	55
Figure 3.3: Two binding modes for 2. a) A low G sulfur-to-sulfur pathway. b) A high G bipodal binding of both thioanisole linkers, with direct Au contact with the Si-Si bond	56
Figure 3.4: An alternate conductance pathway in the disilaacenaphthene system	57
Figure 3.5: Conductance in the Si ₂ and Si ₂ Naph system	58
Figure 3.6: Sekiguchi's bis(silyl radicals) on a benzene core	59

Figure 3.7: An analogous system to Sekuguchi's para isomer	60
Figure 3.8: Retrosynthetic analysis for the synthesis of benzodisilacyclobutene 3.1.....	60
Figure 3.9: Retrosynthetic analysis for the synthesis of ferrocenyl disilane 3.2.....	61
Figure 3.10: Successful formation of the tetramethyl ferrocenyl disilane	62
Figure 3.11: Synthesis attempt of 4.8 via a double Grignard	63
Figure 3.12: Successful formation of the tetramethyl double Grignard product	63
Figure 3.13: Double Grignard attempt with TIPS protected intermediate 3.10.....	64
Figure 3.14: Cold temperature, stepwise Grignard reaction to synthesize 3.11 a) Via dibromide b) Via diiodide	65
Figure 3.15: Successful synthesis of TIPS protected ferrocenyl silane 3.14.....	66
Figure 3.16: Chlorination attempts of 3.14.....	66
Figure 3.17: TIPS deprotection attempts of 3.14.....	67
Figure 3.18: New disulfide targets	67
Figure 3.19: Attempts to synthesize disulfides 3.17 and 3.18.....	68

List of Schemes

Scheme 2.1: Synthesis of allyl quasisilatrane 2.3.....	13
Scheme 2.2: Synthesis of N-Butyl quasisilatrane 2.11.....	15
Scheme 2.3: Synthesis of phenyl quasisilatrane 2.15.....	23
Scheme 2.4: Synthesis of silane 2.16.....	26
Scheme 2.5: Synthesis of 2.20.....	26
Scheme 2.6: Synthesis of chiral silane 2.32.....	31
Scheme 3.1: Synthetic route to access 3.4.....	67
Scheme 3.2: Synthesis of key intermediate 3.7.....	68
Scheme 3.3: Synthesis of key TIPS protected sulfur intermediate 3.10.....	69

List of Tables

Table 2.1: Solvent screen	21
Table 2.2: Chloride binder screen	28
Table 2.3: Temperature screen	28
Table 2.4: Concentration screen	29

List of Abbreviations

DIBAL	diisobutylaluminum hydride
DBU	1,8-diazabicyclo[5.4.0]undec-7-ene
DMF	dimethylformamide
DMSO	dimethylsulfoxide
dr	diastereomeric ratio
ee	enantiomeric excess
HMPA	hexamethylphosphoramide
HPLC	high-performance liquid chromatography
LAH	lithium aluminum hydride
LiHMDS	lithium hexamethyldisilazide
MS	molecular sieves
NMR	nuclear magnetic resonance
NR	no reaction
PG	protecting group
TASF	tris(dimethylamino)sulfonium difluorotrimethylsilicate
TBAB	tetrabutylammonium bromide
TBAF	tetrabutylammonium fluoride
THF	tetrahydrofuran
TIPS	triisopropylsilyl
TLC	thin-layer chromatography
TES	triethylsilyl
TMS	trimethylsilyl

Acknowledgements

Throughout my graduate school career there have been many who have helped and supported me along the way. First, I have to thank my Ph.D. advisor Professor James Leighton for giving me the opportunity to join his group. Over the past 5 years, I have learned much from him and his method of approaching problems in organic chemistry. I appreciate him giving me the chance to explore new and challenging areas of silicon chemistry that our group has not explored as much. I would like to thank Professor Tomislav Rovis for serving on my committee from the very beginning and for his support. I would also like to thank Professors Latha Venkataraman, Gerard Parkin, Xavier Roy and Tianning Diao for serving on my committee.

Navigating through graduate school has not been an easy task and I certainly would not have been able to do it without all the members of the Leighton group, past and present. They have mentored me, allowed me to grow as a scientist, and provided a great and enjoyable working environment. I couldn't ask for a better group of individuals to work with. I would especially like to thank Dr. Isaac Hughes. From the very first day I walked into the lab, until the very end, he has continuously been supportive and helpful, always willing to talk about chemistry or other subjects. I'm happy to have started and ended this journey with him. I would also like to thank Dr. Makeda Tekle-Smith who has always been an inspiration in the lab and Dr. Josh Infantine for his insightful conversations about chemistry and support in my earlier years of grad school.

Outside of the lab, I'd like to thank my fellow 5th years for being part of this journey, in particular Sean who has always been a joy to talk to. I would like to thank the rest of the Columbia chemistry department for providing a fun and enjoyable environment. The research being done in the department would not be possible without people like Socky, Daisy, Alison,

and Dani, who have made administrative and teaching-related duties very simple. A special thank you to John and Michael for all their NMR help, to Brandon for help with the constantly malfunctioning Advion and to Dan for obtaining my crystal structures. I would also like to thank Dr. Karen Phillips who has been a mentor in the teaching realm. I have learned much from her and am grateful I was able to be a teaching assistant for her for many semesters, learning a different and interactive way to teach undergraduates organic chemistry.

I have to thank all my friends outside of Columbia. Their help and support have made the last 5 years more enjoyable. Our travels together have been truly memorable and have inspired me to go farther.

Last, but certainly not least, I have to thank all my family members, especially my mother. They have been very supportive over the last 5 years, and have allowed me to reach this stage in my life. Without them, I would not have accomplished anything and will forever be indebted to them. They have given up much so I could be where I am today and their sacrifices will not be in vain. Thank you.

For my family

Chapter 1: Introduction to Silicon Lewis Acidity and Silylium Ion Catalysis

1.1. Introduction to silicon Lewis acidity

Lewis acid mediated reactions and catalysis form the backbone of organic chemistry's most important reactions. Many of these transformations employ the use of transition metals which are excellent due to their tunability and extremely low catalyst loadings. However, many of these metals can be toxic and expensive, in addition to being low in abundance. It is for these reasons that Lewis acid mediated reactions and catalysis using silicon are of interest. Silicon is widely abundant, low cost and non-toxic. Despite these advantages, a tetracoordinate silane is not inherently Lewis acidic and must first be activated. Traditionally, this has been achieved via Lewis base activation and strain-release Lewis acidity. Hosomi and Sakurai reported one of the first examples of Lewis base activation of silanes in the allylation of carbonyl compounds where TBAF was used as a Lewis base in conjunction with allyltrimethylsilane as the allylating agent (Figure 1.1).¹

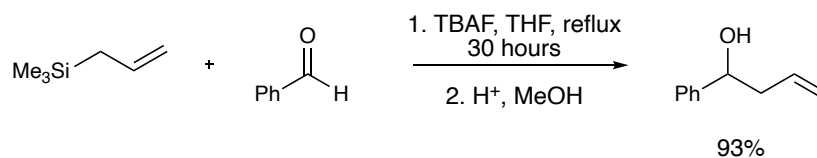


Figure 1.1: Hosomi and Sakurai's Lewis base activation of allylsilanes.

In this method of activation, the Lewis base first coordinates to the silane which results in a pentacoordinate silane with a formal negative charge where the electron density is on the ligands. This creates a silicon center that is more electropositive and therefore a silane that is more Lewis acidic, which allows for easy coordination of the substrate and subsequent allyl transfer. This differs from the commonly known Hosomi-Sakurai reaction where the substrate is first activated by a Lewis acid, and then allyl transfer proceeds and is facilitated by the β -silicon effect.

The other common method employed in rendering silicon Lewis acidic is known as strain-release Lewis acidity. Pioneering work was done by Utimoto where he found that a silicon atom constrained in a 4-membered ring allowed for the allylation of aldehydes, whereas the acyclic silane showed no reaction (Figure 1.2).² Denmark rationalized this remarkable phenomenon by proposing that when silicon is constrained in a 4-membered ring, the bond angle at silicon is compressed to approximately 90°, far from the ideal 109.5°. However, coordination of a substrate or nucleophile allows silicon to rehybridize to a trigonal bipyramidal geometry, accommodating the 90° bond angle much better, thereby relieving the strain of the initial tetrahedral silane (Figure 1.3).³

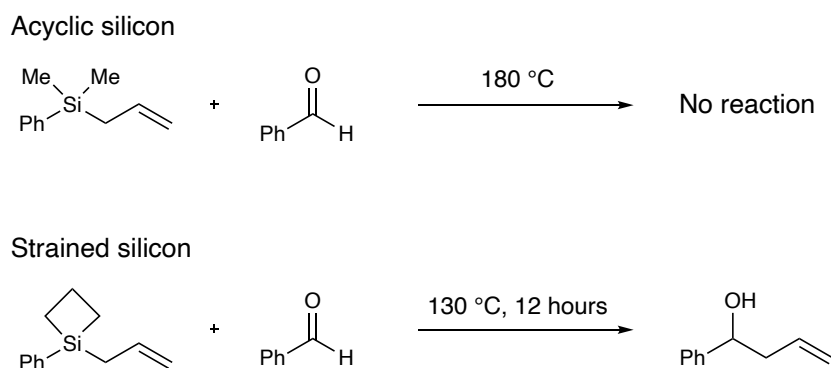


Figure 1.2: Utimoto's strained silane experiments.

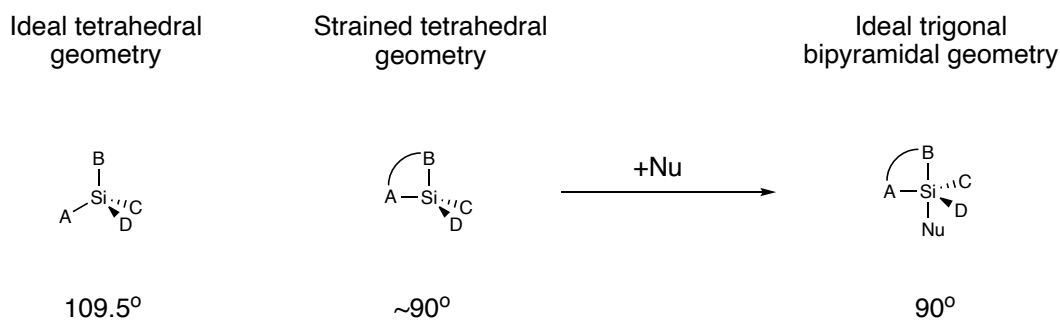


Figure 1.3: Denmark's Strain-release Lewis Acidity rationalization.

This important work done by Denmark and Utimoto has set the foundation for the Leighton group's efforts in exploring silicon Lewis acidity.

1.2. Overview of the Leighton lab's efforts in harnessing silicon Lewis acidity

The Leighton lab has taken advantage of this phenomenon of strain-release Lewis acidity to build a library of strained silane Lewis acids.⁴⁻⁸ Initial results showed that while relatively unstrained silanes **1.2**, **1.3** and **1.4** showed no reactivity in the allylation of benzaldehyde, strained silane **1.1**, based off of the commercially available pinacol backbone, allowed for the allylation of benzaldehyde in good yield. Furthermore, strained silane **1.5**, based off the pseudoephedrine backbone, gave good ee. (Figure 1.4).⁴

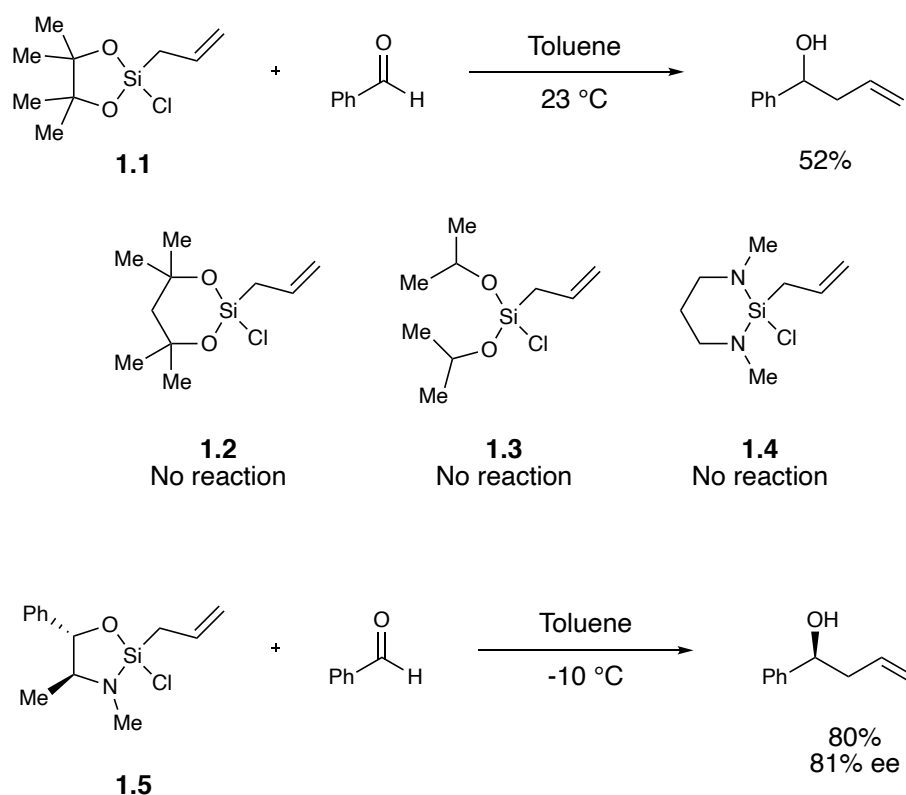


Figure 1.4: The Leighton Group's initial results in developing strained silicon Lewis acids.

Subsequent reports have shown that chiral diamine derived reagents *E*-**1.6** and *Z*-**1.6** have allowed for the highly enantioselective crotylation of aldehydes (Figure 1.5).⁷ *E*-**1.6** and *Z*-**1.6** are bench stable crystalline solids that can be prepared from the corresponding free amines. Mixtures of *E*-**1.6** and *Z*-**1.6** with Sc(OTf)₃ are commercially available as the EZ-CrotylMix.

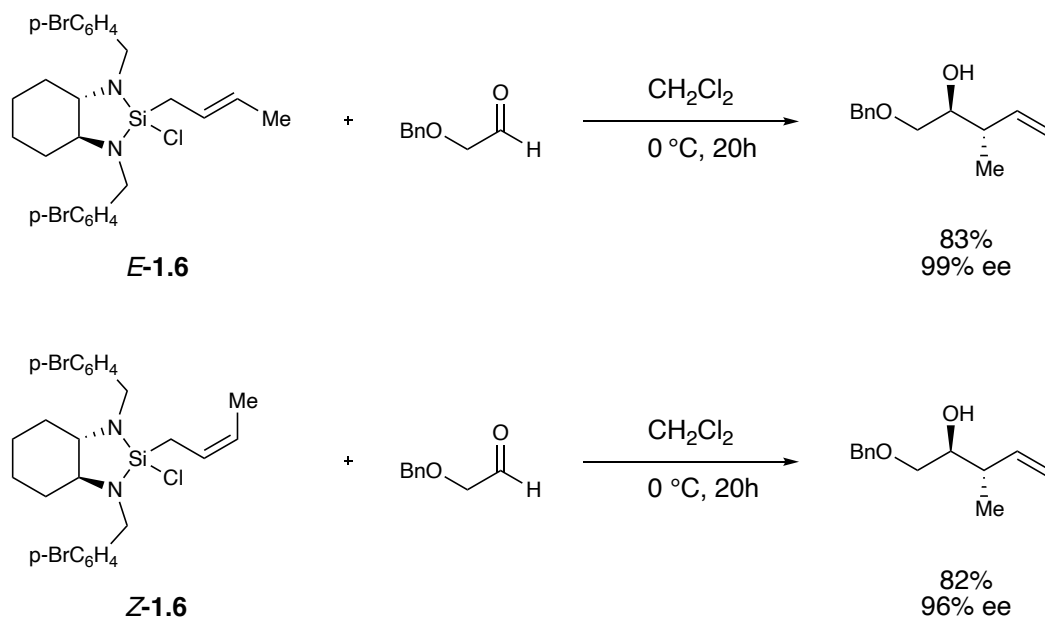


Figure 1.5: Highly enantioselective chiral diamine-based reagents for crotylation.

The next advancement came with the development of the diaminophenol tridentate ligand **1.7**.⁹ The development of this novel ligand was a major improvement over the EZ-CrotylMix as it obviated the need to isolate and purify the strained silane away from the DBU•HCl salts formed during the reaction. Additionally, the increased reactivity of the ligated strained silane eliminates the need for Sc(OTf)₃, thereby allowing for a facile one-pot allylation and crotylation of a wide variety of aldehydes with high yields and enantioselectivities (Figure 1.6). The strength of this methodology has been highlighted in the Leighton group's recent synthesis of a Spongistatin 1 analog.^{10,11}

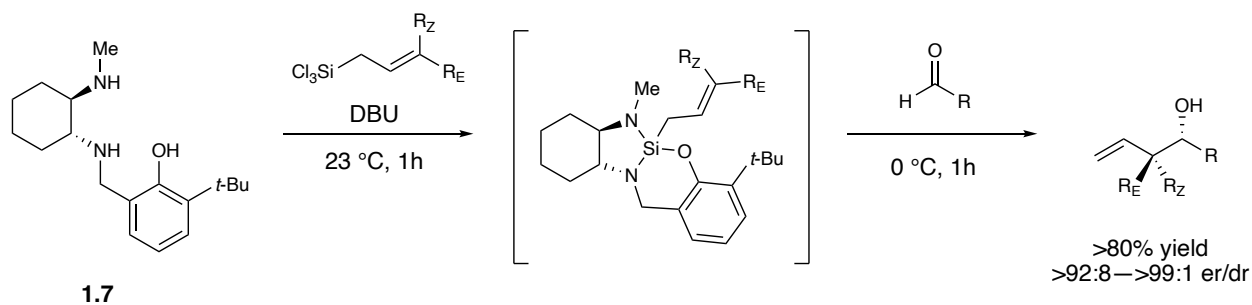


Figure 1.6: One-pot crotylation of aldehydes using the tridentate ligand.

In addition to harnessing silicon Lewis acidity, the Leighton group has also used strain-release and Lewis base activation to develop a silicon Lewis acid catalyst **1.8**, which remains one of the few examples of a highly enantioselective silicon Lewis acid catalyst (Figure 1.7).¹² A drawback of this system however, is that it lacked generality beyond the Diels-Alder reaction. Thus, it remains a challenge in silicon chemistry to develop a simple and general silicon Lewis acid catalyst for asymmetric synthesis.

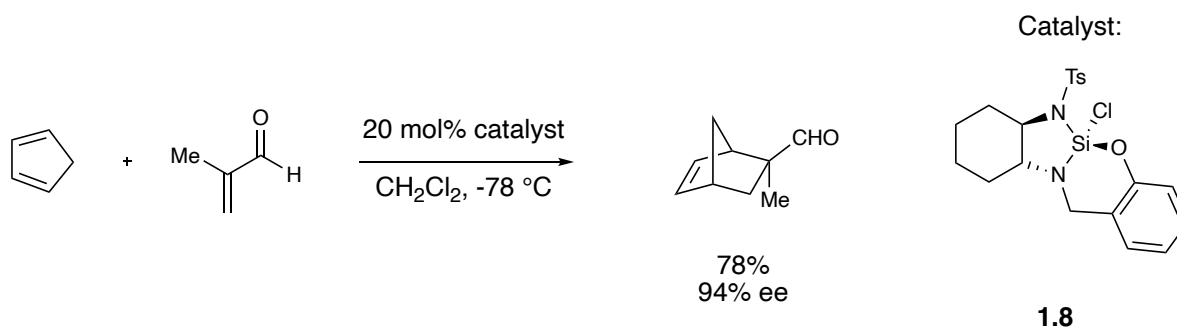


Figure 1.7: Silicon Lewis acid catalyzed Diels-Alder reaction reported by the Leighton group.

1.3. Overview of silylium ions and their potential in silicon Lewis acid catalysis

One promising area where catalysis can be achieved is with the use of cationic silane complexes, also known as silylium ions. Silylium ions are highly reactive species and the tricoordinate versions are quite difficult to prepare compared to their tricoordinate carbon analogs. This can be rationalized by the increased electrophilicity at silicon due its larger electropositivity and size compared to carbon. This results in a poorer orbital overlap and therefore poorer allowance for hyperconjugation from adjacent substituents compared to the analogous carbocation. Truly free tricoordinate silylium ions that do not have further substituents coordinating to them are rare. The crystal structure of one of the first “free” silylium ions **1.9**, reported by J. B. Lambert, was shown to have the solvent toluene coordinate to the silicon center (Figure 1.8a)¹³. Lambert later reported the crystal structure of trimesitylsilylium cation **1.10** (Figure 1.8b),^{14,15} which is considered to be the first truly free tricoordinate silylium ion, confirmed

by both crystal structure and the highly down-field NMR resonance at 225.5 ppm. The two ortho methyl groups on each aryl ring play an extremely important role in shielding the electropositive silicon center from coordinating to a solvent or being attacked by nucleophiles.

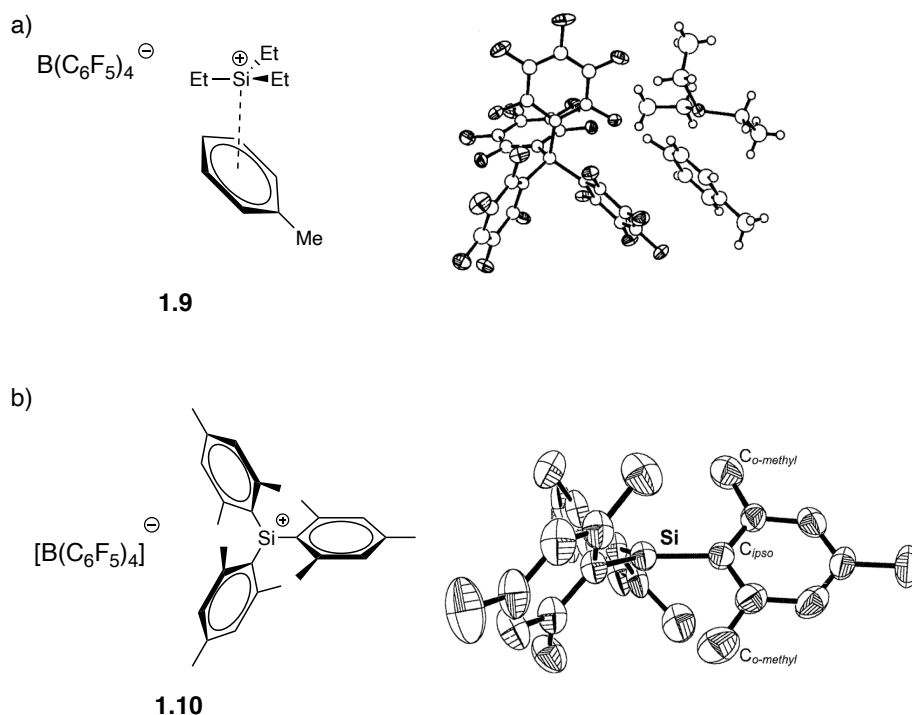


Figure 1.8: a) Crystal structure of solvent coordination to a silylium ion.¹³ b) Crystal structure of a free silylium ion.^{14,15}

While free trivalent silylium ions are rare, there are more examples in the literature of stabilized silylium ions. Stabilization can be provided via σ -donor interactions as in silanes **1.11**¹⁶ and **1.12**¹⁷ where a lone pair of electrons or a σ -bond can coordinate to the silicon center, or via π -donor interactions as in silanes **1.9** and **1.13**¹⁸ where the π -system of the aromatic ring can coordinate to the silylium ion (Figure 1.9). These stabilized silylium ions are more promising candidates for their use as catalysts due to their ability to be handled more effectively, not only in terms of their synthesis and storage, but also in terms of regenerating the silylium ion, since the most challenging aspect of silylium ion catalysis is the ability to consistently regenerate the silyl

cation.¹⁹ Therefore, strong Lewis bases must be avoided as stabilizers and any Lewis pair formation should be reversible.

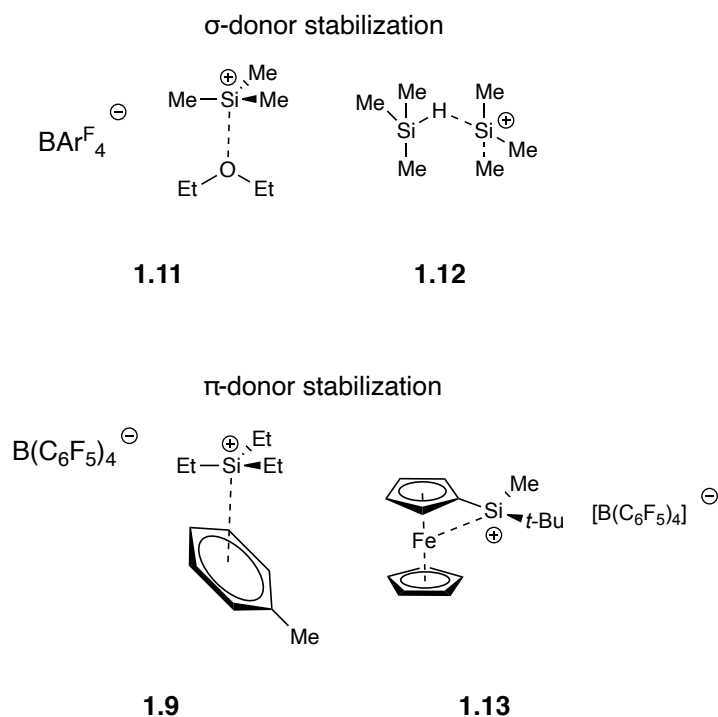


Figure 1.9: Stabilized silylium ions.

1.4. Preparation of silylium ions

Silylium ions have traditionally been prepared via abstraction of a leaving group from the tetracoordinate silane. This can happen via a hydride abstraction as in the original report from Corey where the trityl cation was used to abstract a hydride from the hydrosilane (Figure 1.10a), however the perchlorate counterion used was nucleophilic enough to coordinate to the silane.²⁰ The development and use of weaker coordinating ions such as BArF_4^- ²¹ and $\text{B}(\text{C}_6\text{F}_5)_4^-$ ¹³ have allowed for the preparation of more free silylium cations via hydride abstraction. Silylium ions can also be generated via alkyl or aryl abstraction, as used by Lambert, where an allyl group was abstracted from the allyltrimesityl silane to produce silylium ion **1.10** (Figure 1.10b).¹⁵ An advantage of abstracting an allyl group over other alkyl groups or a hydride ion, is that the allyl

group is farther away from the silicon center, allowing for the synthesis of sterically hindered silylium ions.

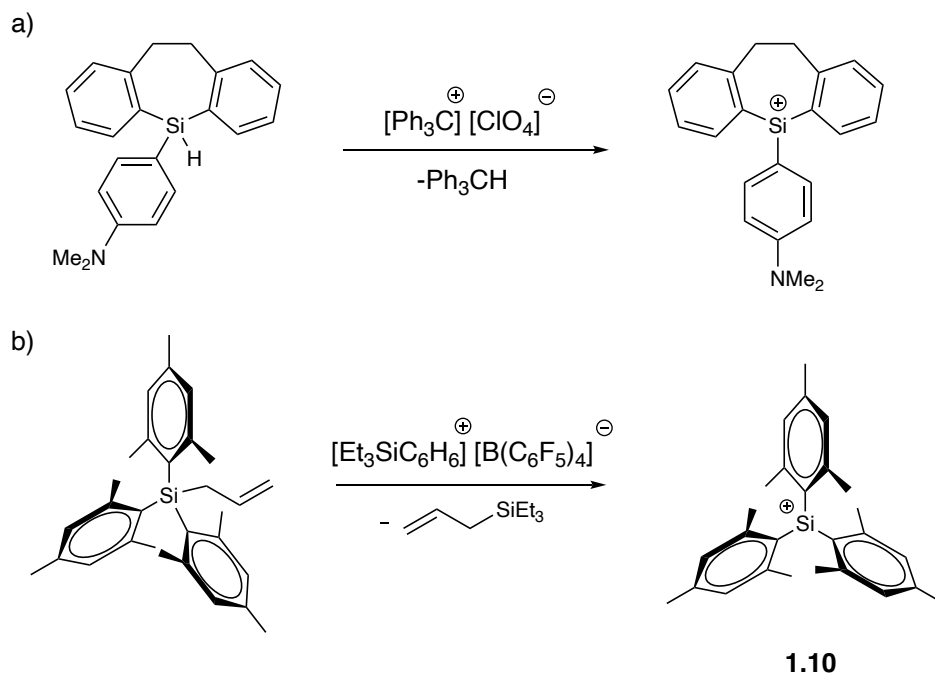


Figure 1.10: Preparation of silylium ions. a) Corey hydride abstraction. b) alkyl abstraction.

1.5. Previous examples of silylium ions used as catalysts

One of the earliest reported examples of a silylium ion catalyst was reported by Ghosez,^{22,23} where TMSNTf₂ silane **1.14** catalyzed the Diels-Alder reaction between cyclopentadiene and methyl acrylate (Figure 1.11a). Sawamura²⁴ reported solvent stabilized silane **1.15** catalyzing the same the Diels-Alder reaction with cyclohexadiene, with catalyst loadings reaching 2 mol%, a remarkable achievement for an organocatalyst (Figure 1.11b). In 2009, Oestreich²⁵ reported ferrocenyl stabilized silane **1.13**, catalyzing the Diels-Alder reaction at low temperature, a testament to the high reactivity of silylium ions and their potential in catalysis (Figure 1.11c). It is important to note that these are some of the very few examples of silylium ion catalysts and they are mostly achiral.

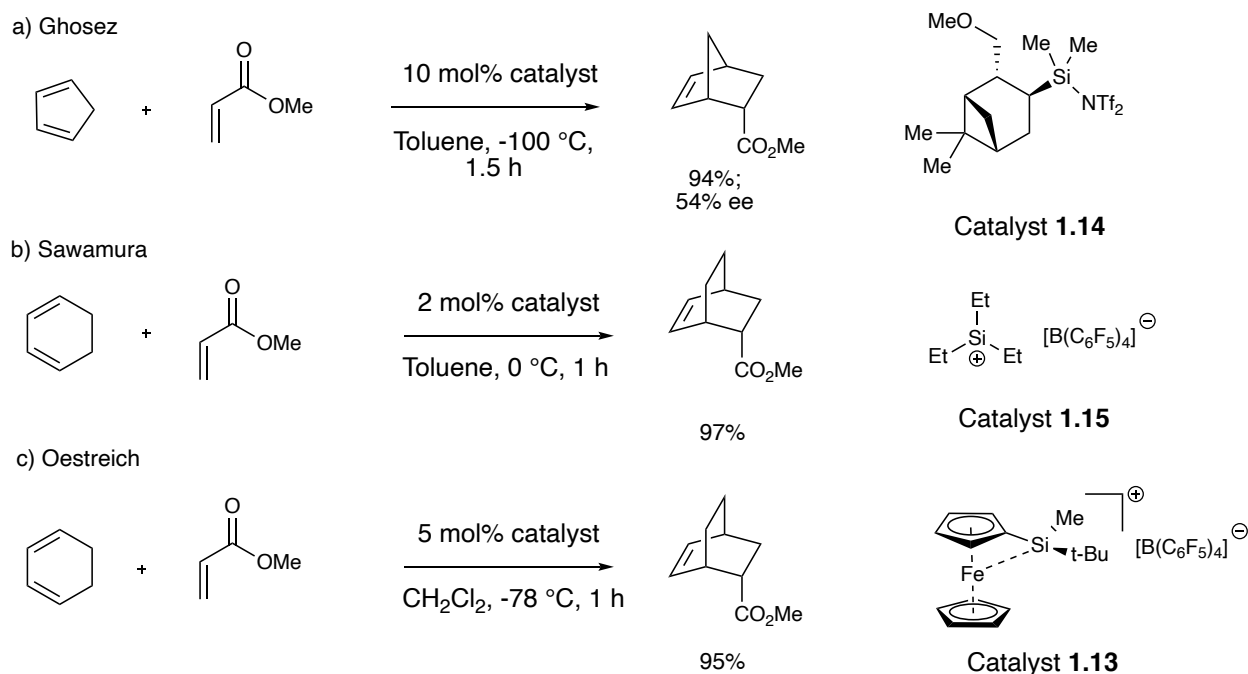


Figure 1.11: Silylium ions used in catalysis.

Since the 2009 report, Oestreich has reported more examples of silylium ion catalysts, including chiral variants (Figure 1.12).²⁶⁻²⁸ Enantioselectivity has remained a challenge in the field due to the high reactivity of the silyl cation and Oestreich's reports are some of the only examples of enantioselective silylium ion catalysts.

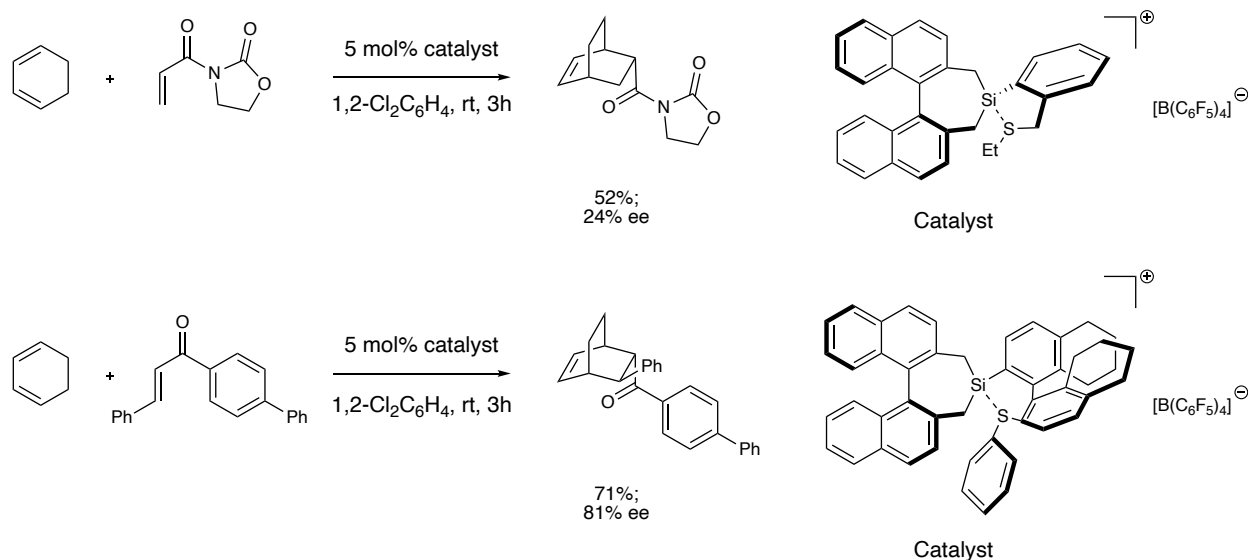


Figure 1.12: Oestreich's chiral silylium ion catalysts.

1.6. Summary and Outlook

A summary of silicon Lewis acidity has been presented, including the Leighton group's use of strain-release Lewis acidity to develop powerful allylation and crotylation reagents. Despite these advances in tuning silicon Lewis acidity, the Diels-Alder catalyst reported from the group in 2006 remains one of the only examples of a highly enantioselective silicon Lewis acid catalyst. The use of silylium ions appears to be a promising area in which a general silicon Lewis acid catalyst could be developed. The following thesis describes (1) my efforts towards developing a novel silylium ion catalyst and (2) my efforts towards synthesizing strained silanes for use in molecular electronic junctions.

1.7. References

- ¹ Hosomi, H.; Shirahata, S.; Sakurai, H. *Tetrahedron Lett.* **1978**, *33*, 3043-3046.
- ² Matsumoto, K.; Oshima, K.; Utimoto, K. *Journal of Organic Chemistry.* **1994**, *59*, 7152-7155.
- ³ Denmark, S. E.; Jacobs, R. T.; Dai-Ho, G.; Wilson, S. *Organometallics.* **1990**, *9* (12), 3015-3019.
- ⁴ Kinnaird, J. W.; Ng, P. Y.; Kubota, K.; Wang, X.; Leighton, J. L. *J. Am. Chem. Soc.* **2002**, *124* (27), 7920-7921.
- ⁵ Wang, X.; Meng, Q.; Nation, A. J.; Leighton, J. L. *J. Am. Chem. Soc.* **2002**, *124* (36), 10672-10673.
- ⁶ Kubota, K.; Leighton, J. L. *Angew. Chemie - Int. Ed.* **2003**, *42* (8), 946-948.
- ⁷ Hackman, B. M.; Lombardi, P. J.; Leighton, J. L. *Org. Lett.* **2004**, *6* (23), 4375-4377.
- ⁸ Wang, X.; Meng, Q.; Perl, N. R.; Xu, Y.; Leighton, J. L. *J. Am. Chem. Soc.* **2005**, *127* (37), 12806-12807.
- ⁹ Suen, L. M.; Steigerwald, M. L.; Leighton, J. L. *Chem. Sci.* **2013**, *4* (6), 2413-2417.
- ¹⁰ Suen, L. M.; Tekle-Smith, M. A.; Williamson, K. S.; Infantine, J. R.; Reznik, S. K.; Tanis, P. S.; Casselman, T. D.; Sackett, D. L.; Leighton, J. L. *Nature Communications.* **2018**, *9*, 4710.
- ¹¹ Tekle-Smith, M. A.; Williamson, K. S.; Hughes, I. F.; Leighton, J. L. *Org. Lett.* **2017**, *19*, 6024-6027.
- ¹² Kubota, K.; Hamblett, C. L.; Wang, X.; Leighton, J. L. *Tetrahedron.* **2006**, *62*, 11397-11401.
- ¹³ Lambert, J. B.; Zhang, S.; Stern, C. L.; Huffman, J. C. *Science.* **1993**, *260*, 1917-1919.
- ¹⁴ Lambert, J. B.; Zhao, Y. *Angew. Chem. Int. Ed. Engl.* **1997**, *36*, 400-40.
- ¹⁵ Kim, K.; Reed, C.; Elliott, D.; Mueller, L.; Tham, F.; Lin, L.; Lambert, J. B. *Science.* **2002**, *297*, 825-827.
- ¹⁶ Kira, M.; Hino, T.; Sakurai, H. *J. Am. Chem. Soc.* **1992**, *114*, 6697-6700.
- ¹⁷ Hoffmann, S. P.; Kato, T.; Tham, F. S.; Reed, C. A. *Chem. Commun.* **2006**, 767-769.
- ¹⁸ Klare, H. F. T.; Bergander, K.; Oestreich, M. *Angew. Chem. Int. Ed.* **2009**, *48*, 9077-9079.
- ¹⁹ Muther, K.; Oestreich, M. *Chem. Commun.* **2011**, 47,334 -336.
- ²⁰ Corey, J. Y. *J. Am. Chem. Soc.* **1975**, *97*, 3237-3238.
- ²¹ Kira, M.; Hino, T.; Sakurai, H. *J. Am. Chem. Soc.* **1992**, *114*, 6697-6700.
- ²² Mathieu, B.; Ghosez, L. *Tetrahedron Lett.* **1997**, *38*, 5497-5500.
- ²³ Mathieu, B.; Ghosez, L. *Tetrahedron.* **2002**, *58*, 8219-8226.
- ²⁴ Hara, K.; Akiyama, R.; Sawamura, M.; *Org. Lett.* **2005**, *7*, 5621-5623.
- ²⁵ Klare, H. F. T.; Bergander, K.; Oestreich, M. *Angew. Chem. Int. Ed.* **2009**, *48*, 9077-9079.
- ²⁶ Schmidt, R. K.; Klare, H. F. T.; Fröhlich, R.; Oestreich, M. *Chem. Eur. J.* **2016**, *22*, 5376-5383.
- ²⁷ Rohde, V. H. G.; Müller, M. F.; Oestreich, M. *Organometallics.* **2015**, *34*, 3358-3373.
- ²⁸ Shaykhtudinova, P.; Oestreich, M. *Org. Lett.* **2018**, *20*, 7029-7033.

Chapter 2: The Development of a Novel Cationic Silicon Lewis Acid and Catalyst

2.1. Introduction

Based on the Leighton group's expertise in developing strained silicon Lewis acids and our 2006 report¹ of a silicon Lewis acid catalyst, we wondered if it would be possible to develop another more general silicon Lewis acid catalyst. To develop such catalyst, the N-Methyldiethanolamine backbone **2.1** was chosen (Figure 2.1). This new backbone was structurally most similar to the pinacol silane developed early on in the Leighton group, except with a nitrogen spacer in the middle. The resulting N-Methyldiethanolamine based silane is known as a quasisilatrane, and falls under the general class of molecules known as silatranes (Figure 2.1). Silatranes and quasisilatranes are pentacoordinate silanes that have been known and studied for their interesting structural features, particularly the N-Si dative bond.²⁻⁶ They have traditionally been synthesized by treating a triethanolamine or diethanolamine with an alkoxy silane.⁶ However, until recently, their use as reagents in organic chemistry has not been explored, with only a few reports in the literature.^{7,8} This therefore represented an excellent opportunity to explore and develop the use of quasisilatranes as potential reagents and catalysts in organic chemistry. Our efforts to develop this catalyst and explore its reactivity will be described in this chapter.

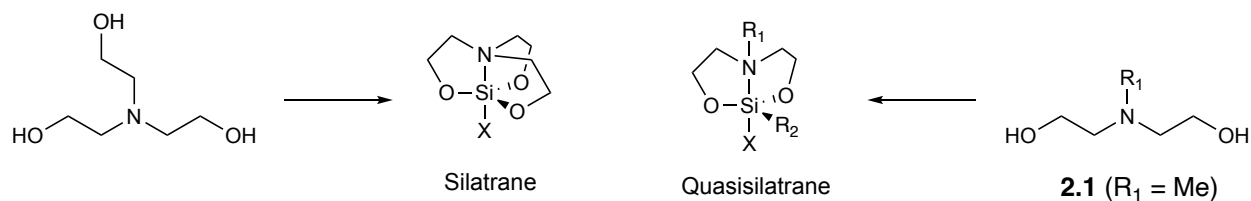
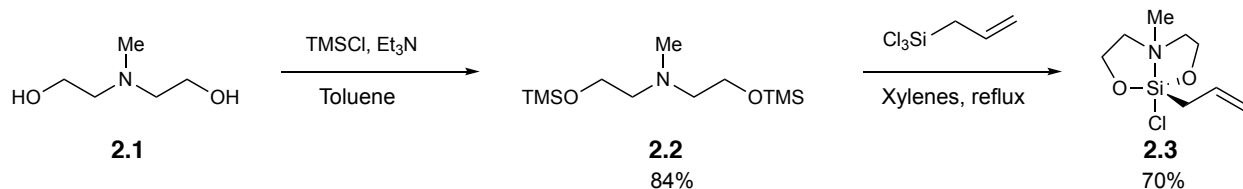


Figure 2.1: General structure of silatrane and quasisilatrane.

2.2. Initial efforts to synthesize the silane

Following the Leighton group's precedent⁹ for synthesizing silanes, N-Methyldiethanolamine was treated with allyltrichlorosilane in the presence of DBU. However, repeated attempts using this procedure did not afford the desired quasisilatrane and resulted in what appeared to be mixtures of oligomerized silane. Following Urtane's method for synthesizing quasisilatrane,¹⁰ N-Methyldiethanolamine was first TMS-protected with TMSCl to produce bis-protected product **2.2**, which was then trans-silylated with allyltrichlorosilane to produce the allyl chloroquasisilatrane **2.3** (Scheme 2.1).



Scheme 2.1: Synthesis of allyl quasisilatrane **2.3**.

Reaction optimization and monitoring of the crude NMR showed that the quasisilatrane could be generated more cleanly at higher temperature, but product isolation still proved to be a challenge. Despite multiple attempts to isolate the purified product via vacuum distillation, including temperatures up to 200 °C, we turned our focus to alternate isolation techniques. Subjecting the crude reaction mixture to sublimation conditions revealed that the product could be isolated to produce a white crystalline solid. A crystal structure was obtained by Dr. Daniel Paley to confirm that the pentacoordinate chloroquasisilatrane **2.3** had indeed been isolated (Figure 2.2). The N-Si bond length in **2.3** is 2.113 Å, which is longer than a typical N-Si bond, but in the range of similar quasisilatrane and the ²⁹Si NMR shift of **2.3** is -54 ppm, which is in the range of pentacoordinate silanes.^{6,10}

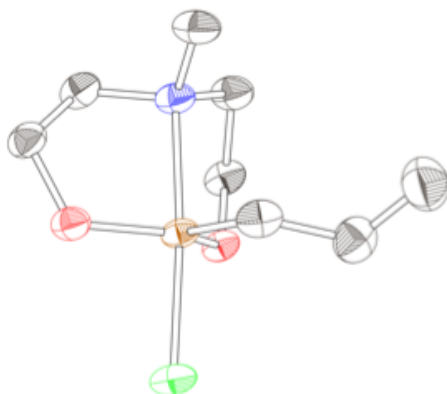


Figure 2.2: Crystal structure of allyl quasisilatrane 2.3.

Having successfully sublimed crystals of **2.3**, it was investigated whether it could be crystallized via traditional, low temperature conditions to ease product isolation and scalability. Initial attempts proved to be unsuccessful and efforts were then turned towards synthesizing a more crystalline silane. Using the aforementioned procedure and the corresponding diethanolamines, silanes **2.4**, **2.5**, **2.6**, **2.7**, **2.8** (Figure 2.3) were unable to be synthesized or isolated by crystallization. It is worth noting that the molecular weights of these silanes are significantly higher than **2.3** and degradation was often observed during attempted sublimation.

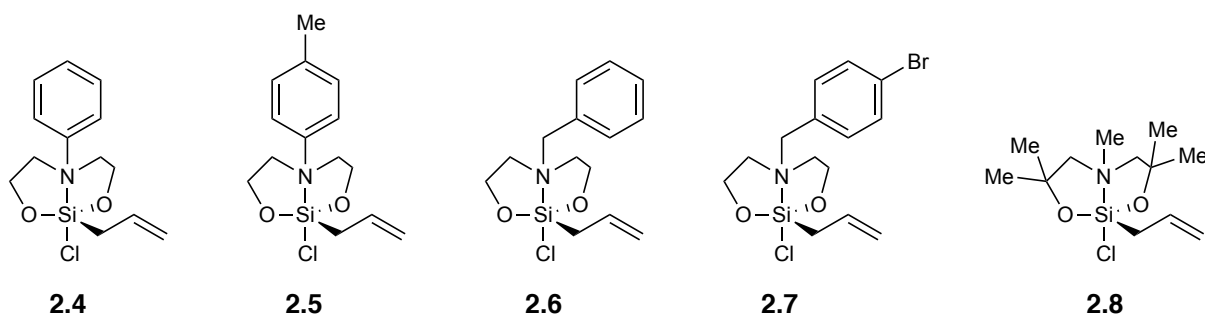
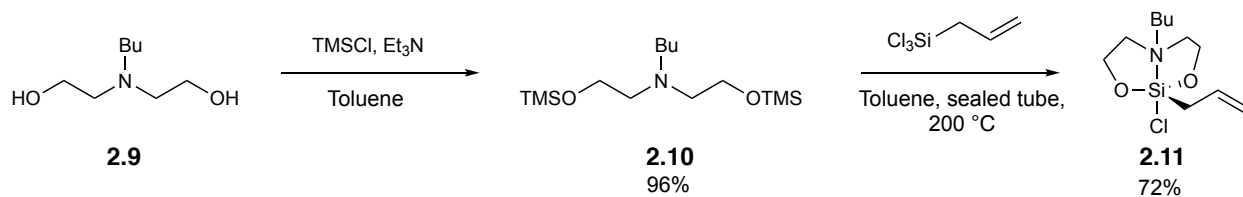


Figure 2.3: More crystalline silanes.

Being unable to generate or isolate a more crystalline silane, efforts were then turned towards generating a less polar silane that could potentially be isolated by distillation. Commercially available N-Butyldiethanolamine **2.9** was treated with TMSCl to provide bis-silylated product **2.10**, which was then trans-silylated with allyltrichlorosilane at high temperature

to produce crude chloroquasisilatrane **2.11** (Scheme 2.2), which, gratifyingly, was able to be purified by vacuum distillation.



Scheme 2.2: Synthesis of N-Butyl quasisilatrane 2.11.

Furthermore, it was discovered that after distillation, **2.11** crystallized upon storage in the freezer. To confirm that **2.11** had not simply frozen at its freezing point, it was warmed back to room temperature, at which point no liquid product was observed, and then heated further, again showing no liquid product, confirming that **2.11** was indeed a crystalline solid at room temperature. A crystal structure of **2.11** was subsequently obtained by Dr. Daniel Paley and its structure was confirmed (Figure 2.4).

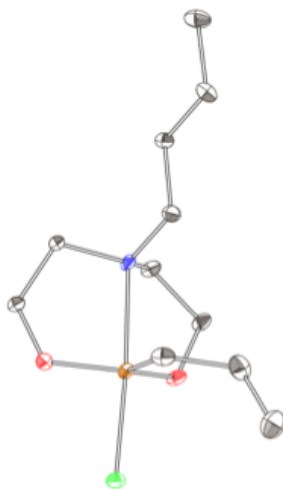


Figure 2.4: Crystal structure of 2.11.

Of note, the N-Si bond length is 2.238 Å, and the ²⁹Si NMR shift is -47.7 ppm. The slightly longer N-Si bond length of **2.11** compared to **2.3** can be understood due to the steric hinderance of the butyl chain. The effect of the elongated bond length is demonstrated in the silicon NMR where

due to a slightly less effective donation of the nitrogen lone pair into the silicon, a downfield shift is observed. The synthesis of **2.11** was repeated on large scale (up to 50g) showing that accessing **2.11** is a scalable process with simple isolation, and additionally it can be stored under inert conditions for months.

2.3. Initial reactivity

Having obtained useful quantities of **2.11**, its reactivity was then tested in simple allylation reactions. The choice of specifically making the allyl silane reagent was not simply to develop another allylsilicon reagent, but rather to explore the reactivity of this new type of quasisilatrane reagent, taking advantage of our group's experience in the field of silicon mediated allylations. It was subsequently discovered that both an aromatic and aliphatic substrate could be allylated in good yield, consistent with our group's previous allyl silane reagents (Figure 2.5). The small quantity of **2.3** that was previously obtained was also tested in these allylations and gave similar results with no distinguishable change in product yield or reaction time. Consequently, **2.11** was used in all future reactions due to its relative ease of isolation compared to **2.3**.

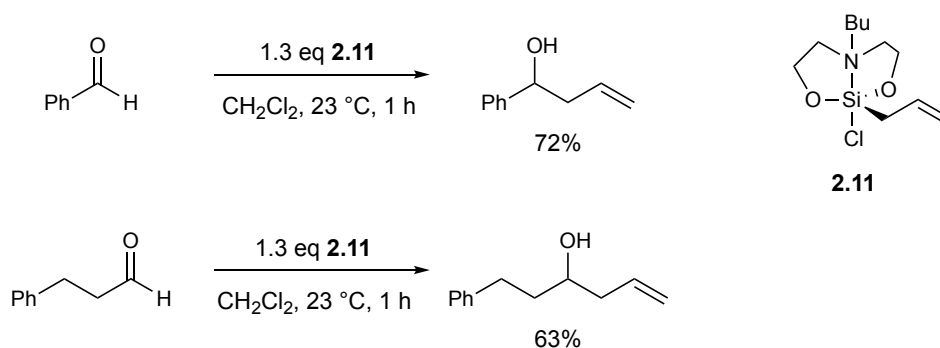


Figure 2.5: Allylation of an aromatic and aliphatic aldehyde with **2.11**.

With the knowledge that aldehydes were easily allylated with this new reagent, efforts were then turned to further investigate the reactivity of **2.11**, by exploring the allylation of ketones, which are more challenging substrates due to their decreased electrophilicity. At the time, our

group had not yet developed chemistry to allylate simple ketones in high yield. Acetophenone was treated with **2.11**, and after 48 hours about 50% allylated product was obtained, with the observation that there was still unreacted acetophenone present in crude mixture (Figure 2.6). This demonstrated that **2.11** was indeed capable of allylating ketones, however the reaction was slow.

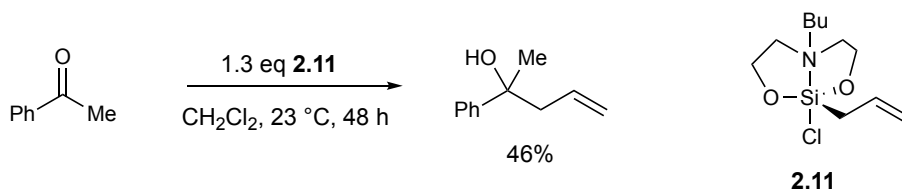


Figure 2.6: Allylation of a ketone with **2.11**.

In order to increase the rate of the reaction a more reactive allyl silane reagent would be needed. It became apparent to us that if the chloride bound to the silicon could be removed by an anion-binding reagent, the resulting silane would have a formal positive charge and therefore we would have generated a silylium ion. Furthermore, this would be a stabilized silylium ion (chapter 1.3), with stabilization provided by the nitrogen lone pair. Consequently, in order to increase the rate of the reaction, Schreiner's thiourea **2.12** was chosen and added to the reaction due its known use as an anion binding catalyst,^{11,12} and gratifyingly, a dramatic rate and yield increase was indeed observed (Figure 2.7).

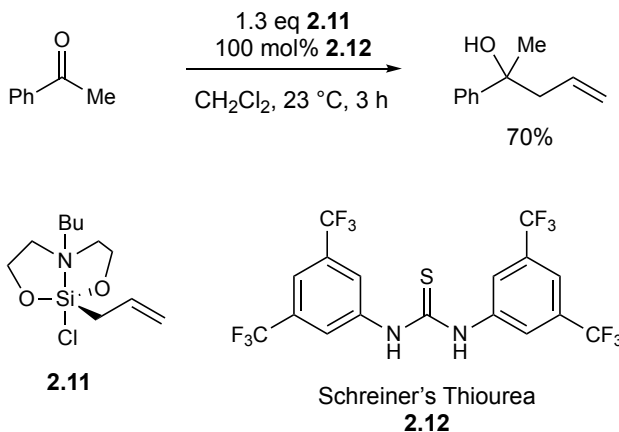


Figure 2.7: Allylation of a ketone with **2.11** and Schreiner's thiourea **2.12**.

Before obtaining the thiourea result, the working mechanistic rationale was that the carbonyl substrate coordinated to the allyl silane reagent forming a hexacoordinate species, with subsequent allyl transfer (Figure 2.8a). However, what appears more likely is that the substrate coordinates to the allyl silane and displaces the chloride, with subsequent allyl transfer (Figure 2.8b). This latter rationale is supported by the thiourea result, where the thiourea binds to the chloride to form a highly reactive stabilized silylium ion **2.13**, which then allows for the facile coordination and allylation of ketones (Figure 2.8c).

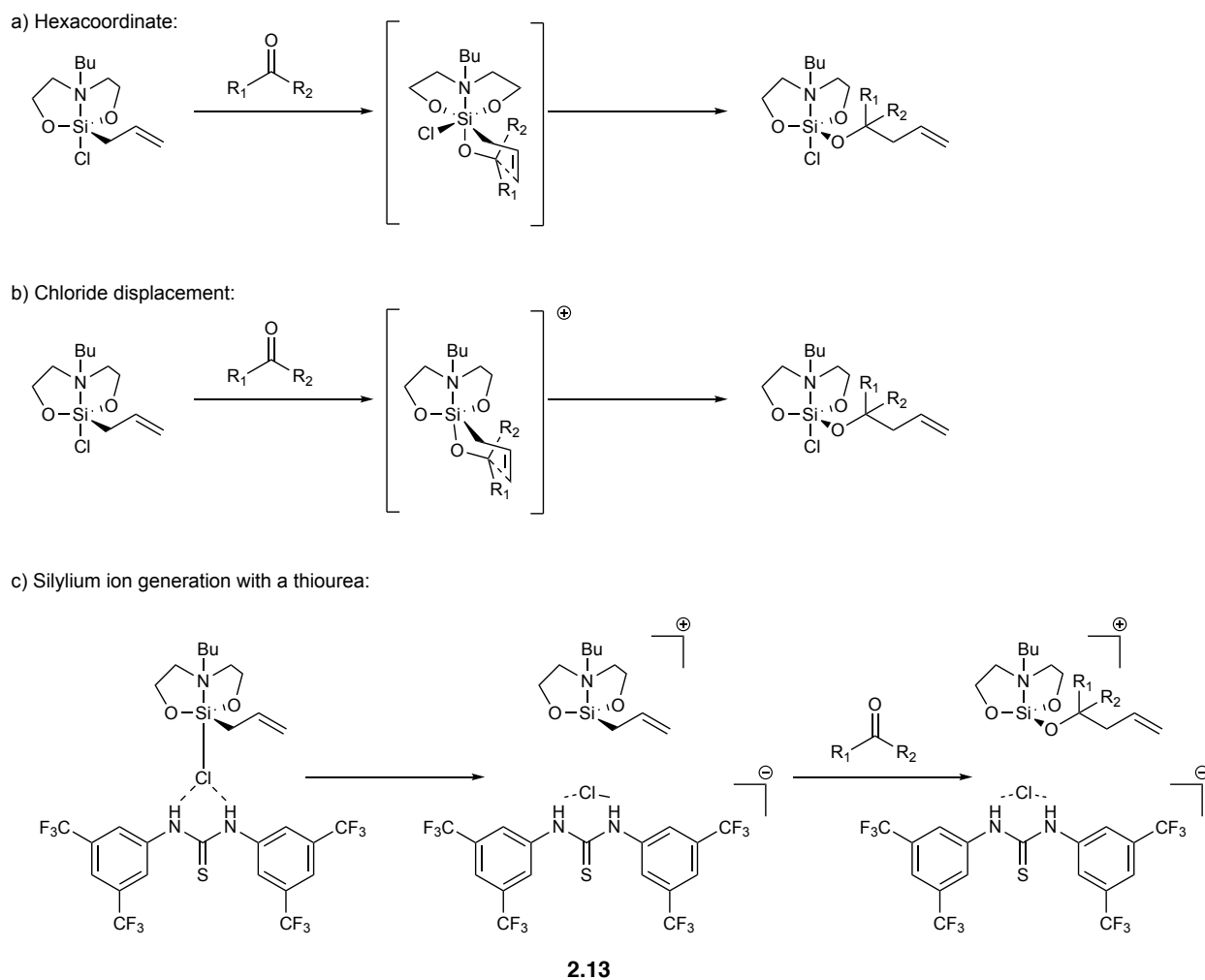


Figure 2.8: Pathways for reactivity. a) Hexacoordinate pathway. b) Chloride displacement pathway. c) Silylium ion-generation by adding a thiourea.

2.4. Thiourea Catalysis

With the knowledge that thiourea accelerated the reaction, we were interested in whether thiourea catalysis was a possibility. However, when 20 mol% of thiourea **2.12** was used, less than 20% of product was observed by NMR (Figure 2.9a). It appeared that the thiourea-chloride-bound species **2.14** was preferred and therefore no free thiourea was available for catalysis (Figure 2.9b).

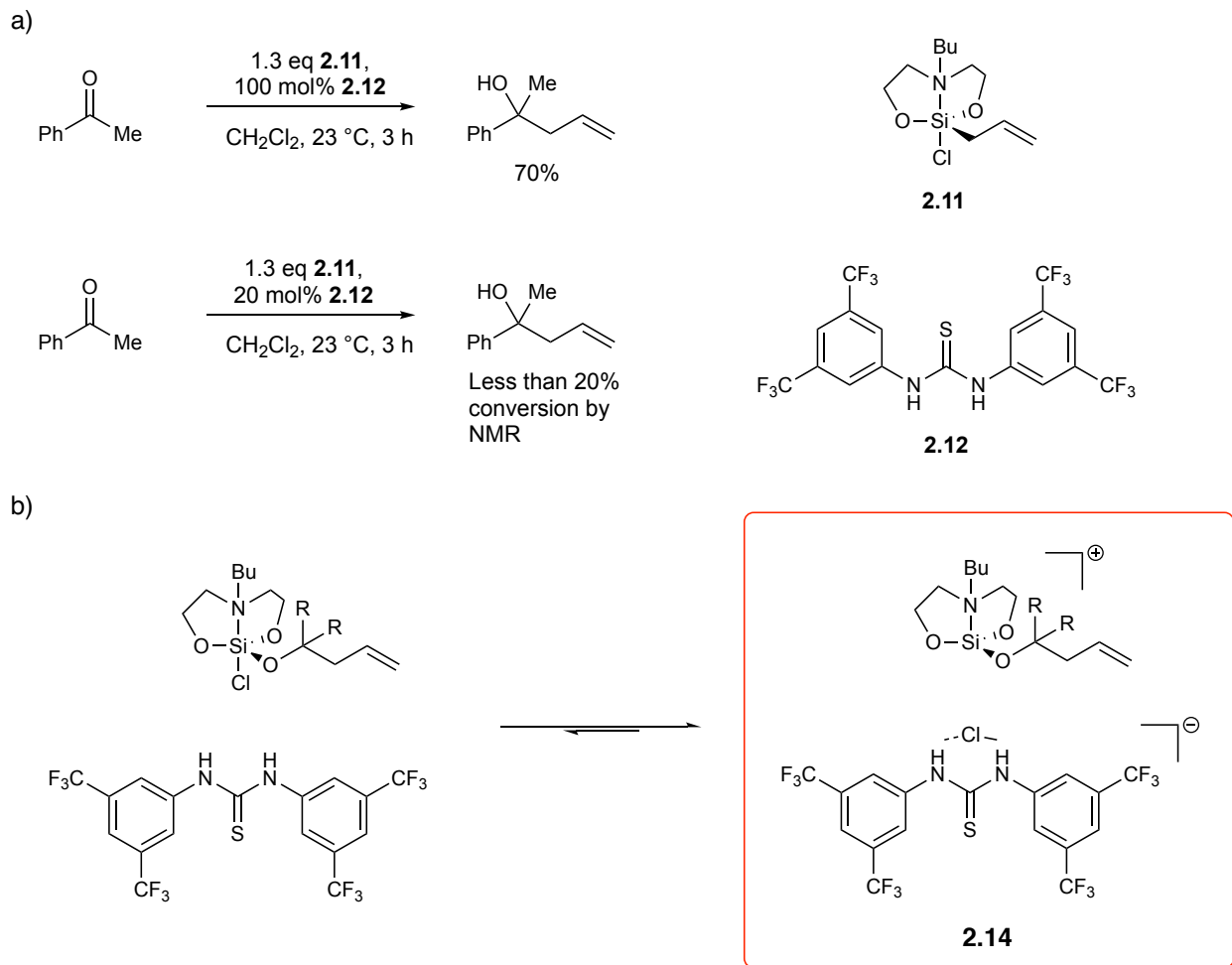


Figure 2.9: a) No catalysis with sub-stoichiometric loading of thiourea. b) Preference of the thiourea-chloride-bound species.

It was proposed that perhaps a different type of thiourea, one that did not bind as strongly to the chloride, was required for our desired catalysis. A thiourea screen was conducted with readily available thioureas obtained from the Owen lab, including electron rich and electron poor thioureas

(Figure 2.10). Unfortunately, all thioureas tested showed no catalysis and confirmed that the lack of catalysis was not unique to thiourea **2.12**.

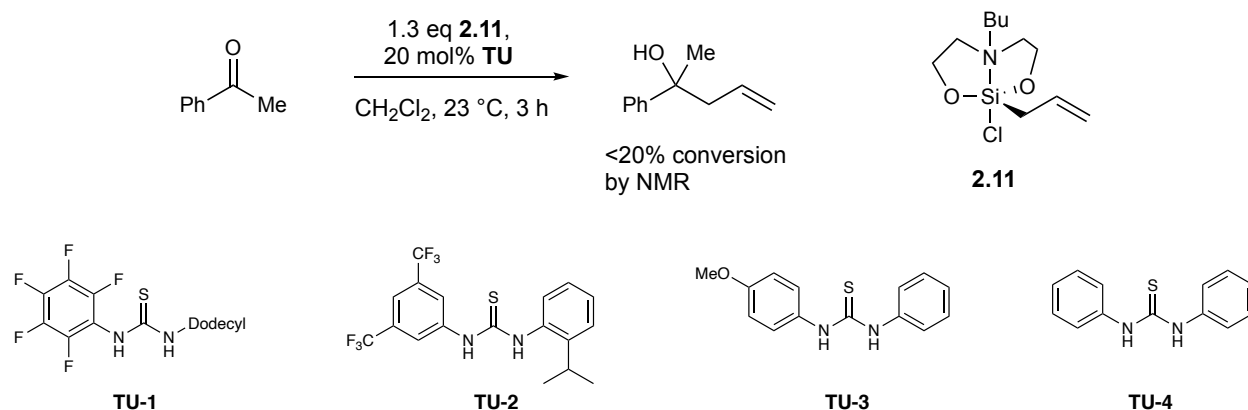
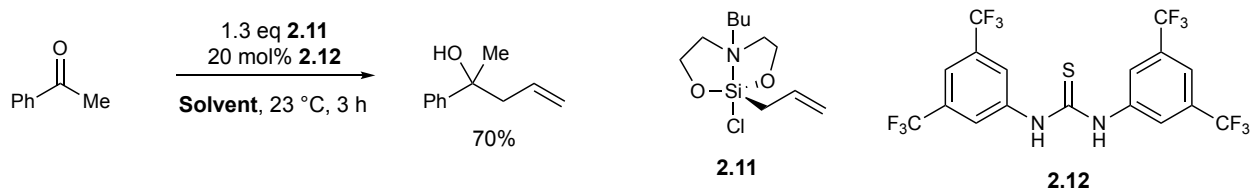


Figure 2.10: Thiourea screen in allylation reactions.

To further probe the lack of thiourea catalysis, it was proposed that a solvent that could stabilize the thiourea-chloride bound complex or further stabilize the silylium ion might allow for thiourea catalysis. Therefore, a solvent screen was then conducted utilizing a range of coordinating and non-coordinating solvents periodically used in silicon-mediated allylation reactions (Table 2.1). It was discovered that dichloromethane, toluene and benzene, all of which are non-coordinating solvents, showed similar results and no catalysis was observed (Table 2.1, entries 1-3). However, the use of coordinating solvents such as ether, THF, DMF, DMSO, and HMPA showed no product formation (Table 2.1, entries 4-8). This was to be expected as these solvents all contain oxygen as their point of coordination, and with silicon, and especially silylium ions, being fairly oxophilic, it was not surprising that no product was obtained due to silane deactivation. A solvent that was more coordinating than dichloromethane, benzene and toluene, but not as coordinating as the oxygen-based solvents was needed, and acetonitrile fit nicely into this range. Gratifyingly, when acetonitrile was used as the solvent with a catalytic amount of thiourea **2.12**, a

91% isolated yield of the allylated product was obtained, demonstrating thiourea catalysis (Table 2.1, entry 9).

Table 2.1 Solvent screen.



Entry	Solvent	% Conversion by NMR
1	CH ₂ Cl ₂	<20%
2	Toluene	11%
3	Benzene	14%
4	Ether	0%
5	THF	0%
6	DMF	0%
7	DMSO	0%
8	HMPA	0%
9	Acetonitrile	91% isolated yield

To confirm that thiourea **2.12** was indeed the active catalyst and not acetonitrile, the control reaction was conducted where acetonitrile was used as the solvent with no added thiourea, and no product was observed (Figure 2.11). This confirmed that acetonitrile on its own was not responsible for catalysis.

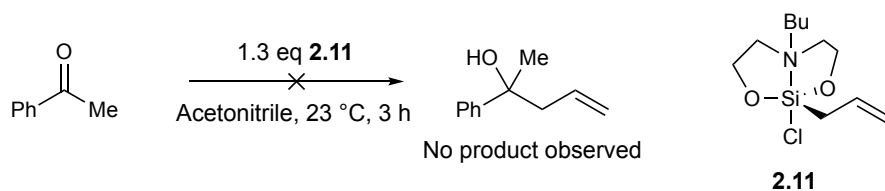


Figure 2.11: Control reaction with only acetonitrile and no thiourea.

It has been shown that acetonitrile can form solvation spheres around halides therefore it was proposed that acetonitrile was stabilizing both the silylium ion species and the chloride, freeing the thiourea from its chloride-bound state and allowing for turnover (Figure 2.12).¹³

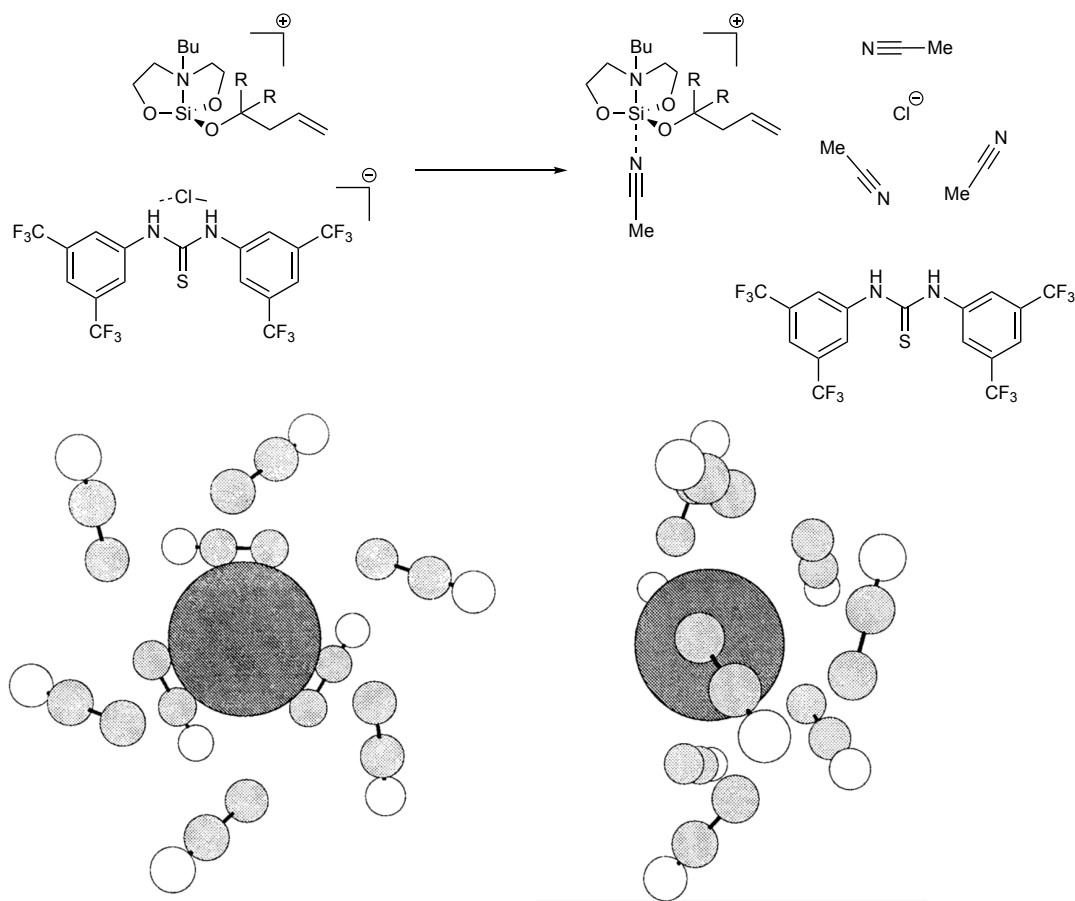


Figure 2.12: Proposed acetonitrile stabilization of silylium ion and solvation sphere around chloride.¹³

In addition to acetophenone, the aliphatic ketone benzylacetone was also tested under these new catalytic conditions and was found to be allylated in excellent yield (Figure 2.13).

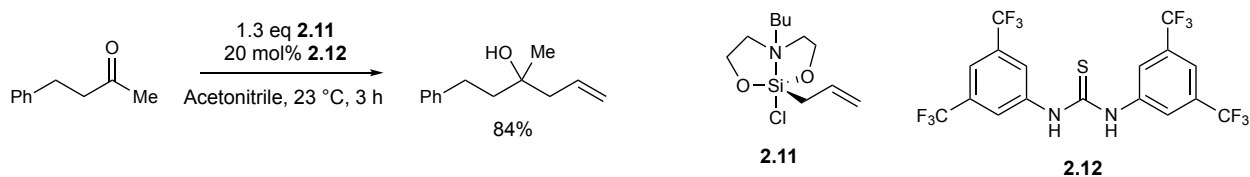
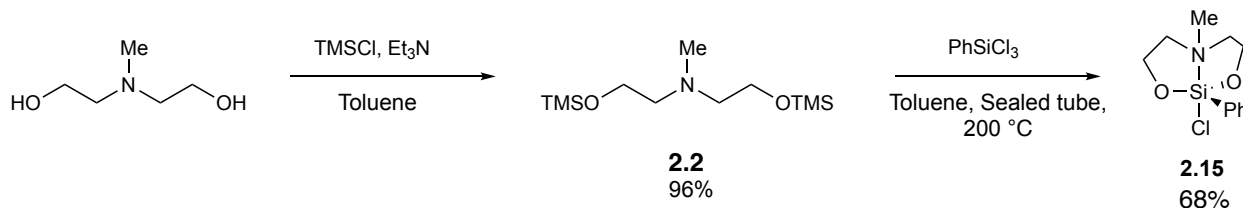


Figure 2.13: Allylation of an aliphatic aldehyde using a catalytic amount of thiourea.

The results and data obtained from both the synthesis attempts and the allylation studies provided us with a deeper understanding of this new silicon Lewis acid and its cationic reactivity pathway. The use of a thiourea to generate the reactive intermediate represents one of the first examples of the merger between anion binding catalysis and silylium ion mediated bond transformations. We used these results to guide us in designing a catalytic version of the silane.

2.5. A more general silicon Lewis acid catalyst

Knowing more about the reactivity of this type of quasisilatrane, we wondered if we could synthesize a more general silicon Lewis acid that could also be used as a catalyst. In order to develop such a general catalyst, a non-transferable substituent would be necessary and consequently the phenyl substituted quasisilatrane **2.15** was chosen as the desired target (Scheme 2.3). As with the synthesis of the allyl quasisilatrane, N-Methyldiethanolamine was TMS protected to afford the bis-silylated product and then trans-silylated with trichlorophenylsilane at an elevated temperature to give **2.15** in a 68% yield (Scheme 2.3). It was observed that as the reaction mixture was cooling to room temperature, crystals started to precipitate. The solvent was removed under pressure and the crude mixture was combined with the crystals and sublimed to afford pure crystals of **2.15**. A crystal structure of **2.15** was obtained by Dr. Daniel Paley (Figure 2.14).



Scheme 2.3: Synthesis of phenyl quasisilatrane **2.15**.

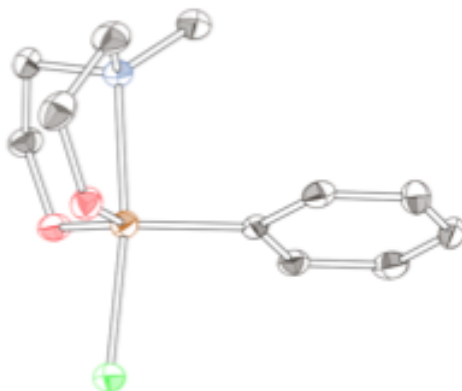


Figure 2.14: Crystal structure of **2.15**.

The N-Si bond length in **2.15** is 2.137Å and the ^{29}Si NMR shift is -70 ppm. The upfield shift of **2.15** compared to the allyl quasisilatrane **2.3** and **2.11** is indicative of the phenyl substituent donating electron density into the silicon center.

2.6. Reactivity of the new catalyst

With pure crystals of **2.15** in hand, we proceeded to investigate its reactivity and the Diels-Alder reaction was chosen as the model reaction. When 20 mol% of catalyst **2.15** was added to the Diels-Alder reaction between cyclopentadiene and methacrolein, a 20% isolated yield of the product was obtained, which represented a promising start (Figure 2.15a). However, as seen in the allylation reactions, when an equivalent amount of thiourea **2.12** was added to the reaction, a dramatic rate increase was observed and this time catalysis was achieved, affording a 90% isolated yield of the cycloadduct (Figure 2.15b).

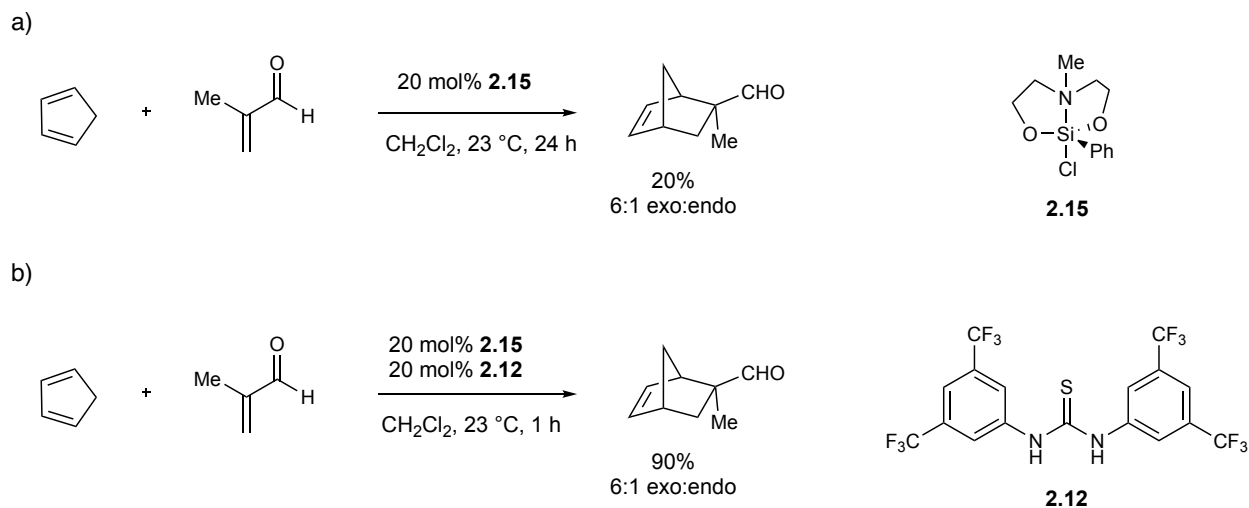


Figure 2.15: Diels-Alder reaction. a) No observed catalysis with 2.15. b) Catalysis after adding thiourea 2.12.

Having achieved catalysis, lower catalyst loadings of both the silane and thiourea **2.12** were tested, but it was observed that at lower catalyst loadings, the reaction stalled and catalysis was no longer achieved. The use of acetonitrile as a solvent, while useful in obtaining thiourea catalysis

in the allylation reactions (section 2.4), did not show any noticeable change in reactivity in these Diels-Alder reactions.

2.7. Investigating the inability to use lower catalyst loadings

The major hypothesis proposed regarding why the reaction failed to show catalysis at lower loadings was that the catalyst was degrading. In order to prevent or slow down degradation, we initially proposed that additional stabilization via an internal tether, such as in **2.16**, would help. We hypothesized that the oxygen at the ortho position in the aromatic ring would be able to coordinate to the silane and provide the suitable stabilization necessary to reduce our catalyst loading (Figure 2.16). One additional advantage is that **2.16** also contained a chiral site close to the silicon center which would be useful for our eventual plans of investigating enantioselectivity.

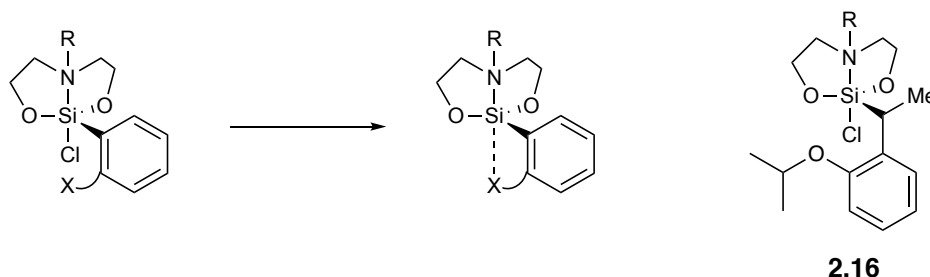
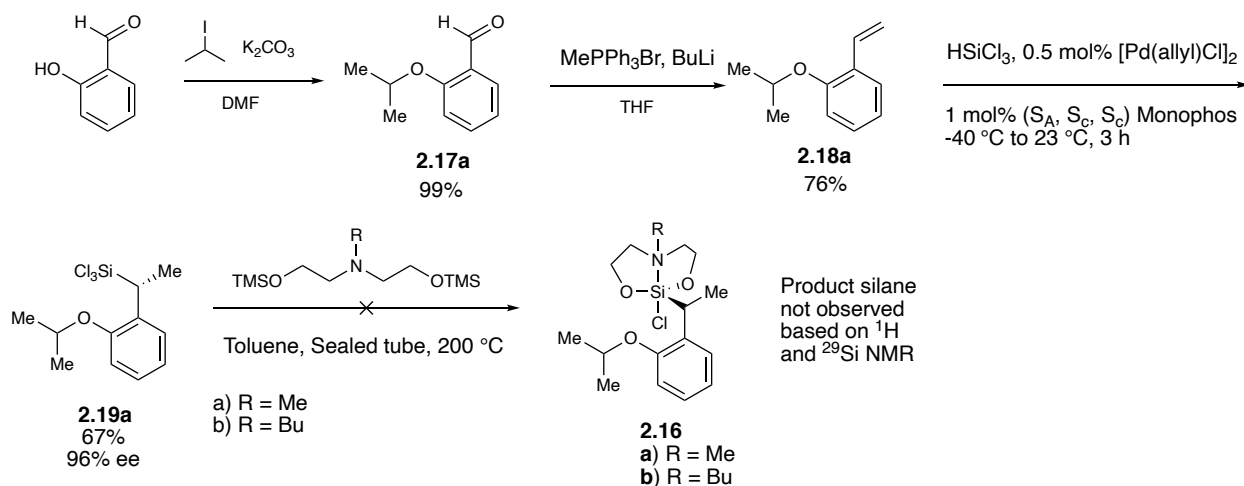


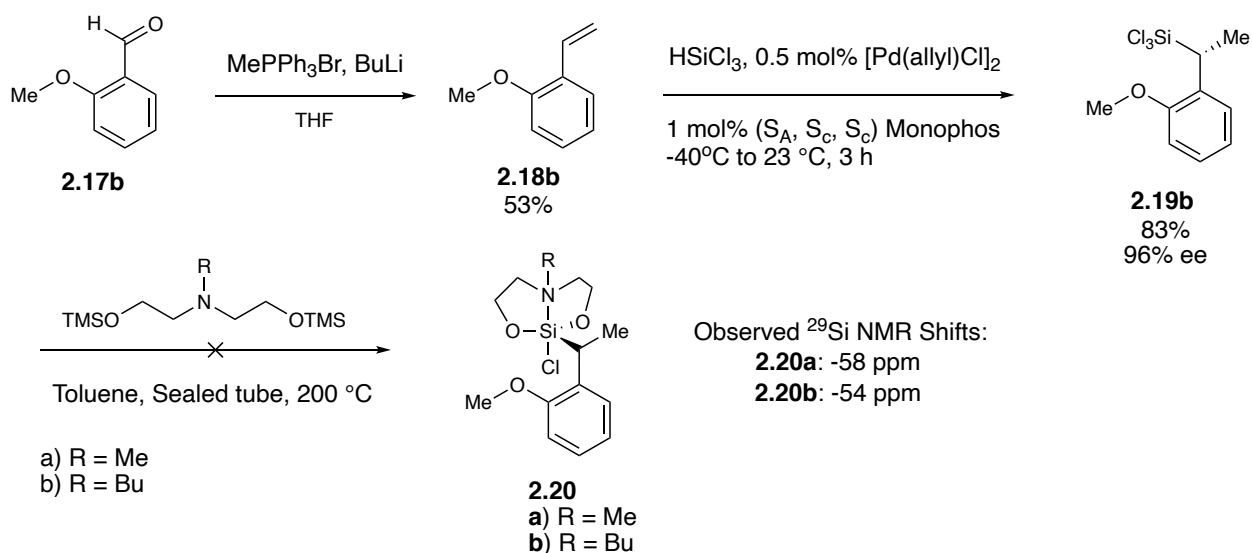
Figure 2.16: Proposed stabilization via internal tether.

We proceeded to synthesize **2.16** by alkylating salicylaldehyde to afford **2.17a**, which via a Wittig reaction afforded styrene **2.18a**, and then upon hydrosilylation afforded the trichlorosilane precursor **2.19a** (Scheme 2.4). However, when **2.19a** was treated with either N-Methyl or N-Butyldiethanolamine, the desired product **2.16** was not observed via ^1H or ^{29}Si NMR.



Scheme 2.4: Synthesis of silane 2.16.

It was proposed that perhaps an isopropoxy group was too bulky and could not be tolerated at the ortho position. Consequently, the *o*-methoxy variant **2.20** was targeted (Scheme 2.5). This time, ^{29}Si NMR shifts were observed for both **2.20a** and **2.20b**, however the product could not be isolated via crystallization, sublimation, or distillation, with the latter 2 methods showing visible signs of decomposition. These results suggested that stabilization via this type of internal tether was not a viable solution to address potential catalyst degradation.



Scheme 2.5: Synthesis of 2.20.

Another solution that was proposed was that more stabilization could be provided by the chloride itself by reducing or adjusting the level of chloride abstraction. This could be achieved by using different types of thioureas whose pKas are known, or other simple chloride binders, as opposed to Schreiner's thiourea **2.12** (Figure 2.17).^{14,15}

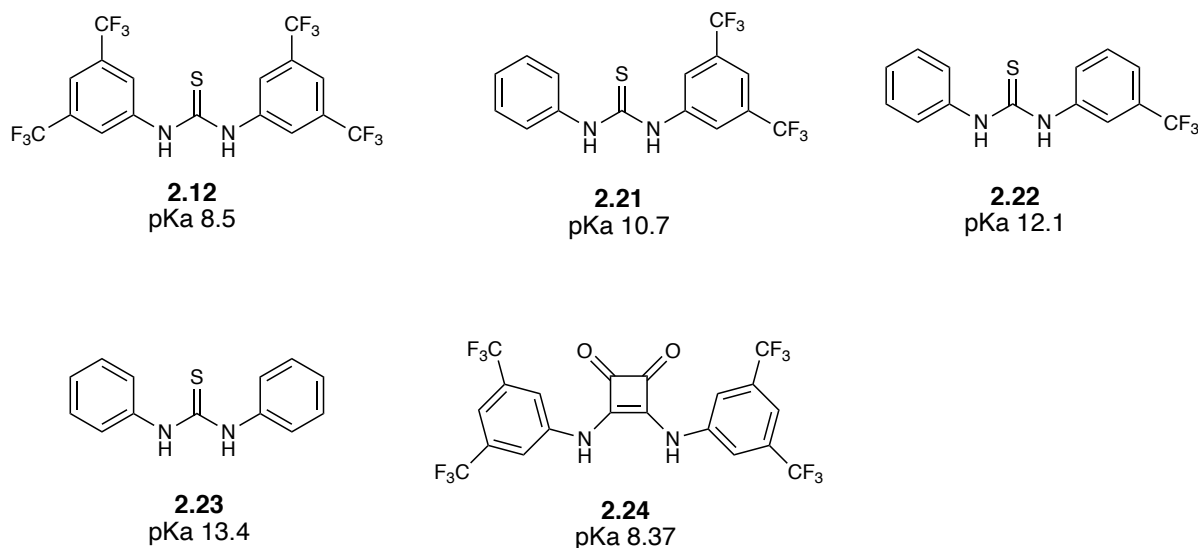
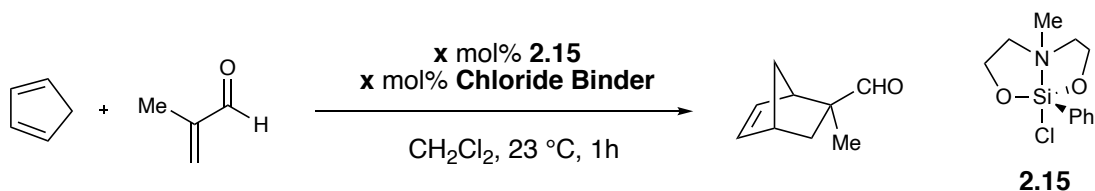


Figure 2.17: pKas of selected thioureas.^{14,15}

However, as shown in Table 2.2, using thioureas with lower pKas did not allow for catalysis at loadings less than 20 mol% (Table 2.2, entries 2, 3, 5, 6, 8, 9), with thiourea **2.23** (Table 2.2, entry 10) not showing complete conversion at 20 mol%, indicating that this was the upper pKa limit. Squaramide **2.24**, while having a slightly lower pKa than Schreiner's thiourea **2.12**, also did not show complete conversion at a loading of 20 mol% (Table 2.2, entry 11).

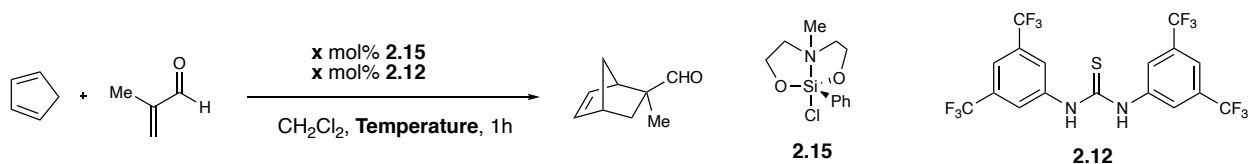
Table 2.2: Chloride binder screen.



Entry	Chloride Binder	Silane and Chloride Binder Catalyst Loading	% Conversion by NMR
1	2.12	20 mol%	>95%
2	2.12	10 mol %	8%
3	2.12	5 mol%	4%
4	2.21	20 mol%	>95%
5	2.21	10 mol %	8%
6	2.21	5 mol%	3%
7	2.22	20 mol%	>95%
8	2.22	10 mol %	8%
9	2.22	5 mol%	3%
10	2.23	20 mol%	33%
11	2.24	20 mol%	43%

Another possible solution to address potential catalyst degradation was lowering the temperature of the reaction (Table 2.3). Fortunately, at 0 °C, -40 °C, and -78 °C (Table 2.3, entries 1-3), catalysis was observed at 10 mol%. However, at loadings of 5 mol%, catalysis was not observed at lower temperatures (Table 2.3, entries 4-6).

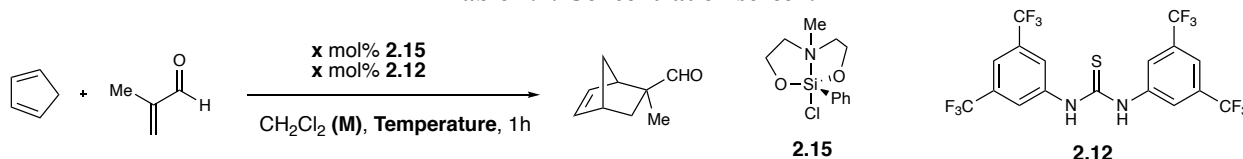
Table 2.3: Temperature screen.



Entry	2.15 and 2.12 Catalyst Loading	Temperature (°C)	% Conversion by NMR
1	10 mol%	0	>95%
2	10 mol %	-40	>95%
3	10 mol%	-78	86%
4	5 mol%	0	6%
5	5 mol %	-40	10%
6	5 mol%	-78	3%

A concentration screen was conducted and it was observed that at room temperature and a concentration of 0.25M (with respect to methacrolein), catalysis was not observed at catalyst loadings below 20 mol% (Table 2.4, entries 2 and 3), while at a concentration of 2M, potential catalysis was observed at lower loadings (Table 2.4, entries 4 and 5). However, when the corresponding control reactions at room temperature were conducted, it was discovered that significant product conversion was obtained in the absence of the catalysts, at a concentration of 2M. Therefore, the product conversions obtained at lower loadings could not be attributed to catalysis, but rather a combination of both the uncatalyzed background reactions and catalysis.

Table 2.4: Concentration screen.



Entry	2.15 and 2.12 Catalyst Loading	Molarity	Temperature	% Conversion by NMR
1	20 mol%	0.25M	23 °C	>95%
2	10 mol%	0.25M	23 °C	9%
3	5 mol %	0.25M	23 °C	4%
4	20 mol %	2M	23 °C	>95%
5	10 mol%	2M	23 °C	>95%
6	5 mol%	2M	23 °C	32%
7	20 mol %	2M	0 °C	>95%
8	10 mol%	2M	0 °C	>95%
9	5 mol%	2M	0 °C	18%

In order to determine whether the uncatalyzed background reaction could be minimized at high concentration, the reactions were repeated at 0 °C. Gratifyingly, at 0 °C and a concentration of 2M, there was no product formation observed in the absence of the catalysts. Upon addition of the catalysts, at 0 °C and a concentration of 2M, catalysis was observed at loadings less than 20 mol% (Table 2.4, entries 8 and 9).

With conditions sorted out to allow for complete product conversion at loadings of 10 mol%, we continued to investigate the reactivity of the silane by proceeding to study the electronic

effects of the phenyl substituent. The primary focus was to determine whether electron rich substituents could further stabilize the silane and allow for catalysis at loadings of 5 mol%. We proceeded to synthesize and test the silanes shown in Figure 2.18 using the corresponding trichlorosilane precursor. However, all silanes tested showed similar levels of product conversion and no definitive trend could be identified.

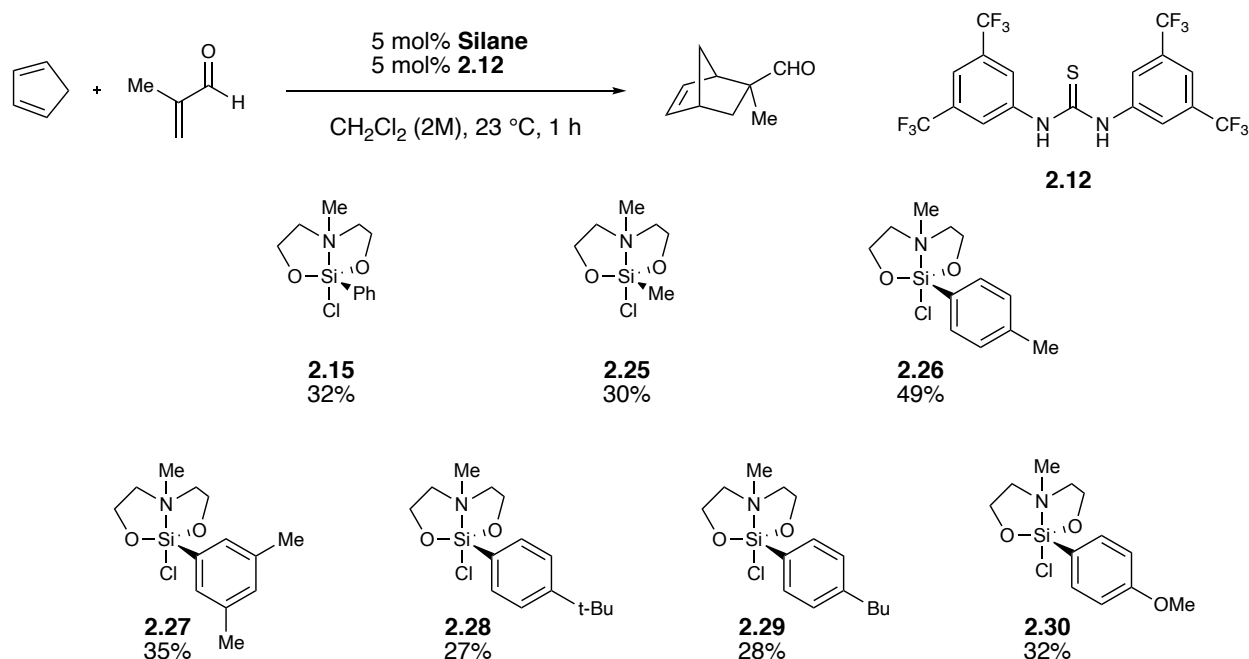
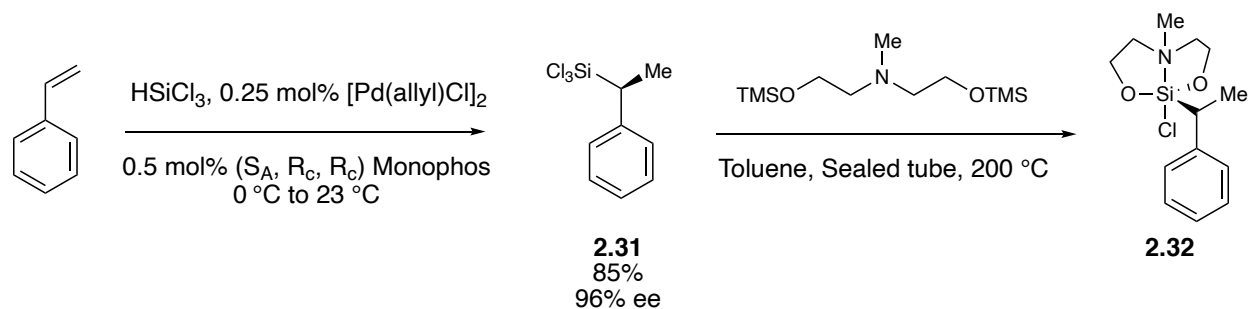


Figure 2.18: Electronic effects of different silanes.

2.8. Efforts to develop enantioselectivity

Having a deeper understanding of the reactivity of this type of quasisilatrane, we proceeded to investigate whether we could achieve enantioselectivity in this reaction. We chose silane **2.32** as our target since it could be synthesized in 2 steps via the chiral hydrosilylation of styrene to generate the trichlorosilane precursor **2.31** (Scheme 2.6). Additionally, the chiral site would be close to the silicon center.



Scheme 2.6: Synthesis of chiral silane 2.32.

However, when attempting to isolate **2.32**, product decomposition was observed upon attempted sublimation, so the crude product was instead used in test reactions. When using 10 mol% of silane **2.32** and thiourea **2.12** at 0 °C, only 8% product conversion was observed (Figure 2.19a). The reaction was then repeated at conditions known to give complete conversion, however the ee was only determined to be 10% (Figure 2.19b). It was determined at this point that the reaction conditions could not be further optimized to give a higher level of enantioselectivity. Furthermore, due to the apparent lower reactivity of alkyl substituted quasisilatrane, and the lower tolerance for substituent variance at this position, it was determined that inducing enantioselectivity via a chiral silane was not feasible.

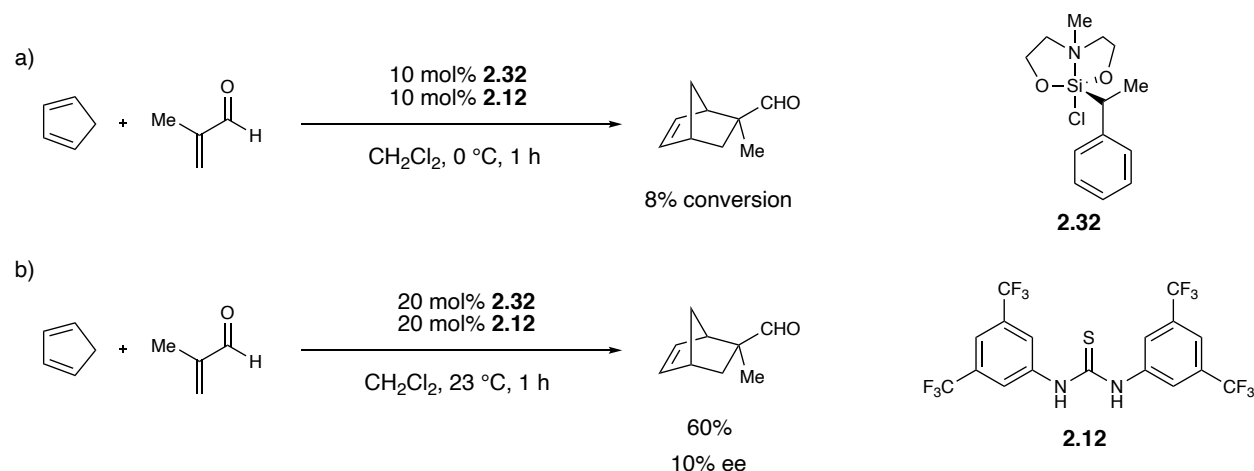


Figure 2.19: Chiral silane catalysis. a) No catalysis at 0 °C. b) Catalysis at room temperature.

Another option for inducing enantioselectivity was via the use of a chiral thiourea and the achiral silane **2.15**. The thioureas shown in Figure 2.20 were subsequently tested, however none of the thioureas used showed any promising level of enantioselectivity. The overall inability to induce enantioselectivity in this system is not surprising due to the highly reactive nature of the cationic silane and the inability to create an effective chiral environment around it.

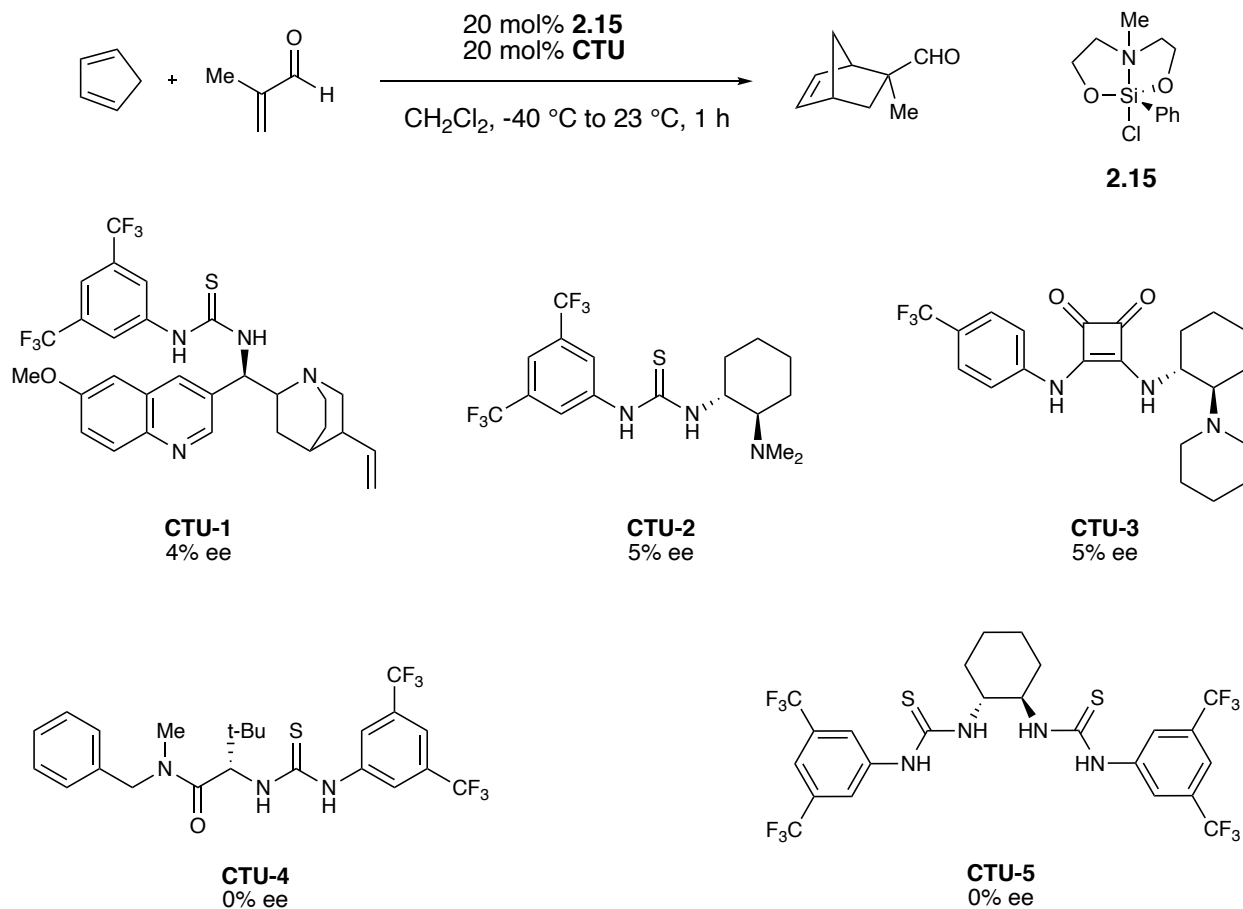


Figure 2.20: Chiral thiourea scope.

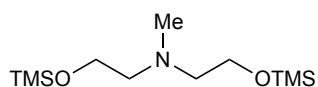
2.9. Summary and Conclusion

We have synthesized and explored the reactivity of a new silicon Lewis acid and a new silicon Lewis acid catalyst. Both the allyl silane reagent and the Diels-Alder catalyst are highly reactive species and show significant increased reactivity when combined with a thiourea, due to the formation of a stabilized silylium ion species. Thiourea catalysis was achieved in the context of the allylation reactions, and multiple strategies were employed to explore the lack of turnover at lower catalyst loadings in the Diels-Alder reaction. While efforts to induce enantioselectivity were not successful, ultimately, a new platform has been developed for silicon Lewis acid catalysis, by combining anion binding catalysis and silylium ion catalysis.

2.10 Experimental procedures

General Information

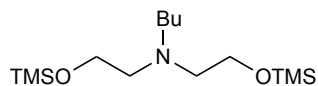
All reactions were carried out under an inert atmosphere of argon in flame-dried glassware with magnetic stirring unless otherwise indicated. Degassed solvents were purified by passage through an activated alumina column. Cyclopentadiene and methacrolein were purified immediately prior to use. All other reagents were purchased from commercial sources and used without further purification unless otherwise noted. Flash chromatography was performed with Silicycle SiliaFlash® P60 silica gel. Thin-layer chromatography (TLC) was carried out on glass backed silica gel TLC plates (250 nm) from Silicycle; visualization by UV, phosphomolybdic acid (PMA), or Potassium Permanganate (KMnO₄). ¹H, and ¹³C data were obtained using Bruker AVIII 500 (500 MHz) spectrometer and are reported in ppm. ¹H NMR spectra were internally referenced to CDCl₃ (7.26 ppm); ¹³C NMR spectra were internally referenced to CDCl₃ (77.23 ppm); Data are reported as follows: (bs= broad singlet, s = singlet, d = doublet, t = triplet, m = multiplet, dd = doublet of doublets, ddd = doublet of doublet of doublets, ddt = doublet of doublet of triplets, td = triplet of doublets; coupling constant(s) in Hz; integration).



2.2

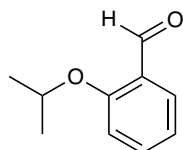
A flame dried flask, equipped with a stir bar, was charged with N-Methyldiethanolamine (310 mmol, 1 equiv) dissolved in CH₂Cl₂ (310 ml). The solution was cooled to 0 °C and TMSCl (775 mmol, 2.5 equiv) was added slowly. The reaction mixture was allowed to stir at room temperature for 4 hours. The reaction mixture was then cooled to 0 °C and methanol was added to quench unreacted TMSCl. The reaction was then diluted with CH₂Cl₂ and H₂O, and the organic layer was

extracted with ether. The organic layer was dried, filtered, concentrated to yield a pale yellow liquid (84%). Spectral data were in agreement with reported values.¹⁶



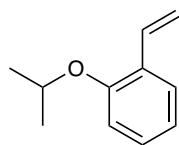
2.10

A flame dried flask, equipped with a stir bar, was charged with N-Butyldiethanolamine (310 mmol, 1 equiv) dissolved in CH_2Cl_2 (310 ml). The solution was cooled to 0°C and TMSCl (775 mmol, 2.5 equiv) was added slowly. The reaction mixture was allowed to stir at room temperature for 4 hours. The reaction mixture was then cooled to 0°C and methanol was added to quench unreacted TMSCl . The reaction was then diluted with CH_2Cl_2 and H_2O , and the organic layer was extracted with ether. The organic layer was dried, filtered, concentrated to yield a pale yellow liquid (96%). Spectral data were in agreement with reported values.¹⁷



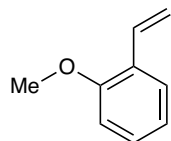
2.17a

Prepared as described in the literature.¹⁸ Spectral data were in agreement with reported values (99%).



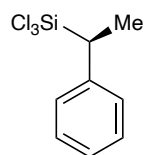
2.18a

Prepared as described in the literature.¹⁹ Spectral data were in agreement with reported values (76%).



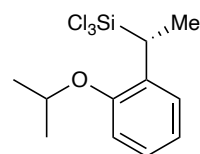
2.18b

Prepared as described in the literature.²⁰ Spectral data were in agreement with reported values (53%).



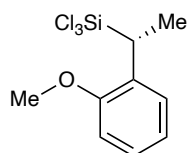
2.31

Prepared as described in the literature.²¹ Spectral data were in agreement with reported values (85%, 96% ee).



2.19a

Prepared using the same method as **2.31**. (67%). ¹H NMR (500 MHz, CDCl₃) δ 7.25 – 7.15 (m, 2H), 6.94 – 6.82 (m, 2H), 4.58 (m, 1H), 3.53 (q, 1H), 1.55 (d, 3H), 1.36 (t, 6H).

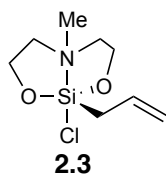


2.19b

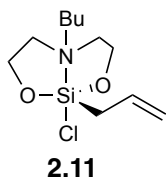
Prepared using the same method as **2.31**. (83%) ¹H NMR (400 MHz, CDCl₃) δ 7.29 – 7.20 (m, 2H), 7.02 – 6.93 (m, 1H), 6.89 (dt, 1H), 3.84 (d, 3H), 3.45 (qd, 1H), 1.60 – 1.53 (m, 3H).

General procedure for synthesis of quasisilatrane

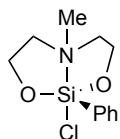
A flame dried pressure tube, equipped with a stir bar was charged with the bis(TMS protected) diethanolamine **2.2** or **2.10** (10 mmol, 1 equiv), dissolved in toluene (10 ml). The trichlorosilane (10 mmol, 1 equiv) was then added. The pressure tube was then tightly sealed and heated to 200 °C for 4 hours. The reaction mixture was then cooled to room temperature and the solvent was distilled off. The crude product was then sublimed or distilled.



Prepared using the general procedure with **2.2** and allyltrichlorosilane. The crude product was sublimed to afford white crystals (70%). ¹H NMR (400 MHz, CDCl₃) δ 5.94 (ddt, 1H), 4.98 – 4.91 (m, 1H), 3.98 – 3.90 (m, 1H), 3.90 – 3.79 (m, 2H), 2.78 (m, 2H), 2.65 (m, 2H), 2.52 (s, 2H), 1.91 (dt, 1H). ¹³C NMR (101 MHz, CDCl₃) δ 133.71, 114.90, 60.88, 55.69, 43.81, 26.63. ²⁹Si NMR (99 MHz, CDCl₃) δ -55.51.

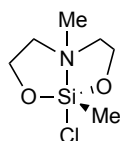


Prepared using the general procedure with **2.10** and allyltrichlorosilane. The crude product was then distilled to afford a clear liquid, which was then stored in the freezer to induce crystallization (72%). ¹H NMR (500 MHz, CDCl₃) δ 5.86 (ddt, 1H), 5.00 – 4.90 (m, 2H), 3.90 – 3.73 (m, 5H), 2.74 – 2.61 (m, 7H), 1.87 (dt, 2H), 1.53 – 1.43 (m, 2H), 1.31 – 1.23 (m, 2H), 0.91 (t, 3H). ¹³C NMR (126 MHz, CDCl₃) δ 133.12, 115.05, 61.87, 53.91, 52.06, 25.91, 25.54, 20.65, 14.05. ²⁹Si NMR (99 MHz, CDCl₃) δ -47.75.



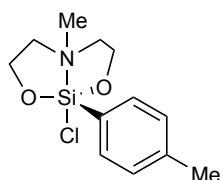
2.15

Prepared using the general procedure with **2.2** and trichlorophenylsilane. The crude product was then sublimed to afford white crystals (60%). ^1H NMR (500 MHz, CDCl_3) δ 7.48 (dd, 2H), 7.35 – 7.26 (m, 3H), 4.03 (dh, 4H), 2.85 (dt, 2H), 2.61 (dt, $J = 12.0, 5.8$ Hz, 2H), 1.63 (s, 3H). ^{13}C NMR (126 MHz, CDCl_3) δ 138.31, 130.23, 128.93, 128.15, 59.95, 54.06, 43.30. ^{29}Si NMR (99 MHz, CDCl_3) δ -70.07.



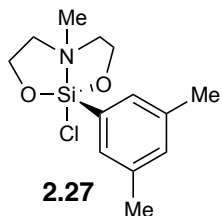
2.25

Prepared using the general procedure with **2.2** and trichloromethylsilane. The crude product was sublimed to afford white crystals (57%).



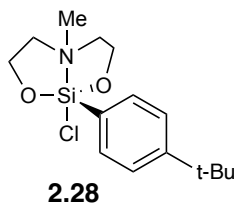
2.26

Prepared using the general procedure with **2.2** and p-tolyltrichlorosilane. The crude product was sublimed to afford white crystals (40%).

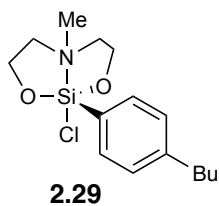


2.27

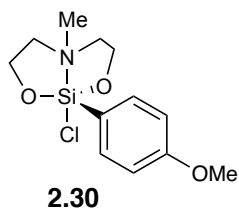
Prepared using the general procedure with **2.2** and trichloro(3,5-dimethylphenyl)silane. The crude product was sublimed to afford white crystals (27%).



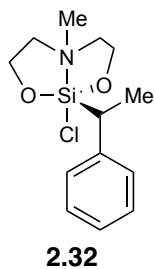
Prepared using the general procedure with **2.2** and (4-*tert*-butyl)phenyl)trichlorosilane. The crude product was sublimed to afford white crystals (28%).



Prepared using the general procedure with **2.2** and 4-butylphenyltrichlorosilane. The crude product was sublimed to afford white crystals (22%).



Prepared using the general procedure with **2.2** and trichloro(4-methoxyphenyl)silane. The crude product was sublimed to afford white crystals (24%).

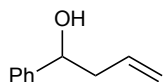


Prepared using the general procedure with **2.2** and **2.31**. The crude product was unable to be purified and was used as is.

General procedure for allylation reactions

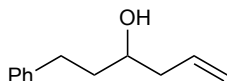
A flame dried vial, equipped with a stir bar, was charged with catalyst **2.11** (1.3 mmol, 1.3 equiv), Schreiner's thiourea **2.12** (1.3 mmol, 1.3 equiv), and dissolved in dry acetonitrile (1 mL). The aldehyde or ketone substrate (1.0 mmol, 1 equiv) was then added dropwise to the reaction mixture and stirred for 1 hour at room temperature. The reaction mixture was then cooled to 0°C and treated with *n*-Bu₄NF (1M in THF, 1.2 mL, 1.2 mmol, 1.2 equiv) and stirred for 1 hour at 0°C. The mixture was then passed through a silica plug with EtOAc and concentrated to give the crude product, which was purified by flash column chromatography.

1-phenylbut-3-en-1-ol



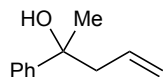
Prepared using the general procedure with benzaldehyde. Purified by silica gel flash column chromatography (0–10% EtOAc/Hexanes) to give the product as a clear oil (87% yield). Spectral data were in agreement with reported values.²²

1-phenylhex-5-en-3-ol



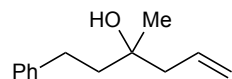
Prepared using the general procedure with hydrocinnamaldehyde. Purified by silica gel flash column chromatography (0–10% EtOAc/Hexanes) to give the product as a clear oil (63% yield). Spectral data were in agreement with reported values.²³

2-phenylpent-4-en-2-ol



Prepared using the general procedure with acetophenone. Purified by silica gel flash column chromatography (0–10% EtOAc/Hexanes) to give the product as a clear oil (91% yield). Spectral data were in agreement with reported values.²²

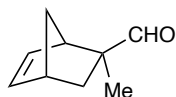
3-methyl-1-phenylhex-5-en-3-ol



Prepared using the general procedure with hydrocinnamaldehyde. Purified by silica gel flash column chromatography (0–10% EtOAc/Hexanes) to give the product as a clear oil (84% yield). Spectral data were in agreement with reported values.²⁴

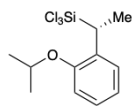
General procedure for the Diels-Alder reaction

2-methylbicyclo[2.2.1]hept-5-ene-2-carbaldehyde:

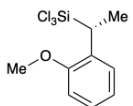
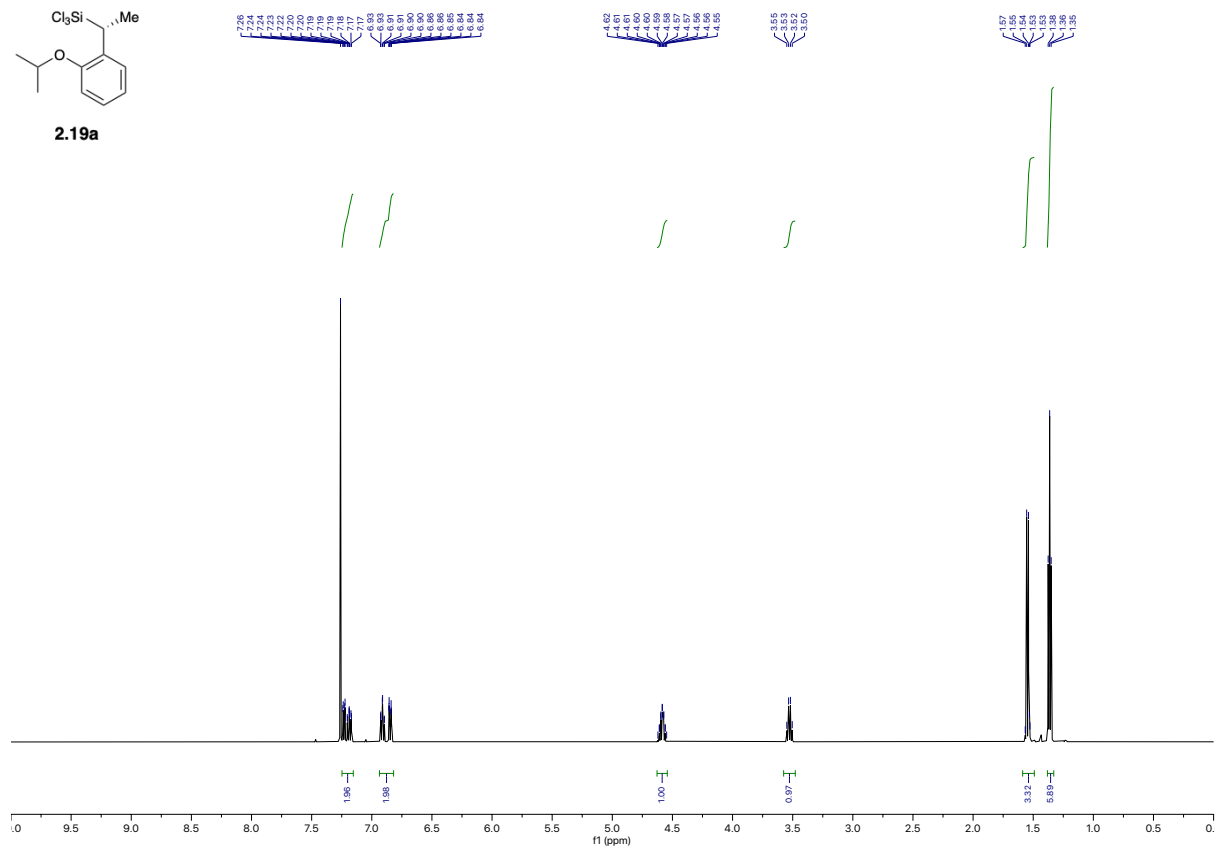


A flame dried vial, equipped with a stir bar, was charged with catalyst **2.15** (0.20 mmol, 0.20 equiv), Schreiner's thiourea **2.12** (0.20 mmol, 0.20 equiv), dissolved in dry CH₂Cl₂ (1 mL). Cyclopentadiene (0.25 mL, 3.8 mmol, 3.8 equiv) was added, followed by methacrolein (1.0 mmol, 1 equiv) dropwise. After 1 hour, the mixture was diluted with CH₂Cl₂ (1.0 mL) and quenched with a solution of 4:1 MeOH/H₂O (0.25 mL). The organic layer was washed with brine (1x1 mL), dried over Na₂SO₄, and concentrated. The residue was purified by flash chromatography (0-20%

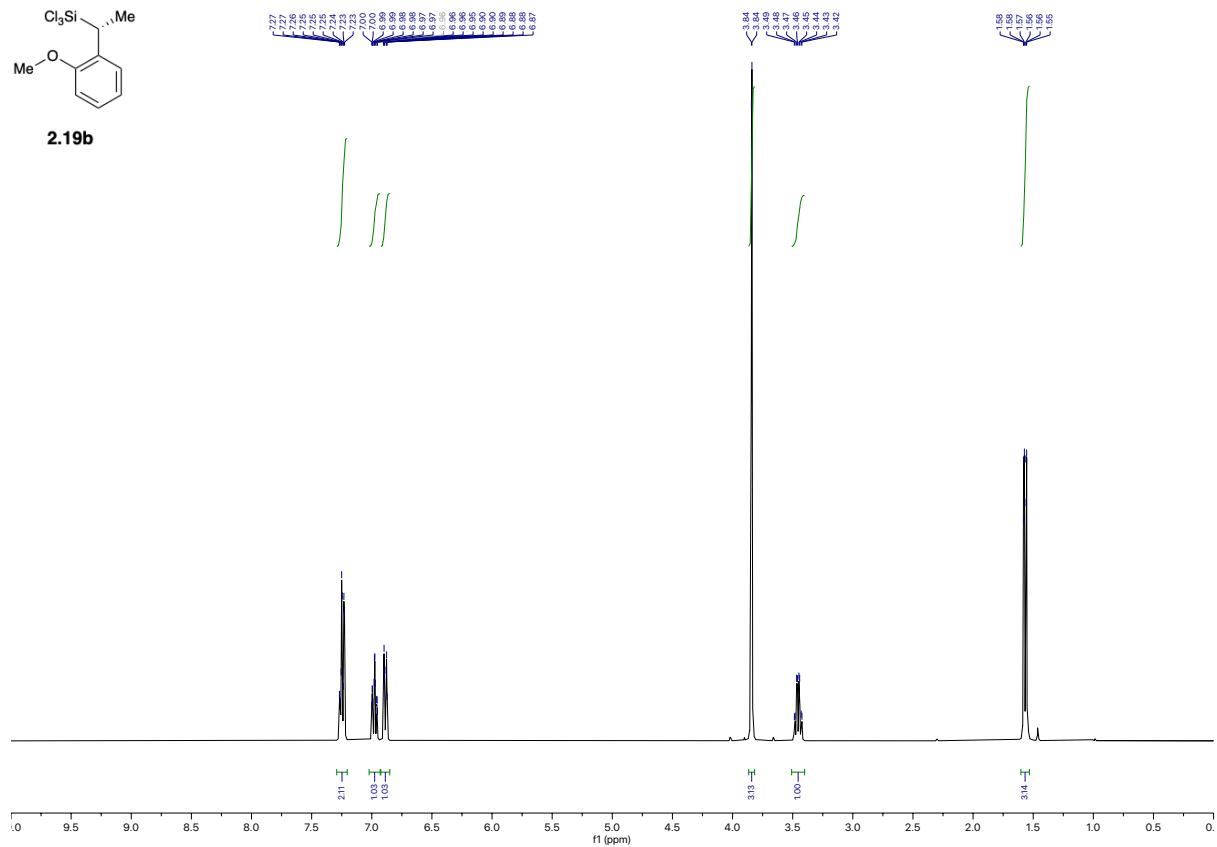
Et₂O/pentane) to afford the pure bicyclic aldehyde product. Spectral data for this compound matched previously reported data. The diastereoselectivity (exo:endo ratio = 6:1) was determined by ¹H NMR (400 MHz, CDCl₃) integration: δ 9.69 (s, 1H,CHO,exo), 9.39 (s, 1H, CHO, endo). The enantioselectivity was determined by reduction with NaBH₄ to the corresponding alcohol, conversion to the (R)-MTPA ester derivative, and ¹H NMR integration: ¹H NMR (500 MHz,CDCl₃) δ 4.34 (d, 1H, one of CH₂O-(R)-MTPA, major), 4.31 (d, 1H, one of CH₂O-(R)-MTPA, minor), 4.25 (d, 1H,one of CH₂O-(R)-MTPA, minor), 4.22 (d, 1H, one ofCH₂O-(R)-MTPA, major).

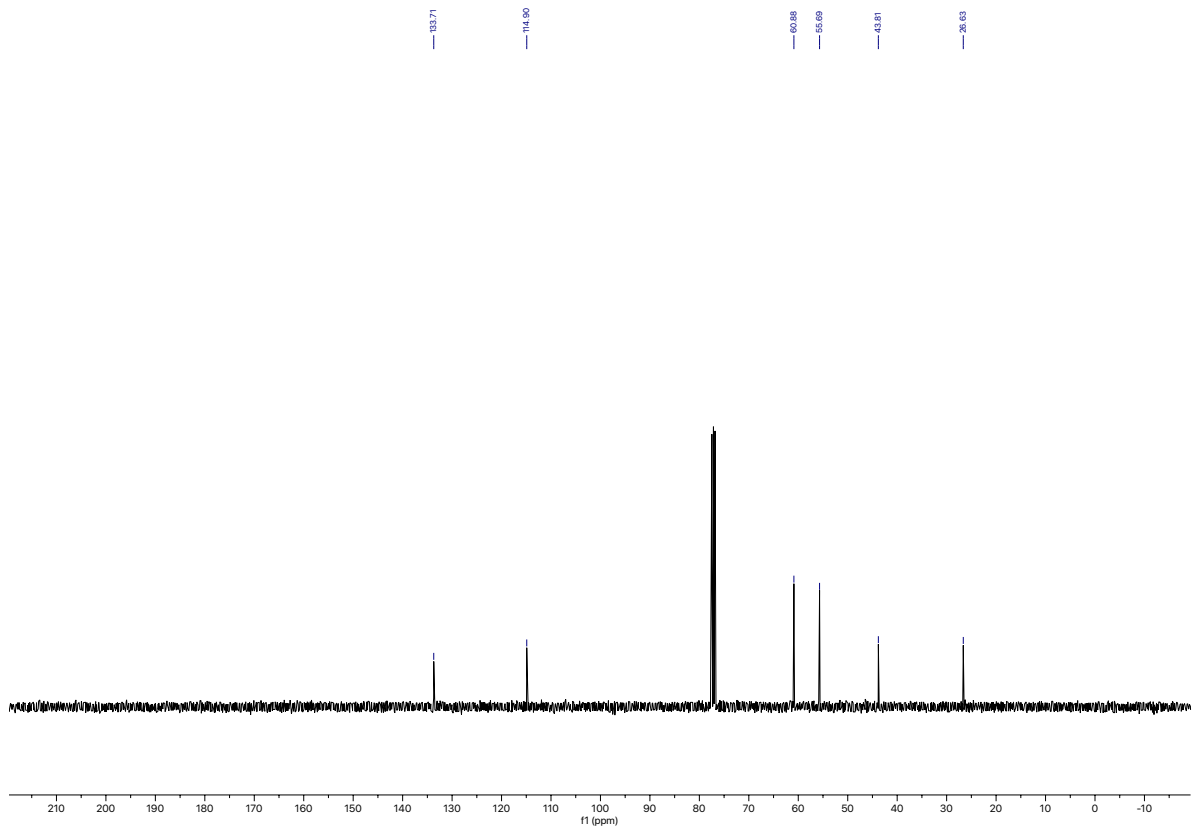
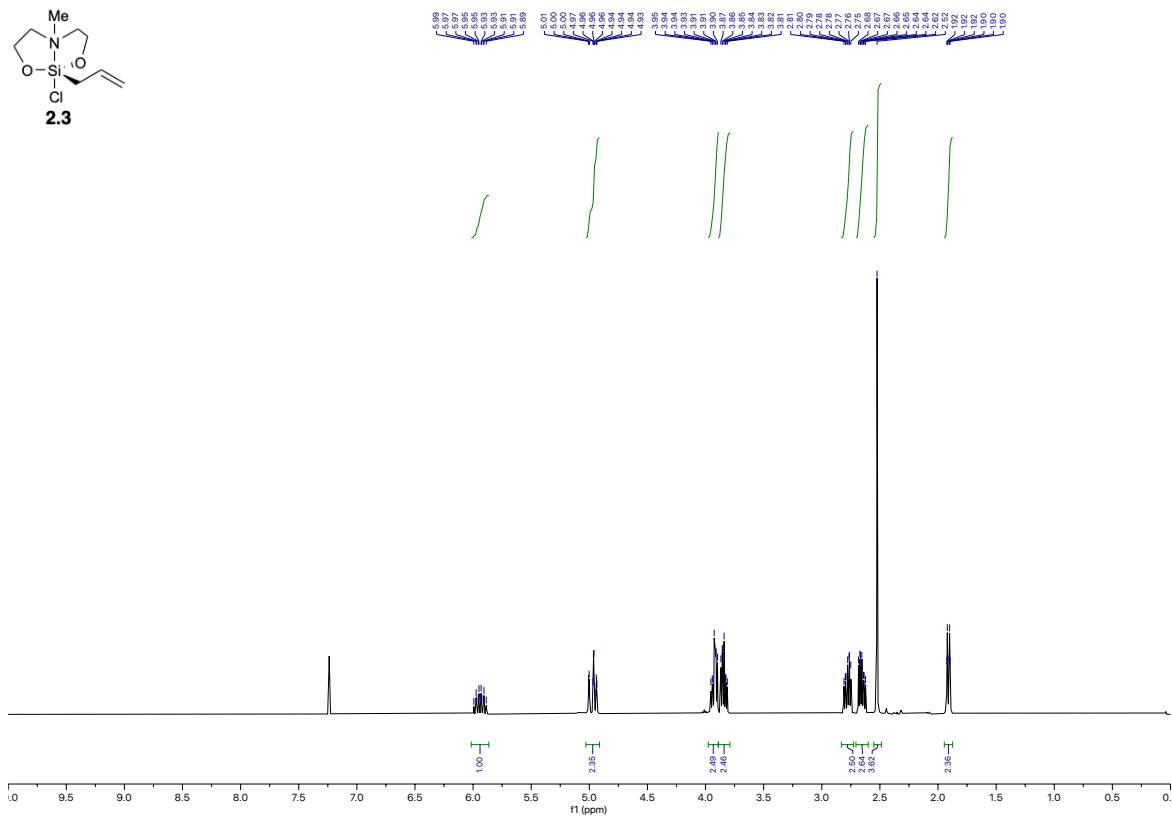
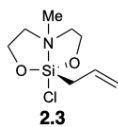


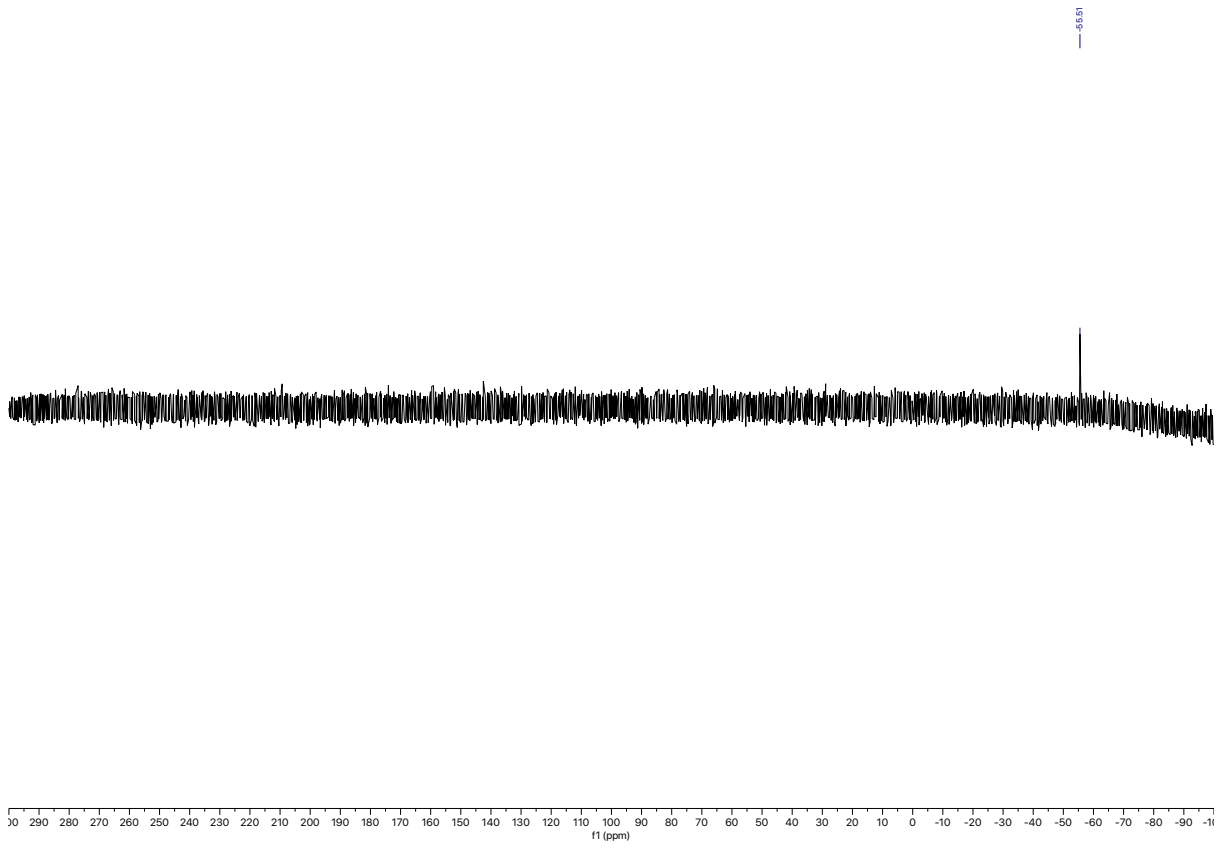
2.19a

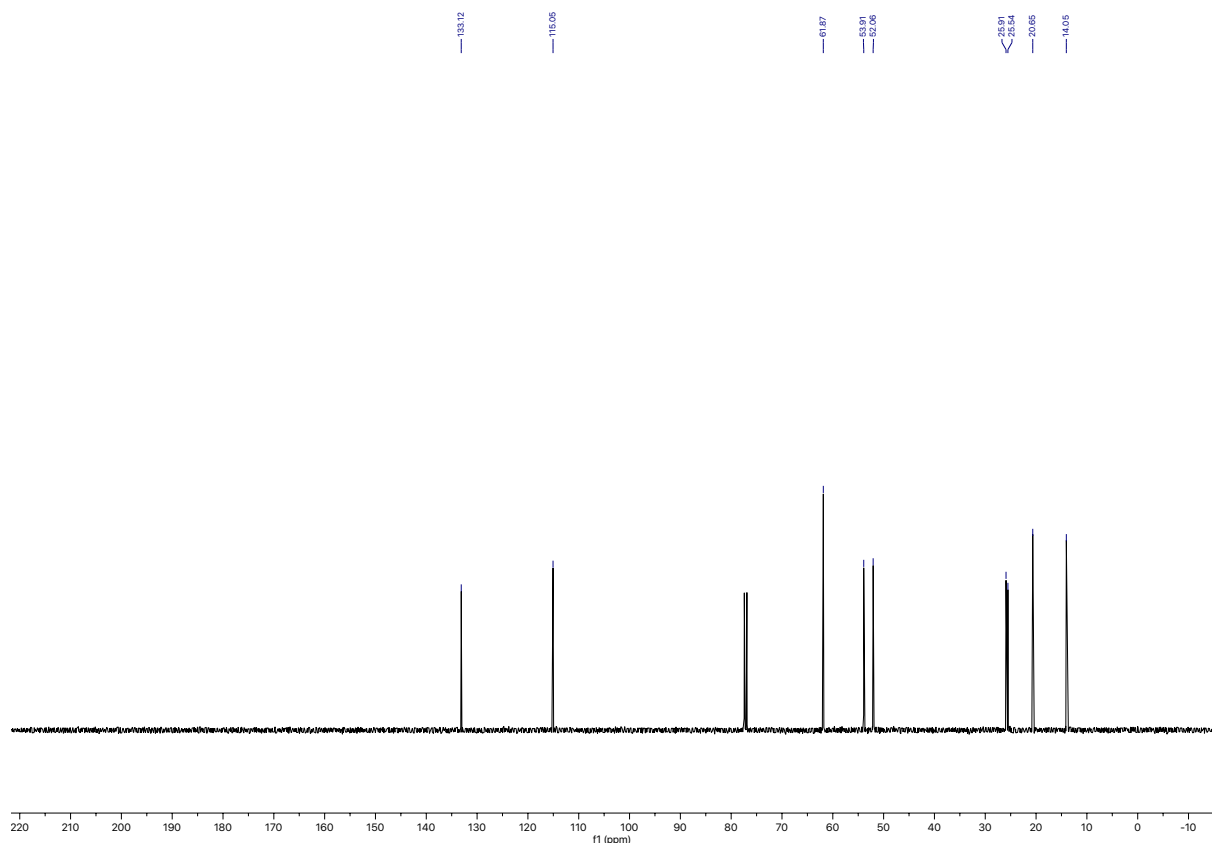
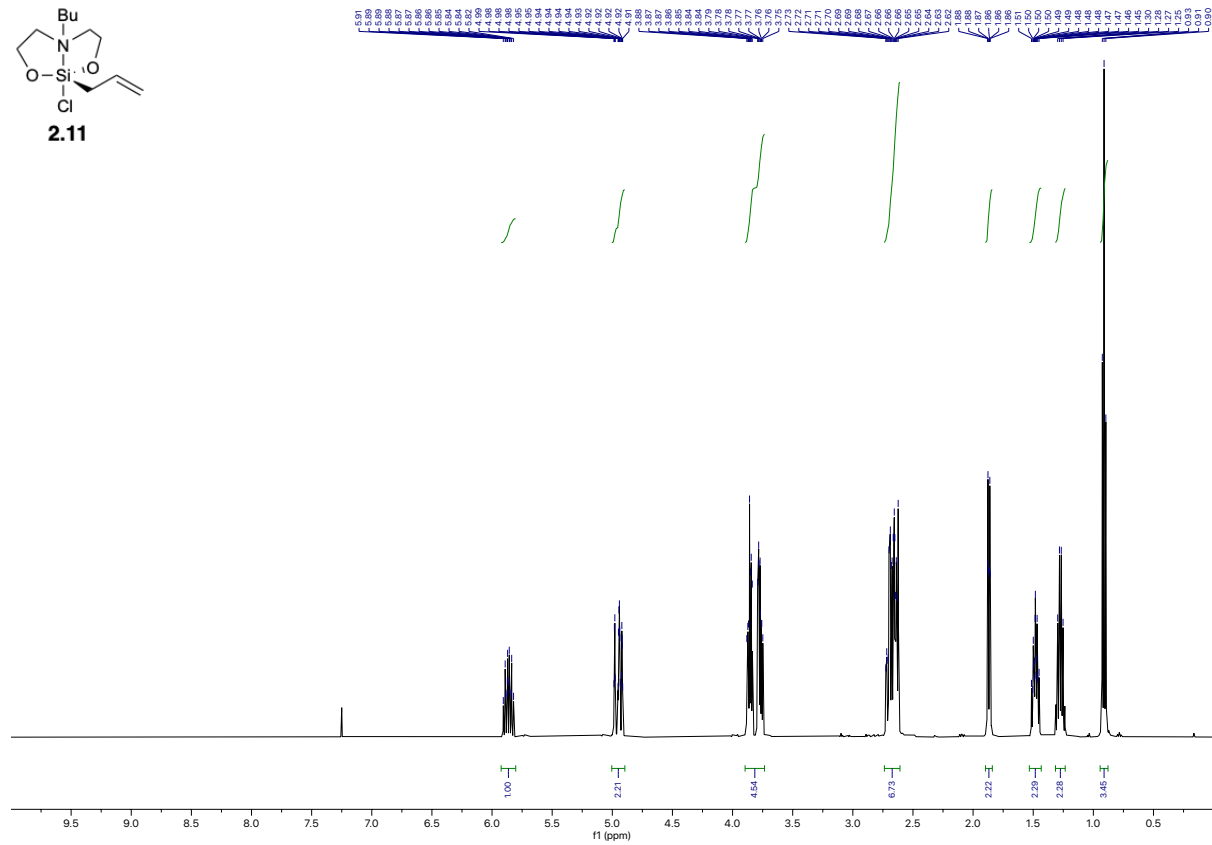
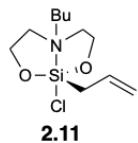


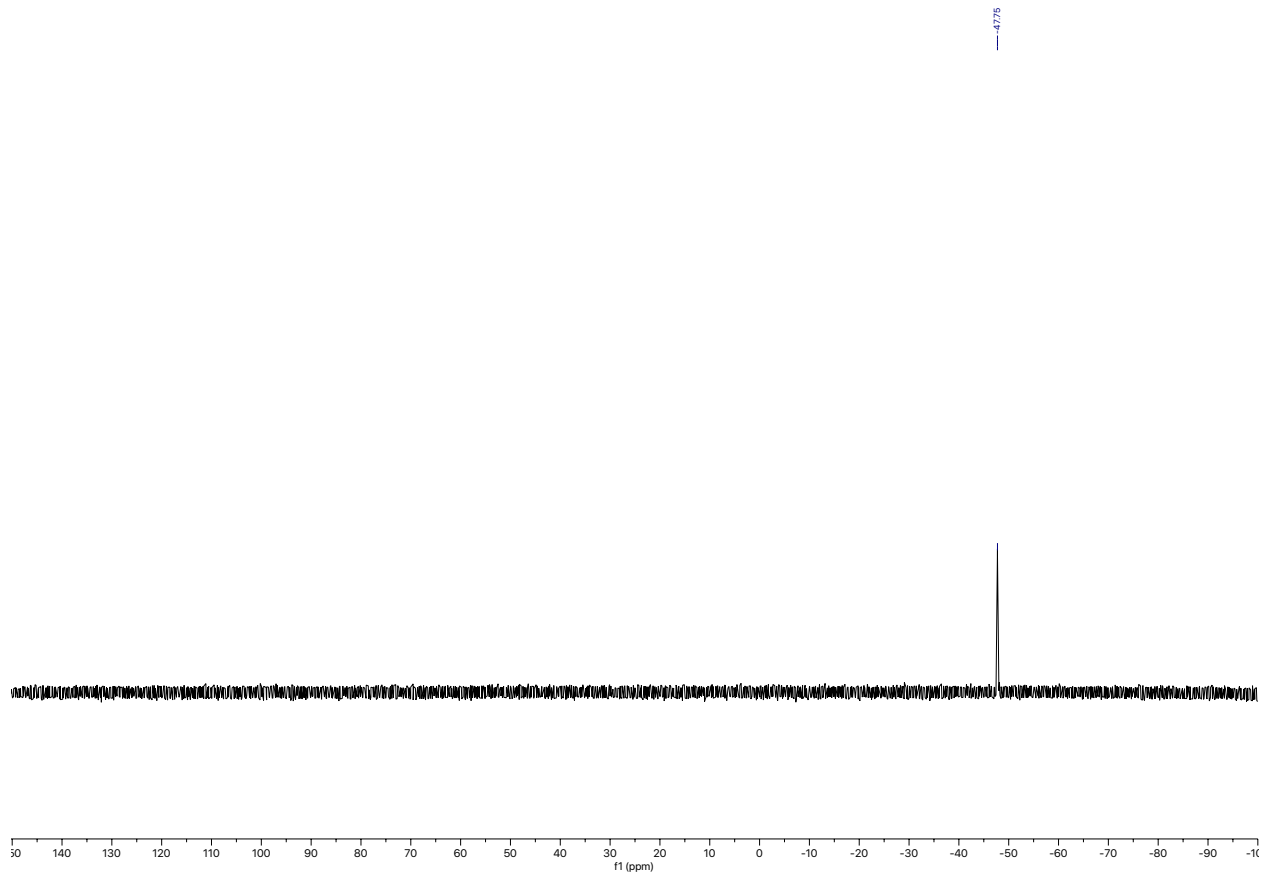
2.19b

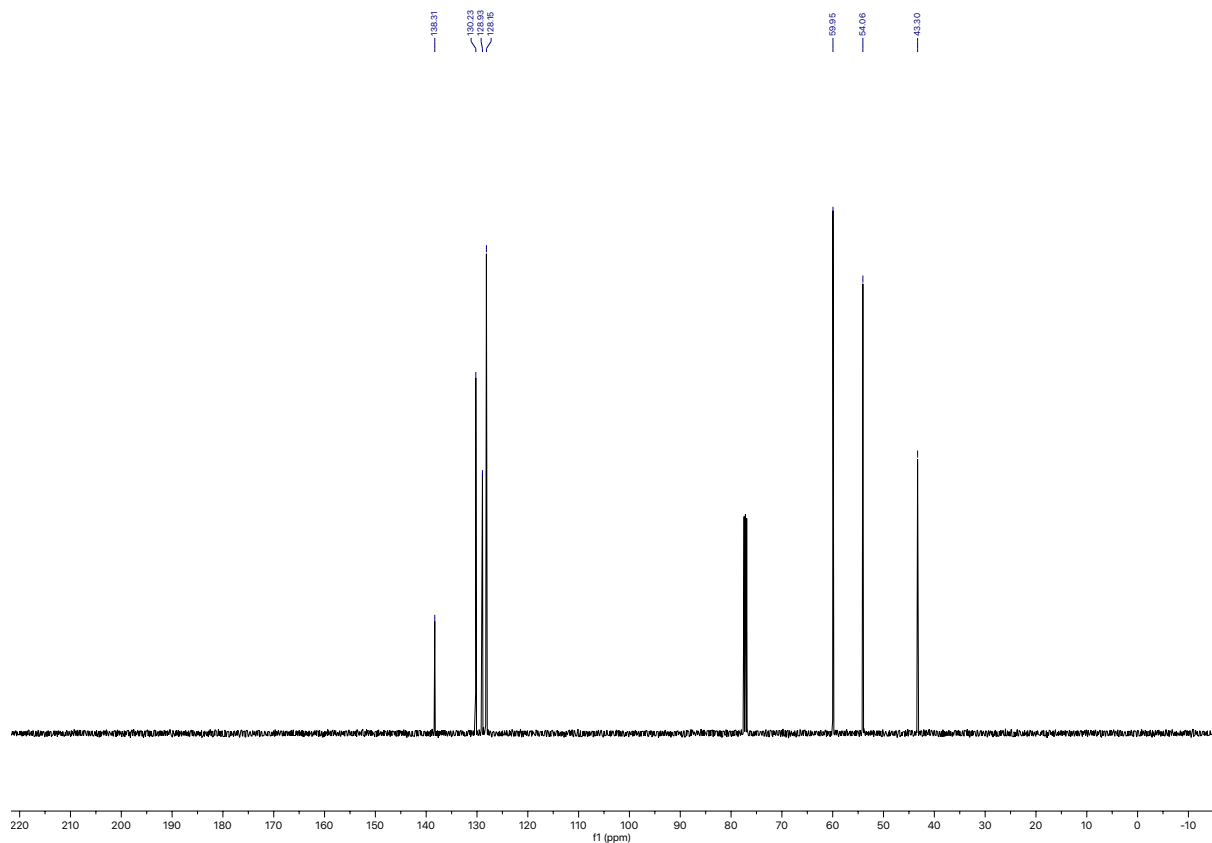
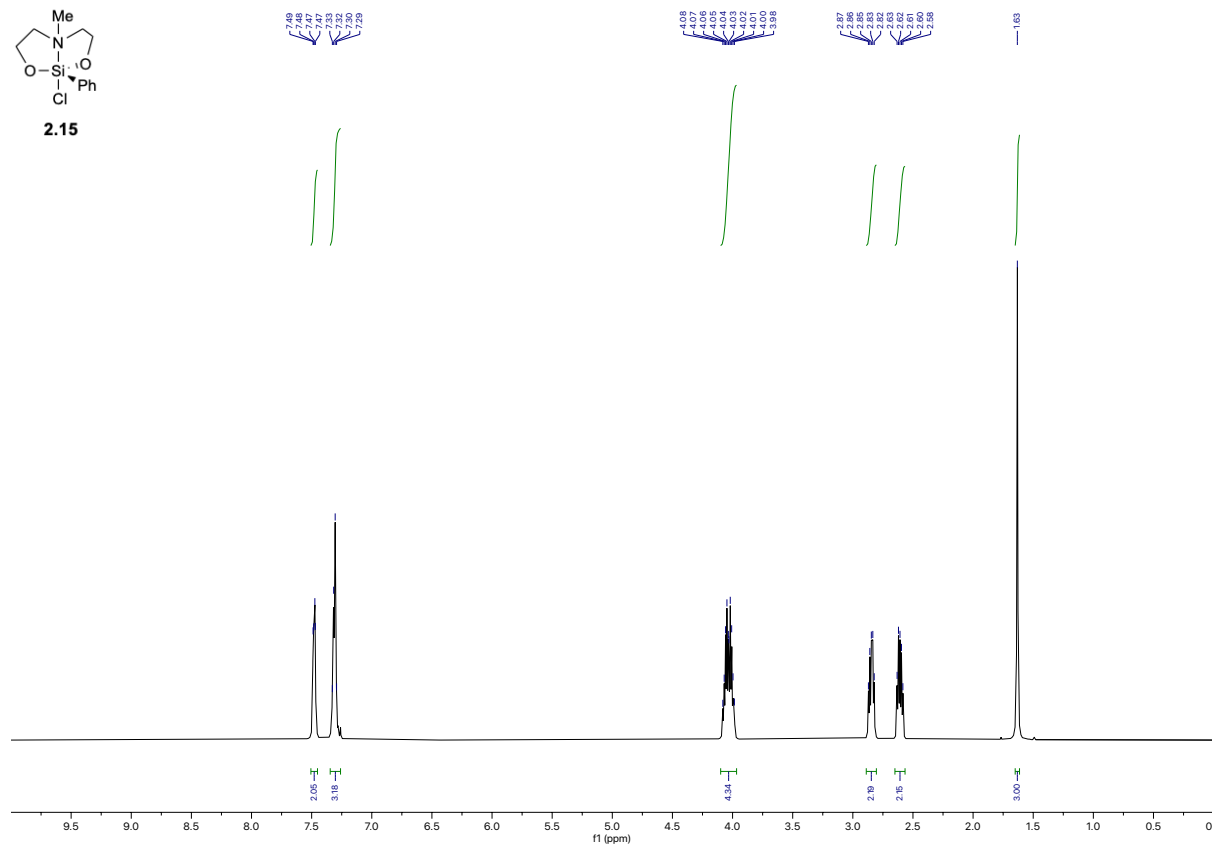
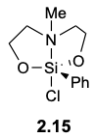


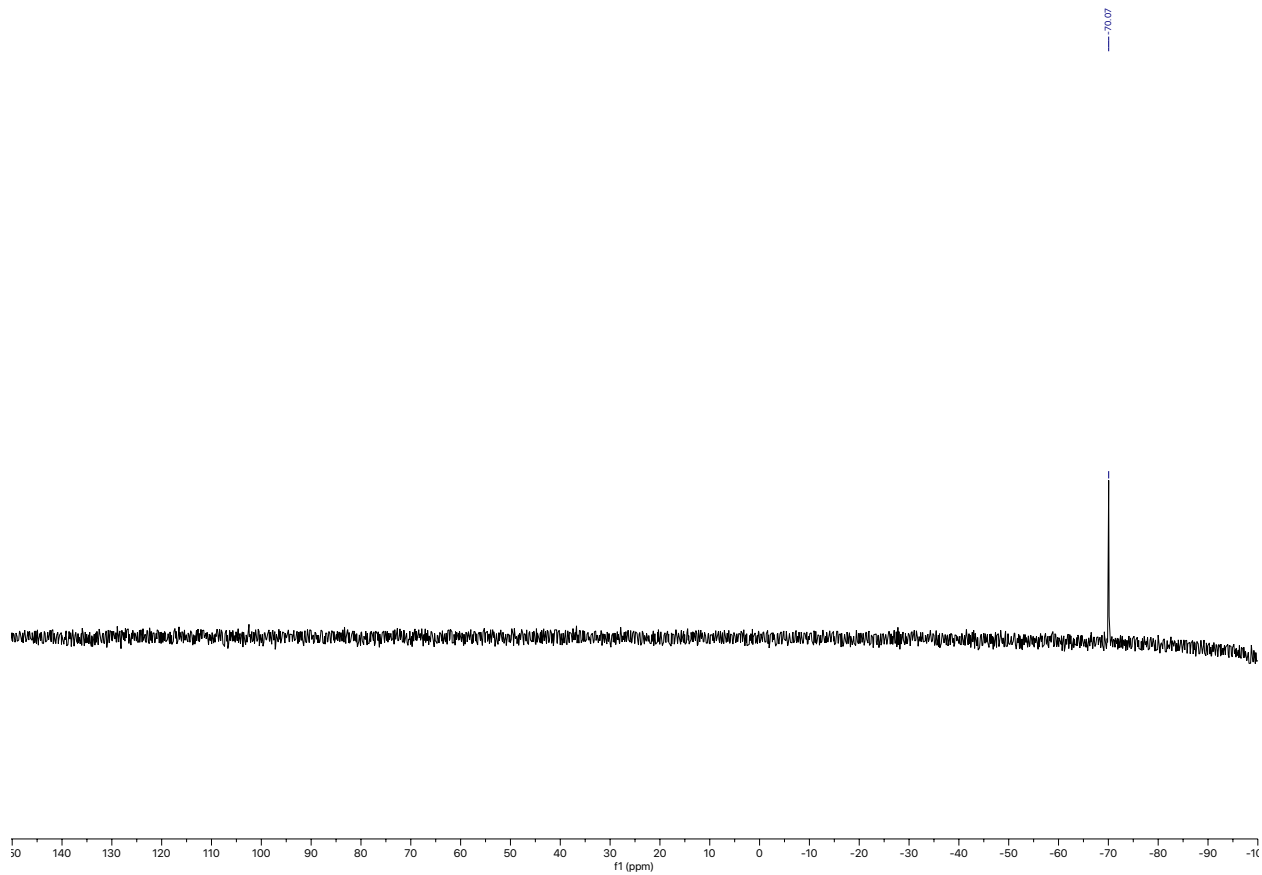


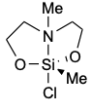




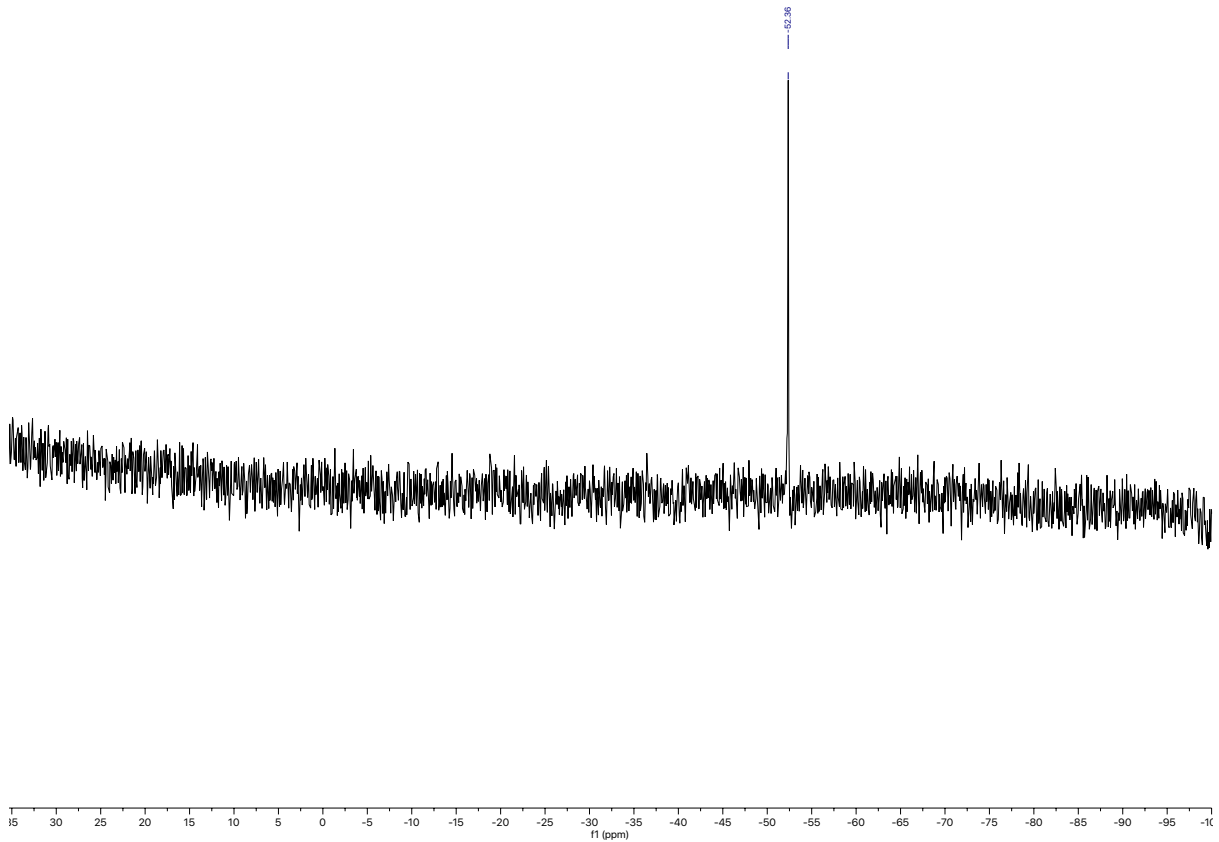
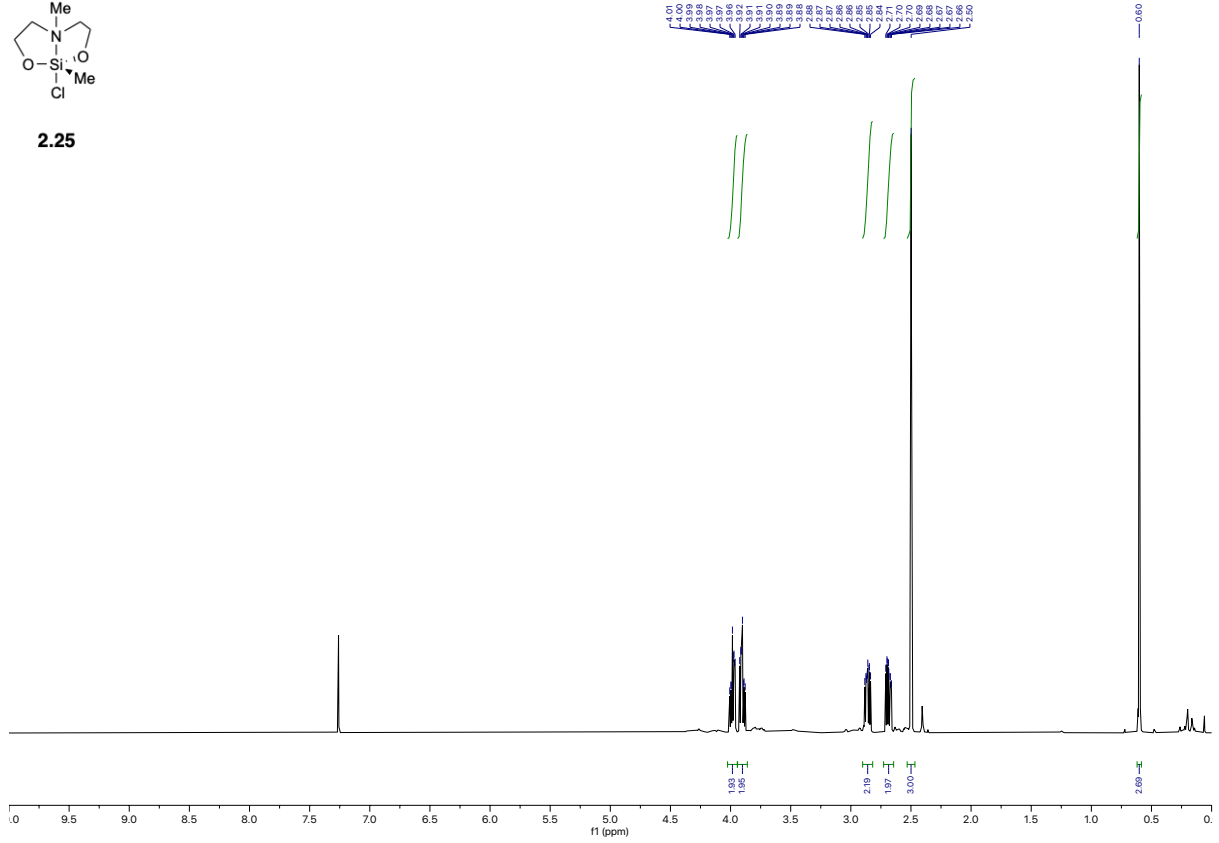








2.25



2.11 References

- ¹ Kubota, K.; Hamblett, C. L.; Wang, X.; Leighton, J. L. *Tetrahedron*. **2006**, 62, 11397-11401.
- ² Frye, C. L.; Vogel G. E.; Hall, J. A. *J. Am. Chem. Soc.* **1961**, 83, 996-997.
- ³ Pestunovich, V. A.; Kirpichenko, S. V.; Voronkov, M. G. *The Chemistry of Organic Silicon Compounds*, 2, John Wiley & Sons Ltd., **1998**, 1447-1537.
- ⁴ Verkade, J. G. *Acc. Chem. Res.* **1993**, 26, 9, 483-489.
- ⁵ Verkade, J. G.; *Coord. Chem. Rev.* **1994**, 137, 233-295.
- ⁶ Puri, J. K.; Singh, R.; Chahal, V. K. *Chem. Soc. Rev.* **2011**, 40, 1791-1840.
- ⁷ Attar-Bashi, M. T.; Eaborn, C.; Vencel, J.; Walton, R. D. *J. Organomet. Chem.* **1976**, 117, 87-89.
- ⁸ Skrypai, V.; Hurley, J. J. M.; Adler, M. J. *Eur. J. Org. Chem.* **2016**, 2207-2211.
- ⁹ Suen, L. M.; Steigerwald, M. L.; Leighton, J. L. *Chem. Sci.* **2013**, 4, 6, 2413-2417.
- ¹⁰ Urtane, I. P.; Zelchan, G. I.; Lukevics, E. Z. *Annorg. Allg. Chem.* **1985**, 520, 179-195
- ¹¹ Visco, M. D.; Attard, J.; Guan, Y.; Mattson, A. E. *Tetrahedron Letters*, **2017**, 58, 2623-2628.
- ¹² Taylor, M. S.; Jacobsen, E. N. *J. Am. Chem. Soc.* **2004**, 126, 10558.
- ¹³ Markovich, G.; Perera, L.; Berkowitz, M. L.; Cheshnovsky, O. *J. Chem. Phys.* **1996**, 105, 7, 15.
- ¹⁴ Jakab, G.; Tancon, C.; Zhang, Z.; Lippert, K. M.; Schreiner, P. R. *Org. Lett.*, **2012**, 14, 7, 1724-1727.
- ¹⁵ Ni, X.; Li, X.; Wang, Z.; Cheng, J. *Org. Lett.* **2014**, 16, 1786-1789.
- ¹⁶ Aldridge, S.; Calder, R. J.; Coombs, D. L.; Jones, C.; Steed, J. W.; Coles, S.; Hursthouse, M. B. *New. J. Chem.* **2002**, 26, 6, 677 - 686.
- ¹⁷ Robert, D.; Gawad, H. A.; Riess, J. G. *Bull. Soc. Chim. Fr.* **1987**, 3, 511 - 516.
- ¹⁸ McQuaid, K. M.; Long, J. Z.; Sames, D. *Org. Lett.* **2009**, 11, 14, 2972-2975.
- ¹⁹ Krause, J. O.; Nuyken, O.; Wurst, K.; Buchmeiser, M. R. *Chem. Eur.* **2004**, 10, 3, 777 - 784.
- ²⁰ Wipf, P.; Hopkins, C.R.; *J. Org. Chem.* **2001**, 66, 9, 3133-3139.
- ²¹ Jensen, J. F.; Svendsen, B. Y. la Cour, T. V.; Pedersen, H. L.; Johannsen, M. *J. Am. Chem. Soc.* **2002**, 124, 17, 4558-4559.
- ²² Das, M.; O'Shea, D. F. *J. Org. Chem.* **2014**, 79, 12, 5595-5607.
- ²³ Felpin, F. X.; Lebreton, J. *J. Org. Chem.* **2002**, 67, 9192-9199.
- ²⁴ Fandrick, K. R.; Fandrick, D. R.; Gao, J. J.; Reeves, J.T.; Tan, Z.; Li, W.; Song, J. J.; Lu, B.; Yee, N. K.; Senanayake, C. H. *Org. Lett.* **2010**, 12, 17, 3748-3751.

Chapter 3: Efforts Towards the Synthesis of New Silanes for High Bias-induced Bond Rupture Experiments

3.1. Introduction

The modern age of technology and the remarkable achievements made in recent decades are hallmarks of the current era. At the core of all these technologies and devices lies the molecular framework of bulk silicon which forms the basis of electronic circuits. These silicon semiconductors have charge transport abilities that can be turned on and off. However, as the size of modern age devices decrease, the size of the transistors found within them must also continue to decrease. Moore's Law states that the number of transistors found on a chip continues to double every 2 years. Eventually, the limit to how small these silicon transistors can be fabricated will be reached.¹⁻³ While smaller transistors can be developed, the on and off states of charge transport cannot reliably be controlled anymore as electrons start to flow between transistors via quantum tunneling.¹ A further complication is the financial cost and economic feasibility of producing such small transistors.⁴

One potential alternative to this miniaturization approach lies in chemical synthesis. Instead of cutting down silicon to nanoscale sizes, precise silicon transistors can be synthesized at the molecular level. This obviates the need for developing new and potentially expensive lithographic techniques, and relies instead on the use of readily available starting materials used in chemical synthesis. Additionally, chemical synthesis enables the exact size and composition of the silicon transistor to be controlled. The ability to tune conductance in single molecules will be crucial, analogous to the tuning of semiconductors from bulk silicon.⁵⁻⁸ Therefore, the field of single molecule electronics^{9,10} is a promising one, with high impact to the development of modern technologies.

3.2. Strained silanes as molecular junctions

The Leighton group has long been interested in strained silanes and the impact of strain on silicon Lewis acidity (see chapter 1). This has led to our group's interest in the conductance properties of such silanes and how charge transport can be impacted. Previously, the Leighton, Nuckolls, and Venkataraman groups have reported the conductance of a strained silacyclobutane attached via a phenylmethylsulfide as a linker, with two distinct conductance pathways corresponding to a low G pathway and a high G pathway (Figure 3.1a).¹¹ In this example, the low G state occurred via a sulfur-to-sulfur pathway while the high G state occurred via a sulfur-to-silacycle pathway, where there is direct contact between the Au electrode and the silicon center (Figure 3.1b). When the dimethyl acyclic silane analog and the silacyclopentane analog were tested, only a single low conductance was observed and the removal of a thioanisole linker showed no conductance, demonstrating that the second Au-S contact is necessary and that the Au-Si contact is a weak interaction (Figure 3.1c). Furthermore, the conductance pathways could be switched simply by altering the tip-substrate distance. This work represented the first example of obtaining conductance measurements from strained silanes.

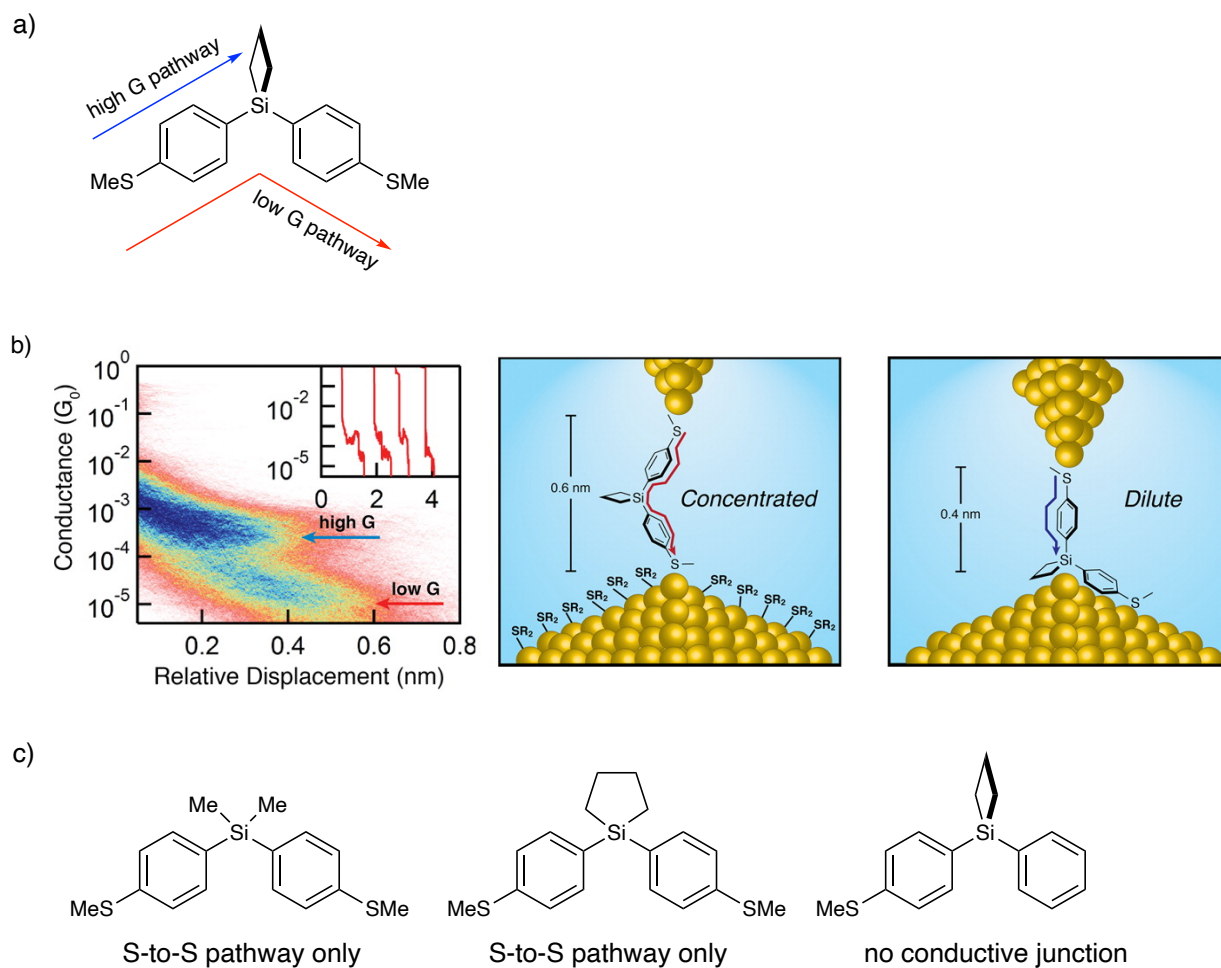


Figure 3.1: Conductance of a strained silacyclobutane. a) A high and low G pathway. b) Conductance histogram. c) Conductance in similar molecules.¹¹

Based on these results the Leighton group sought to further explore the silicon-electrode interaction and the effect of ring strain by examining the conductance properties of 1,2-disilaacenaphthenes.¹² The trans diastereomer **1** showed only a single low conductance peak while the cis diastereomer **2** showed both a high conductance peak and a low conductance peak (Figure 3.2).

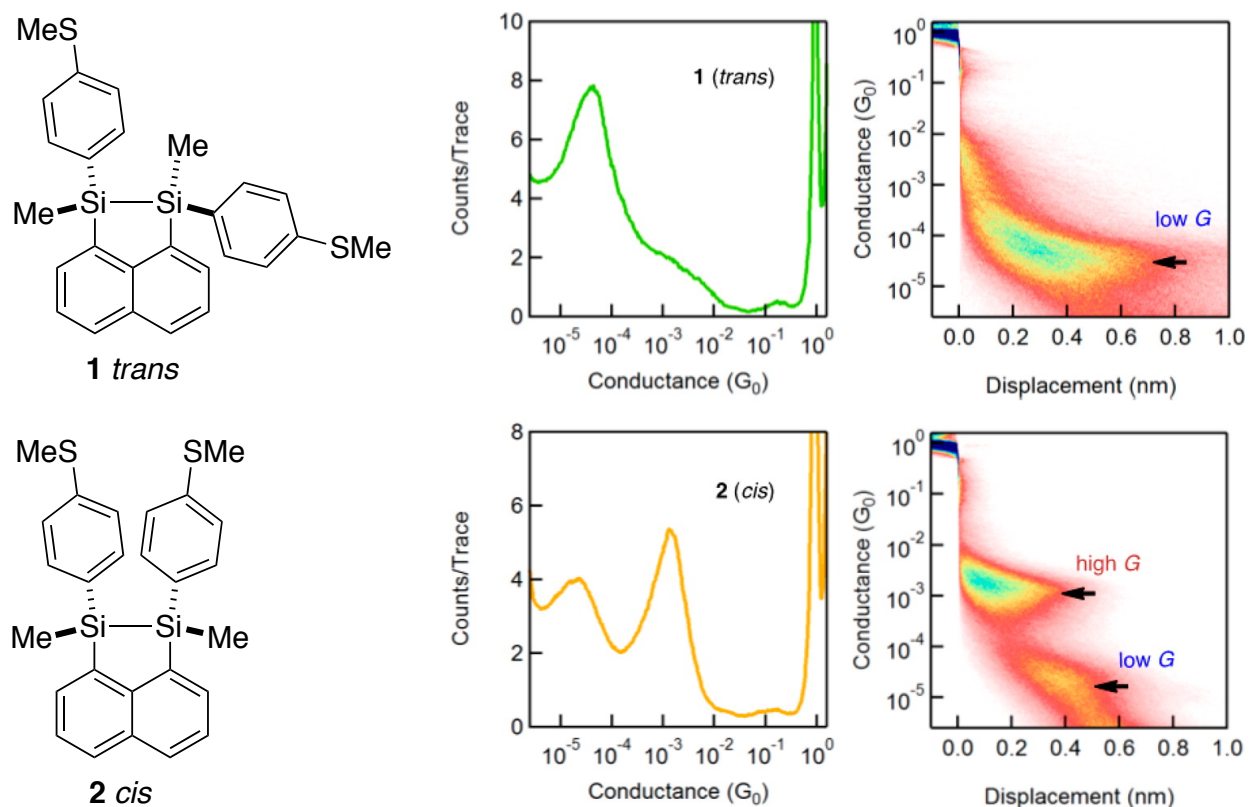


Figure 3.2: Conductance histograms for *cis* and *trans* 1,2-disilaacenaphthenes.

As in the case of the previously reported silacyclobutane, the low G pathway could be attributed to the sulfur-to-sulfur pathway in both diastereomers (Figure 3.3a). However, the high G pathway was found to be due to a rigid, bipodal binding arrangement of the sulfur linkers with the gold electrode, and direct Si-Si to Au interaction (Figure 3.3b). This type of binding arrangement would not be possible with the *trans* diastereomer. Furthermore, conductance switching characteristics were also examined, where the impact of a 0.2nm junction elongation on junction conductance was analyzed. A switch from the high- G state to the low- G state in **3.2** was observed in 35% of the traces, while the high- G junction was maintained in 11% of the traces, and broken 54% of traces.

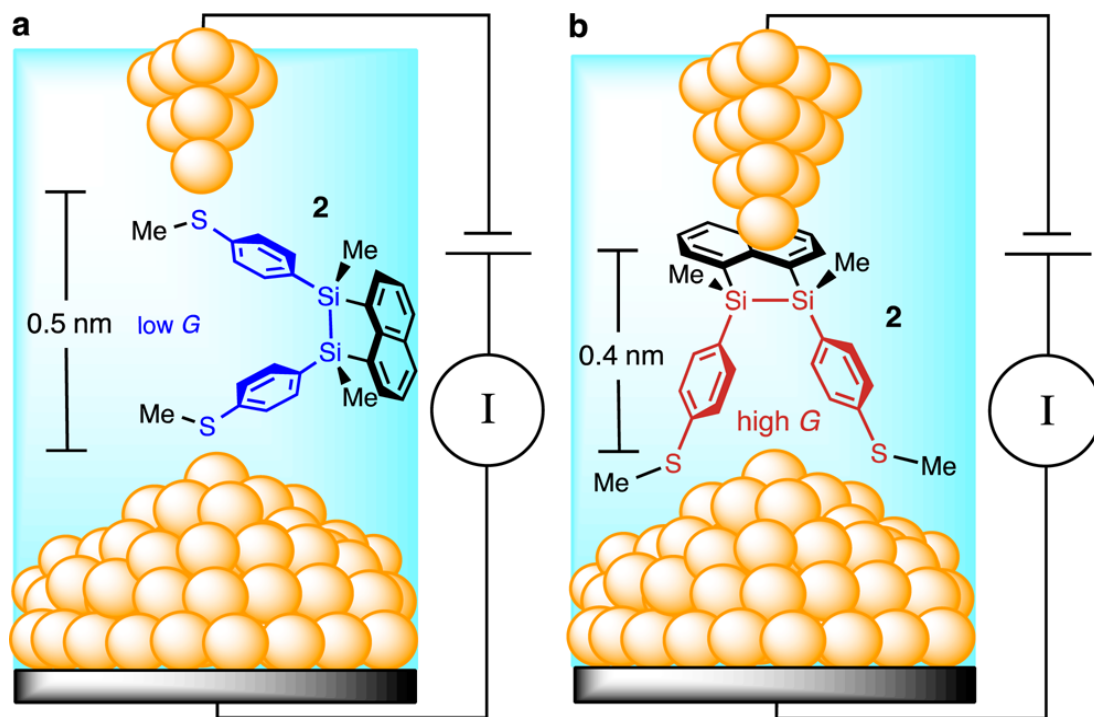


Figure 3.3: Two binding modes for 2. a) A low G sulfur-to-sulfur pathway. b) A high G bipodal binding of both thioanisole linkers, with direct Au contact with the Si-Si bond.

Motivated by our desire to further understand the effects of straining silicon in molecular junctions, the Leighton group has also investigated the high bias-induced bond rupture of strained silanes.¹³ Previously, Li et al. had developed a method to test electric field breakdown, by using thiols (-SH) as linkers, due to their covalent bond with the Au electrode and their ability to resist high voltage bias-induced rupture, whereas linkers such as methylsulfides (-SMe) that formed dative contacts with the electrode were more prone to rupture after applying a voltage bias.¹⁴ Furthermore, it was shown that molecules containing Si-Si bonds could be ruptured above 1 V, while molecules containing Si-C bonds could be maintained at high voltages. However, these results did not eliminate the possibility of bond breakage at other locations.

Using the method developed by Li et al. the Leighton group investigated the high-bias induced bond rupture of 1,2-disilaacenaphthenes equipped with thiol linkers. The choice of this system was based on the fact that once the Si-Si bond was broken, unlike the previously tested

molecules, the molecular junction would not be broken and could still be maintained via an alternate conductance pathway (Figure 3.4). Furthermore, the strain present in the system allowed for the weakening of the Si-Si bond and therefore a more selective bond rupture.

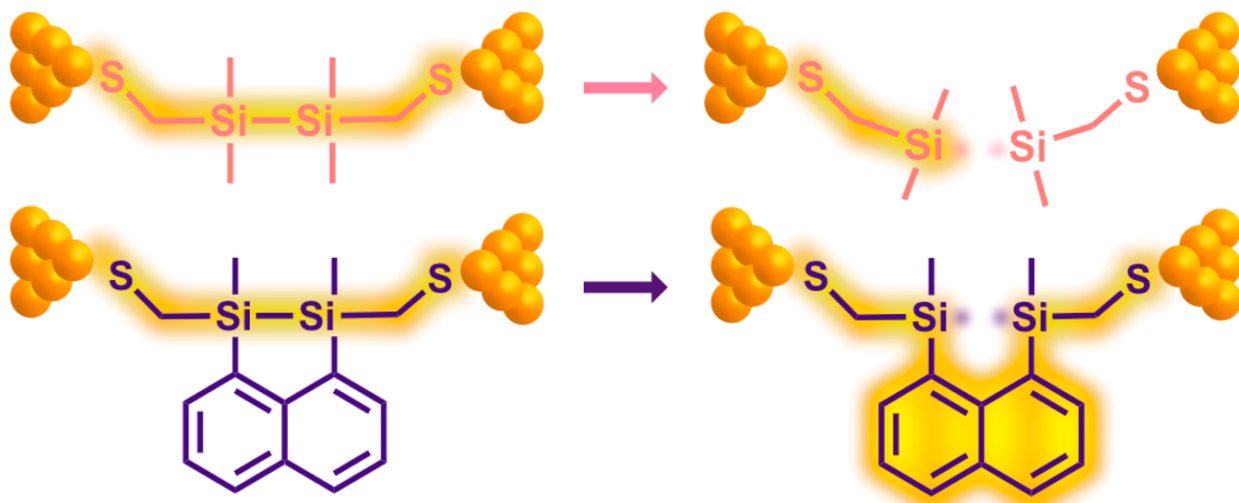


Figure 3.4: An alternate conductance pathway in the disilaacenaphthene system.¹³

It was indeed observed that unlike the acyclic system **Si2** where the conductance falls to the noise floor after bond rupture, in the cyclic **Si2Naph** system, a second conductance was measured (Figure 3.5).

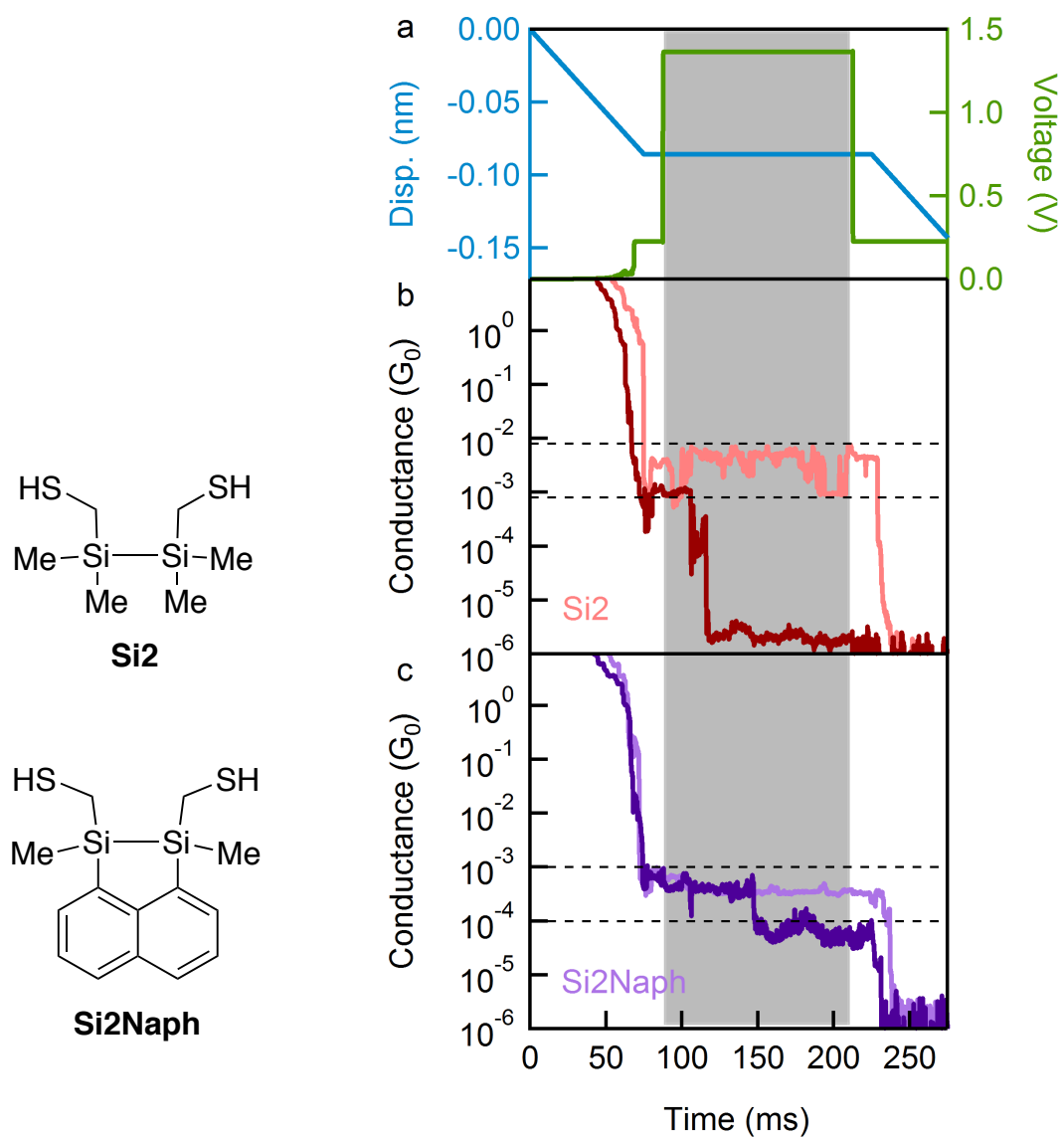


Figure 3.5: Conductance in the Si2 and Si2Naph system. (a) Piezo displacement (blue; left) and applied voltage (green; right) plotted against time in each pull-hold-pull measurement. (b) and (c) Two sample traces measured with Si2 (Si2Naph) showing a molecular junction sustain (light color) or rupture (dark color) under a 0.9 V applied bias.¹³

To show that **Si2Naph** could conduct through the naphthalene via the σ system, a 1,8-disubstituted naphthyl disulfide was synthesized and its conductance measured, confirming that charge transport could be maintained after rupturing the Si-Si bond.

3.3. New motifs for high bias-induced bond rupture experiments

Motivated by our previous results, the Leighton group sought to further understand the nature of the intermediates in the high bias-induced bond rupture of strained silanes. The individual conductance traces for **Si2Naph** seen in Figure 3.5 showed the persistence of the ruptured species even after the voltage was reduced and the junction only broke when the electrodes were pulled further apart. This raised the question of why the Si-Si bond did not reform after the voltage was reduced. One possible explanation for this is that the singlet diradical that is formed undergoes rapid intersystem crossing to the triplet state that may have a longer lifetime. This is precedented in the work of Sekiguchi who had generated bis(silyl radicals) on a benzene system and had found that the para isomer exists in the singlet and fully conjugated planar state, while the meta isomer exists as an isolable triplet with the silyl radicals orthogonal to the benzene π -system (Figure 3.6).¹⁵ Furthermore, for both the meta and para isomers, the bis(silyl radicals) could be converted to the dihydrides after treatment with 1,4-cyclohexadiene.

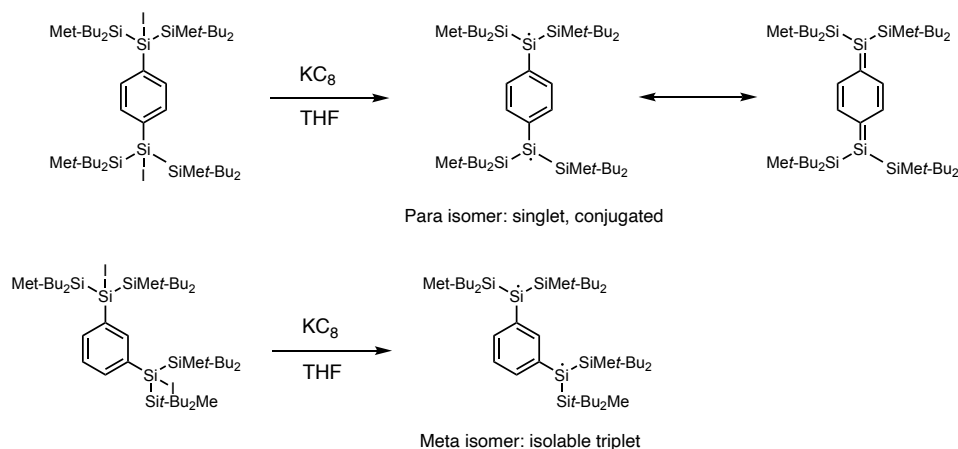


Figure 3.6: Sekiguchi's bis(silyl radicals) on a benzene core.

Considering that our 1,2-disilaacenaphthene system had the silyl radicals on the 1 and 8 positions of the naphthalene ring, this system could be considered analogous to Sekiguchi's meta

isomer. We therefore wondered if we could design a system analogous to Sekiguchi's para isomer and we settled on the highly strained benzodisilacyclobutene system **3.1** (Figure 3.7).

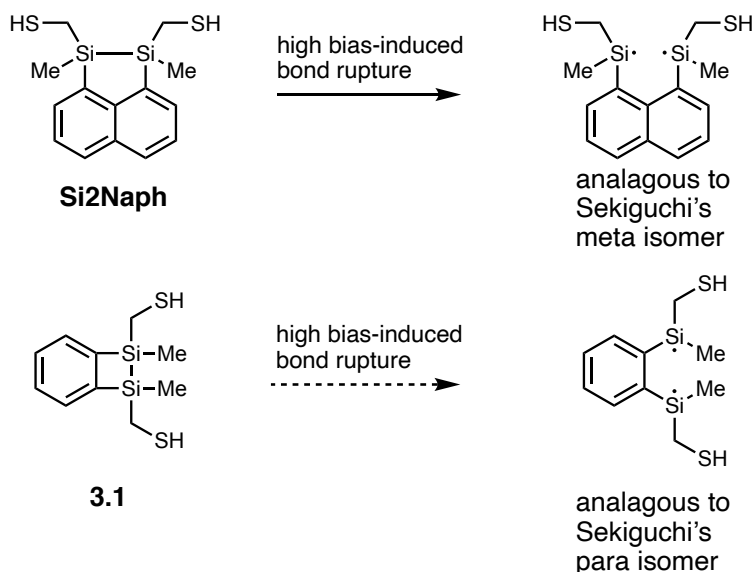


Figure 3.7: An analogous system to Sekiguchi's para isomer.

Ishikawa had developed methods for the synthesis of these strained benzodisilacyclobutenes, albeit with only alkyl groups attached to the silicon atoms.¹⁶ Our plan was to use this chemistry, and our previously developed conditions to install a CH₂SH linker on the benzodisilacyclobutene system, which would allow us to investigate the high bias-induced bond rupture of this system (Figure 3.8).

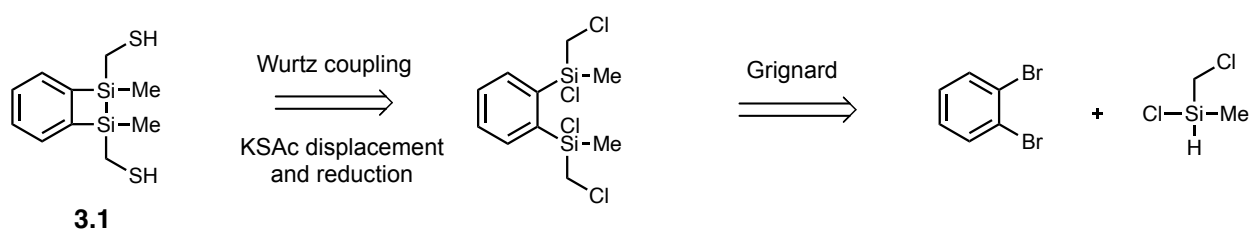


Figure 3.8: Retrosynthetic analysis for the synthesis of benzodisilacyclobutene 3.1.

The diradical generated would be expected to be a conjugated singlet considering their ortho relationship, in direct analogy to the para isomer developed by Sekiguchi, and it would be interesting to see how conjugation affects the conductance of the diradical. We would also attempt

to trap the diradical in the presence of 1,4-cyclohexadiene to form the dihydride, both in solution and in the single molecule conductance experiment, and we would try to characterize the conductance of the dihydride. It would be expected that the dihydride would have a different conductance compared to the diradical, as the diradical would no longer be conjugated.

In addition to the benzodisilacyclobutene system, we also planned to synthesize and study the high bias-induced bond rupture of ferrocenyl disilane **3.2** (Figure 3.9). Ishikawa had reported the synthesis of the tetramethyl ferrocenyl disilane,¹⁷ and using our previously developed conditions, **3.2** should be readily accessible. This system is very different from the 1,2-disilaacenaphthene system and benzodisilacyclobutene system in that any conductance after the Si-Si bond is ruptured must pass through the ferrocene and it would be interesting to characterize this conductance. Similarly, questions about the nature of the diradicals formed, whether they are electronically coupled, and how the ferrocene influences the probability of bond rupture are also important.

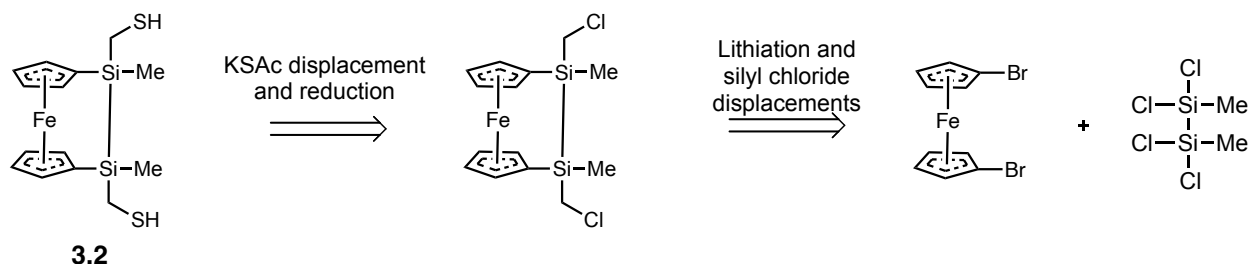
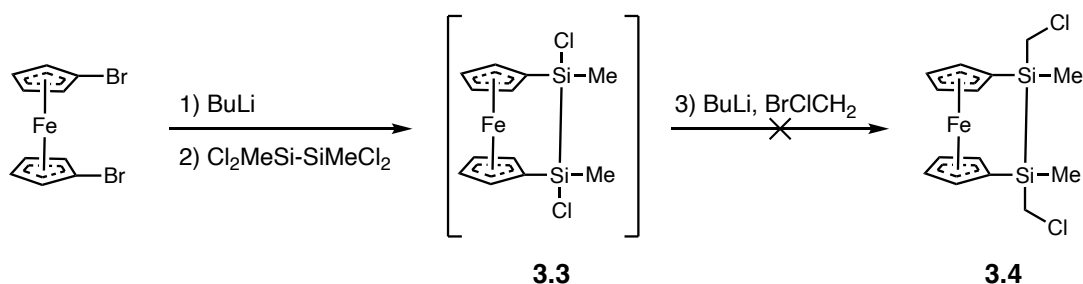


Figure 3.9: Retrosynthetic analysis for the synthesis of ferrocenyl disilane **3.2**.

3.4. Initial synthesis efforts to form the chloromethyl silanes

We decided to proceed with the synthesis of **3.2** initially using the same conditions our group had developed for the synthesis of 1,2-disilaacenaphthenes.¹⁸ We treated 1,1'-dibromoferrocene with butyllithium and commercially available 1,1,2,2-tetrachloro-1,2-dimethyldisilane to generate the dichlorodisilane **3.3** in situ, followed by the addition of more butyllithium and bromochloromethane to generate the chloromethyldisilane **3.4** (Scheme 3.1).



Scheme 3.1: Synthetic route to access 3.4.

Reaction monitoring by NMR showed consumption of the starting dibromoferrocene, and peaks corresponding to **3.4**. Unfortunately, despite significant isolation attempts, **3.4** was unable to be isolated. Multiple purification methods were employed, including crystallization and chromatography using different stationary phases. It appeared that any product that was forming, was degrading during purification. In order to confirm that these ferrocenyl disilanes could be isolated, the known tetramethyl disilane **3.5** was successfully synthesized and isolated by silica gel chromatography (Figure 3.10).

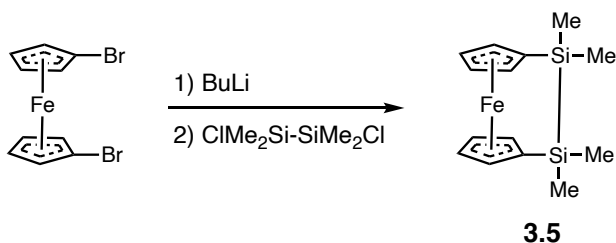
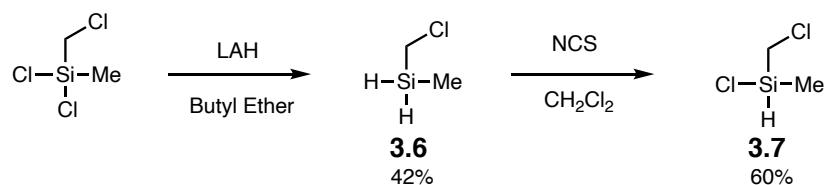


Figure 3.10: Successful formation of the tetramethyl ferrocenyl disilane.

Considering our initial difficulties, we decided that the primary chloride might not be a viable route to access our desired disilanes. However, before trying an alternative route, we looked at the benzene system to investigate whether the primary chloride would be problematic here too, in which case we could address this issue on both the ferrocenyl and benzene systems simultaneously. Commercially available dichloro(chloromethyl)methylsilane was reduced with lithium aluminum hydride to generate the dihydride **3.6**, which was then monochlorinated with N-chlorosuccinimide to generate chlorosilane **3.7** (Scheme 3.2).



Scheme 3.2: Synthesis of key intermediate 3.7.

However, when 1,1-dibromobenzene was treated with **3.7** in the presence of magnesium, the double Grignard product **3.8** was unable to be formed or isolated (Figure 3.11).

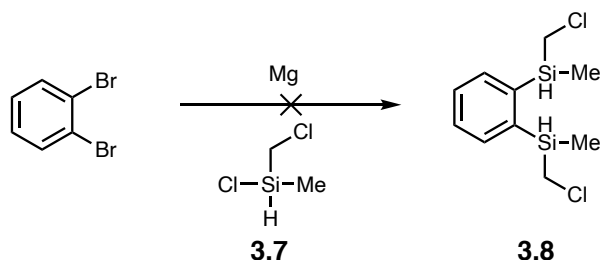


Figure 3.11: Synthesis attempt of 3.8 via a double Grignard.

To confirm that we could indeed form a 1,2-disilylbenzene, we treated 1,2-dibromobenzene with chlorodimethylsilane and successfully formed the Grignard product (Figure 3.12). Once again, it appeared that the primary chloride was an issue and that we would need an alternative solution.

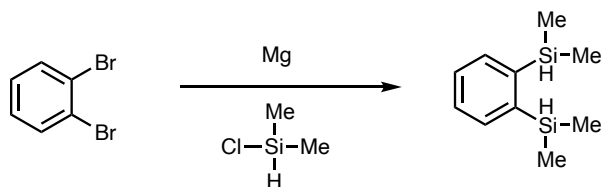
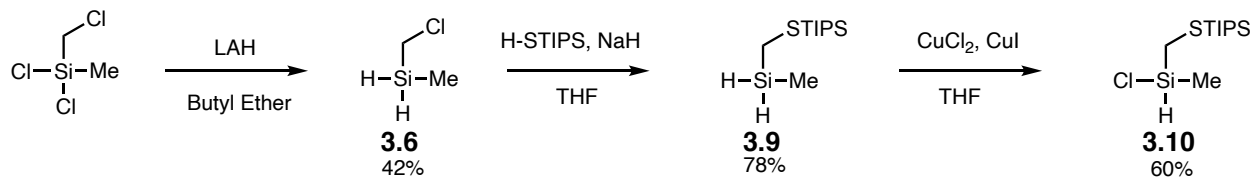


Figure 3.12: Successful formation of the tetramethyl double Grignard product.

3.5. Attaching a protected thiol as a chloromethyl alternative

Due to the complications associated with forming the chloromethyl silanes, we hypothesized it would be possible to displace the chloride with a protected thiol, which could then be deprotected at a later stage. This was an appealing alternative due to the fact that the chloride would eventually have to be displaced to form our desired thiol linker. However, the choice of the

protection group would be crucial since it would have to be robust enough to withstand lithiation and Grignard conditions, but also be easily removable without affecting the silicon-benzene or silicon-ferrocene core. This greatly reduced the number of available options and we decided on using the commercially available TIPS protected thiol triisopropylsilanethiol (H-STIPS). This silyl protected thiol was chosen due to the weaker nature of the S-Si bond, but with the isopropyl groups providing extra stability compared to a TMS or TES protected thiol. Having chosen our protected thiol, we proceeded to reduce dichloro(chloromethyl)methylsilane with lithium aluminum hydride to generate dihydride **3.6**, which then underwent chloride displacement with triisopropylsilanethiol in the presence of sodium hydride to generate the sulfur protected silane **3.9**. Finally, monochlorination of **3.9** with CuCl₂ and CuI generated chlorosilane **3.10** (Scheme 3.3).



Scheme 3.3: Synthesis of key TIPS protected sulfur intermediate 3.10.

Having successfully made chlorosilane **3.10**, we proceeded to try the Grignard reaction with dibromobenzene (Figure 3.13). However, after multiple attempts, the desired Grignard product **3.11** was unable to be formed or isolated, with the crude NMR showing numerous peaks.

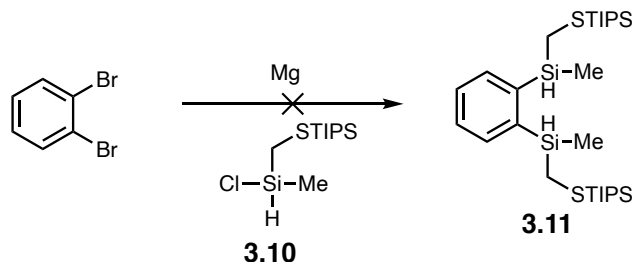


Figure 3.13: Double Grignard attempt with TIPS protected intermediate 3.10.

It was decided that a cleaner Grignard reaction might be necessary and low temperature, stepwise Grignard reactions were investigated. Dibromobenzene was treated with an

$i\text{PrMgCl}\cdot\text{LiCl}$ solution at $-15\text{ }^{\circ}\text{C}$ followed by 1 equivalent of **3.10** and gratifyingly the monosilylated product **3.12** was cleanly formed. **3.12** was then treated with another equivalent of **3.10** under the same conditions, but once again, the disilylated product was unable to be formed (Figure 3.14a). The diiodo starting material was also tested, but only the monosilylated product **3.13** was formed and the disilylated product was not obtained (Figure 3.14b). Based on these results it appeared that the Grignard route to form the 1,2-disilylbenzene would not be feasible most likely due to the steric bulk of the STIPS group and an alternate route had to be considered.

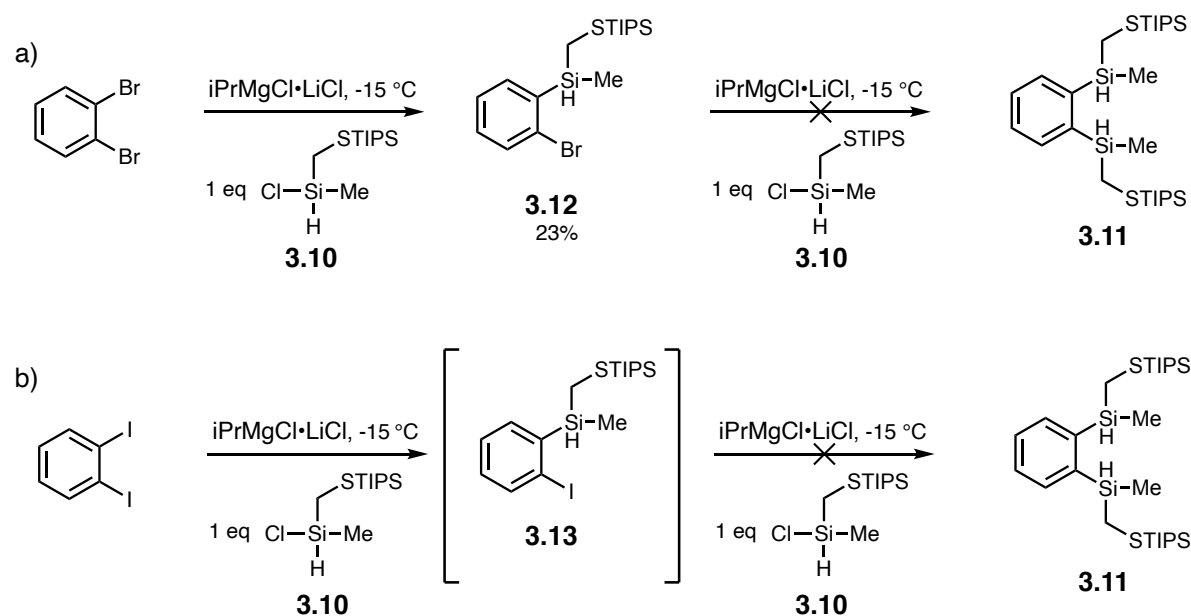


Figure 3.14: Cold temperature, stepwise Grignard reaction to synthesize **3.11** a) Via dibromide b) Via diiodide.

The issue of steric bulk of the STIPS group appeared to be less of a concern on the ferrocene system, so we proceeded to treat dibromoferrocene with butyllithium and **3.10** and fortunately we were able to obtain the disilylated **3.14** (Figure 3.15).

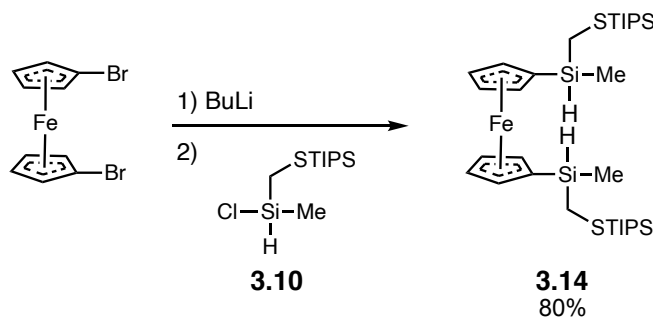


Figure 3.15: Successful synthesis of TIPS protected ferrocenyl silane 3.14.

Having obtained **3.14**, we proceeded to investigate chlorinations of the disilyl product in accordance with our plan of forming the Si-Si bond via a Wurtz coupling. Generating a clean product was crucial due to the inability to easily purify the chlorinated silane because of the high molecular weight which precluded distillation, the greasy nature of the silyl groups, which precluded crystallization, and the moisture sensitivity of the chlorosilane, which precluded chromatographic techniques. However, after trying multiple chlorination conditions including NCS, Cu, Pd, and chlorine gas, we were unable to find conditions that would give us pure chlorinated silane **3.15** (Figure 3.16).

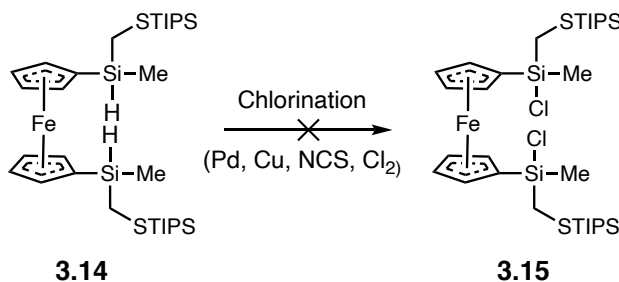


Figure 3.16: Chlorination attempts of 3.14.

We decided it was worth investigating the TIPS deprotection at this stage since it would eventually have to be removed to form our desired thiol linker and the deprotected product might be slightly easier to subsequently chlorinate and isolate. Furthermore, the deprotected product **3.16** is also specifically of interest since it is the resulting dihydride formed if the break junction experiment of **3.2** were to be performed in the presence of 1,4-cyclohexadiene (Figure 3.17).

However, after employing various deprotection strategies using different fluoride and methanol sources, we were unable to selectively deprotect the TIPS groups (Figure 3.17). This was a disappointing result though not completely unsurprising since the silicon directly bonded to the ferrocene is the most unhindered and selectively cleaving the TIPS protected sulfur over this bond is not trivial.

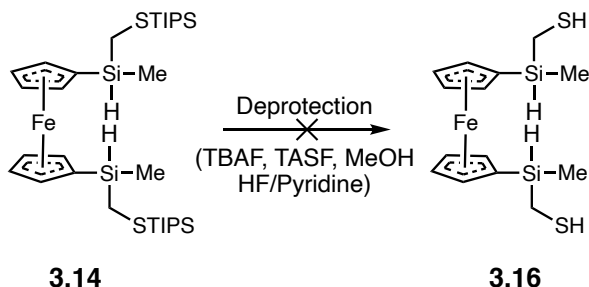


Figure 3.17: TIPS deprotection attempts of 3.14.

3.6. Other routes to access 3.1 and 3.2

Our results showed us that for both the benzene and ferrocene systems, the use of a protected thiol would not be a feasible path to reaching our targets **3.1** and **3.2** and therefore we had to consider other routes. An alternative to using a dedicated protecting group was to synthesize disulfides such as **3.17** and **3.18** (Figure 3.18) which would allow us to install our “protected” sulfur linker and reduce the disulfide at a later stage to afford us the free thiol linker.



Figure 3.18: New disulfide targets.

We proceeded to synthesize **3.17** and **3.18** by taking dihydro silane **3.6** and displacing the chloride to generate thioacetate **3.19**. However, upon using basic methanolysis conditions and either S-Methyl thiomethanesulfonate or iodine, we were unable to generate **3.17** or **3.18**, respectively (Figure 3.19). The propensity for methoxide to bond to silicon most likely disrupted

the desired reaction pathway. Other reagents such as lithium aluminum hydride were employed to reduce the thioacetate to the thiol first, but the volatility of this thiol, analogous to propanethiol, prevented easy handling and use and was not a viable option. Currently, other disulfide routes are being pursued, in addition to other methods for accessing the benzene and ferrocenyl disilane systems.

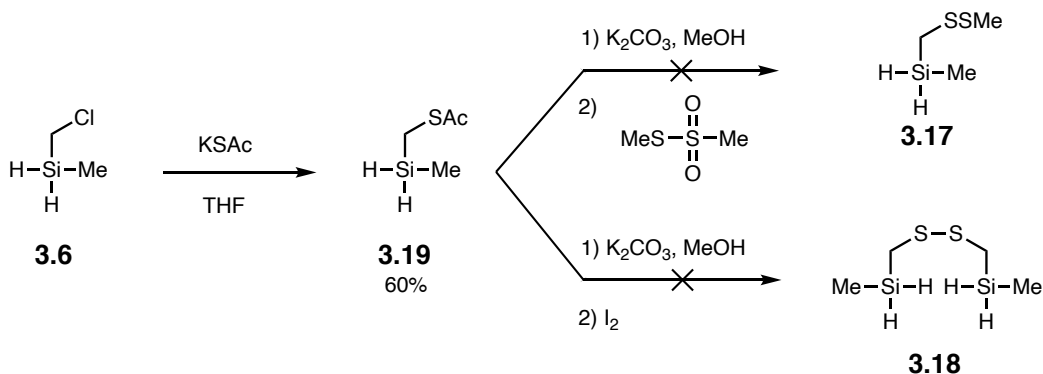


Figure 3.19: Attempts to synthesize disulfides 3.17 and 3.18.

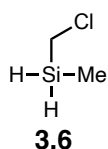
3.7. Summary and conclusion

An overview of the Leighton group's previous contributions to single molecule electronics has been presented. Our questions about the nature of the bond-ruptured species has led us to propose new targets for high bias-induced rupture experiments. These highly strained silanes are very challenging synthetic targets and our efforts to synthesize these molecules has been presented, including our attempts to install the thiol linker and circumventing the issues faced with using the primary chloride. These efforts are ongoing and the synthesis of these disilanes will allow us to further understand silicon molecular junctions and contribute to the development of molecular circuitry.

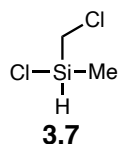
3.8. Experimental procedures

General Information

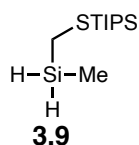
All reactions were carried out under an inert atmosphere of argon in flame-dried glassware with magnetic stirring unless otherwise indicated. Degassed solvents were purified by passage through an activated alumina column. Cyclopentadiene and methacrolein were purified immediately prior to use. All other reagents were purchased from commercial sources and used without further purification unless otherwise noted. Flash chromatography was performed with Silicycle SiliaFlash® P60 silica gel. Thin-layer chromatography (TLC) was carried out on glass backed silica gel TLC plates (250 nm) from Silicycle; visualization by UV, phosphomolybdic acid (PMA), or Potassium Permanganate (KMnO₄). ¹H, and ¹³C data were obtained using Bruker AVIII 500 (500 MHz) spectrometer and are reported in ppm. ¹H NMR spectra were internally referenced to CDCl₃ (7.26 ppm); ¹³C NMR spectra were internally referenced to CDCl₃ (77.23 ppm); Data are reported as follows: (bs= broad singlet, s = singlet, d = doublet, t = triplet, m = multiplet, dd = doublet of doublets, ddd = doublet of doublet of doublets, ddt = doublet of doublet of triplets, td = triplet of doublets; coupling constant(s) in Hz; integration).



Prepared as described in the literature.¹⁹ Spectral data were in agreement with reported values (42%).

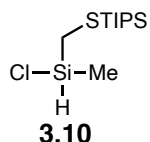


Prepared as described in the literature.²⁰ Spectral data were in agreement with reported values (60%).



A flame dried flask, equipped with a stir bar, was charged with NaH (5.3 mmol, 1.01 eq), suspended in THF (5.3 mL) and cooled to 0 °C. Triisopropanethiol (5.25 mmol, 1 eq) was then slowly added dropwise and the reaction was let to stir for 5 minutes. **3.6** (5.25 mmol, 1 eq) was then added slowly at the reaction was stirred for 5 minutes and then warmed to room temperature and stirred for 30 minutes. The reaction mixture was then filtered, concentrated and purified by silica gel flash chromatography (100% pentane) to yield a pale oil (78%).

¹H NMR (400 MHz, CDCl₃) δ 3.89 (q, 2H), 1.75 (t, 2H), 1.32 – 1.25 (m, 3H), 1.12 (d, 23H), 0.27 (t, 18H).



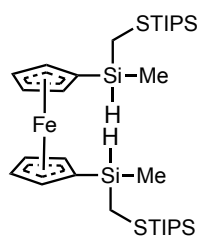
To a flame dried flask, equipped with a stir bar, was added CuCl₂ (8.11 mmol, 2.02 eq) and CuI (0.198 mmol, 0.05 eq), suspended in THF (12 mL). **3.9** (4.02 mmol, 1 eq) was then added dropwise and the reaction was stirred at room temperature for 1 hour. The reaction mixture was filtered,

concentrated and the crude product was then distilled to afford a clear liquid (60%). $^1\text{H NMR}$ (500 MHz, CDCl_3) δ 4.81 (ddd, 1H), 2.05 – 1.86 (m, 2H), 1.29 (ddd, 3H), 1.12 (d, 18H), 0.62 (d, 3H).



3.12

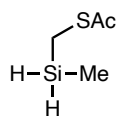
To a flame dried flask, equipped with a stir bar, was added a solution of $i\text{PrMgCl}\cdot\text{LiCl}$ in THF (1.3M in THF, 0.77 mL) and then cooled to $-15\text{ }^\circ\text{C}$. 1,1-dibromobenzene (1 mmol, 1 eq) was then added and the reaction was stirred for 2 hours at $-15\text{ }^\circ\text{C}$. **3.10** (1 mmol, 1 eq) was then added and the reaction was removed from the cold temperature bath stirred for 18 hours while warming to room temperature. The reaction mixture was then added to water, extracted with pentane, dried with Na_2SO_4 , filtered, and concentrated. The crude product was purified by silica gel flash chromatography (100% pentane), to yield a clear liquid (23%). $^1\text{H NMR}$ (400 MHz, CDCl_3) δ 7.57 – 7.49 (m, 2H), 7.34 – 7.23 (m, 2H), 4.56 (ddd, 1H), 2.12 – 1.97 (m, 2H), 1.34 – 1.23 (m, 3H), 1.11 (dd, 18H), 0.56 (d, 3H). $^{13}\text{C NMR}$ (126 MHz, CDCl_3) δ 137.44, 137.32, 132.39, 131.49, 130.54, 126.59, 18.59, 12.61, 6.15, -5.99 .



3.14

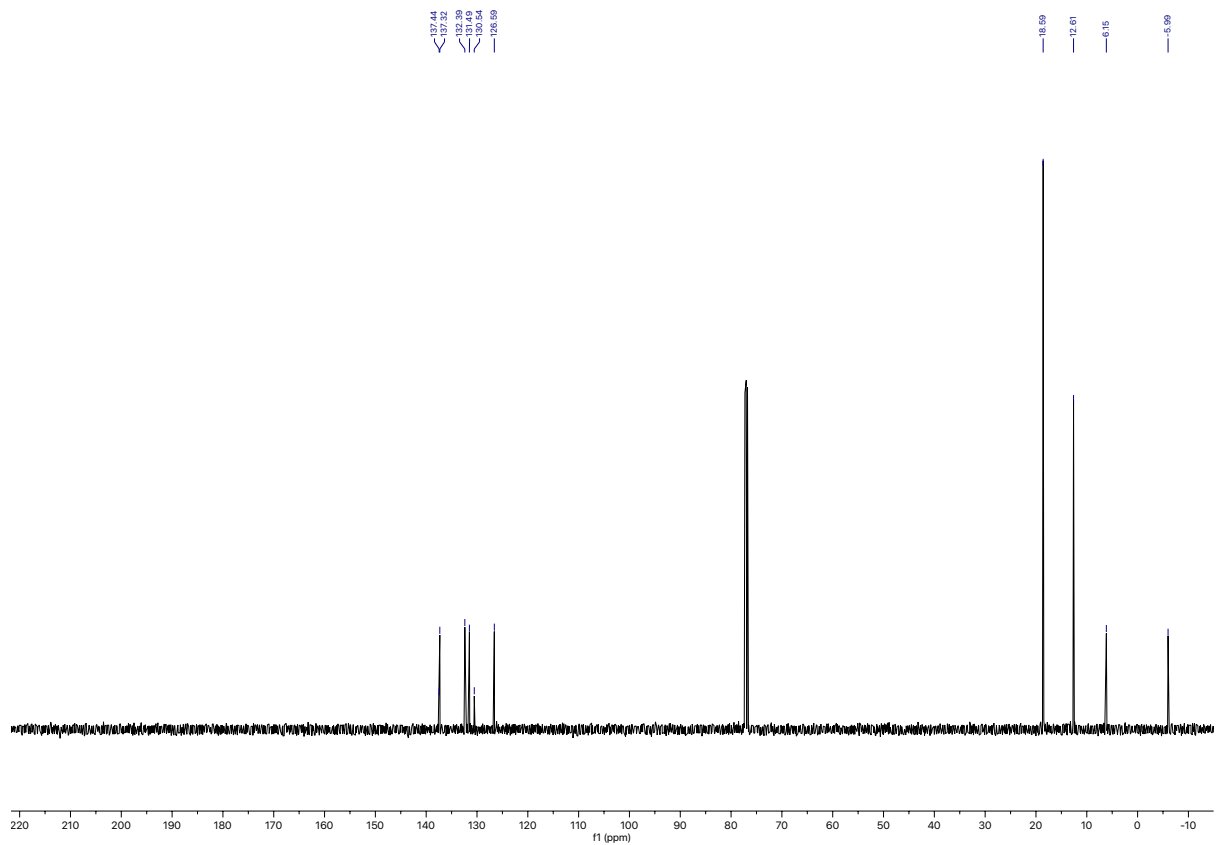
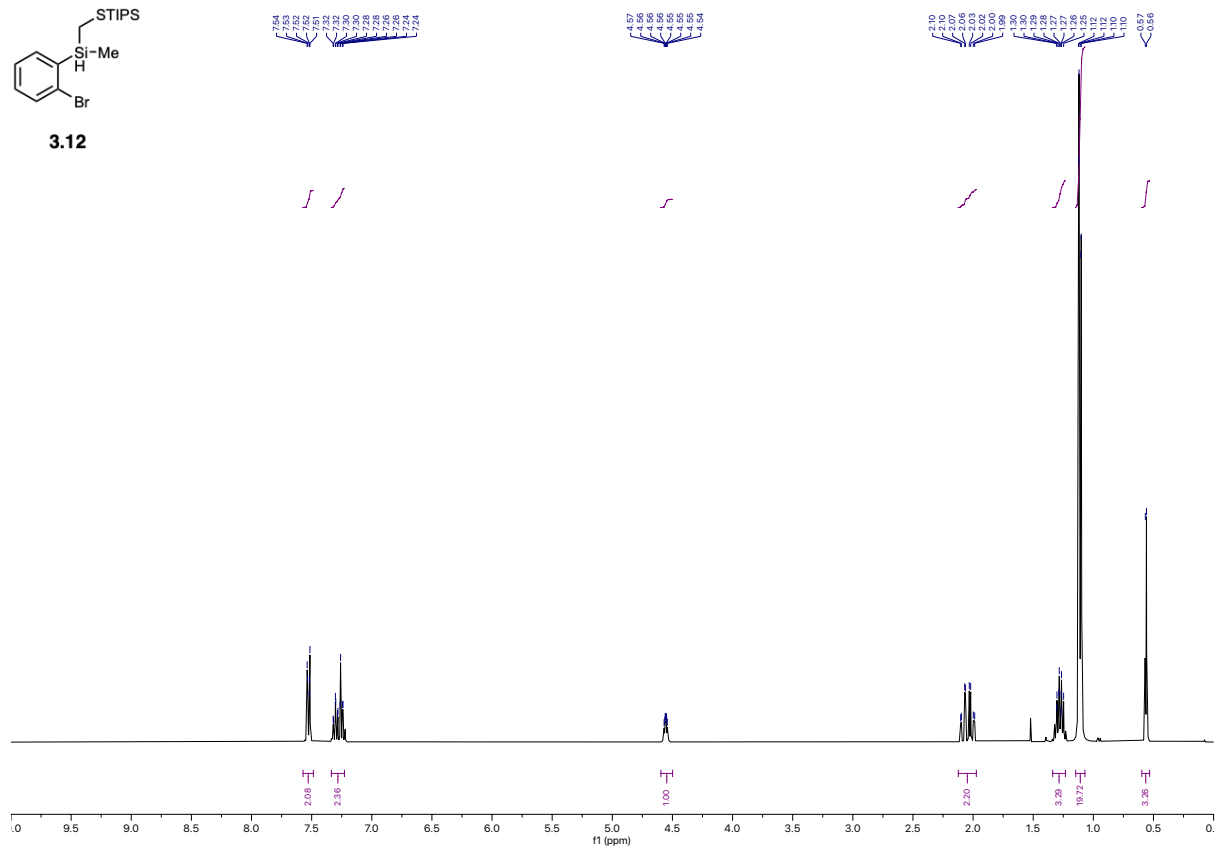
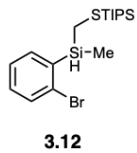
To a flame dried flask, equipped with a stir bar, was added a solution of 1,1'-dibromoferrocene (2.91 mmol, 1 eq) in ether (11.6 mL). The reaction was cooled to $0\text{ }^\circ\text{C}$, a solution of BuLi (2.5M

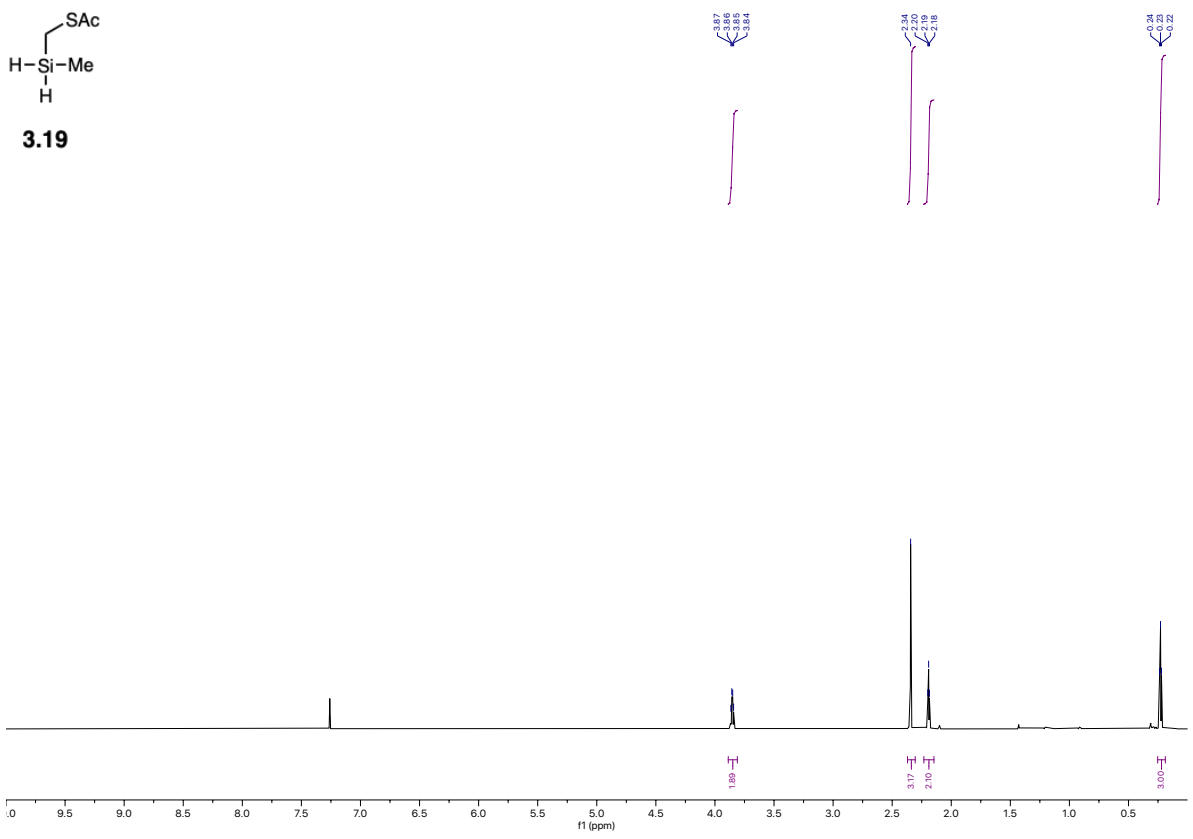
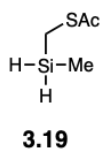
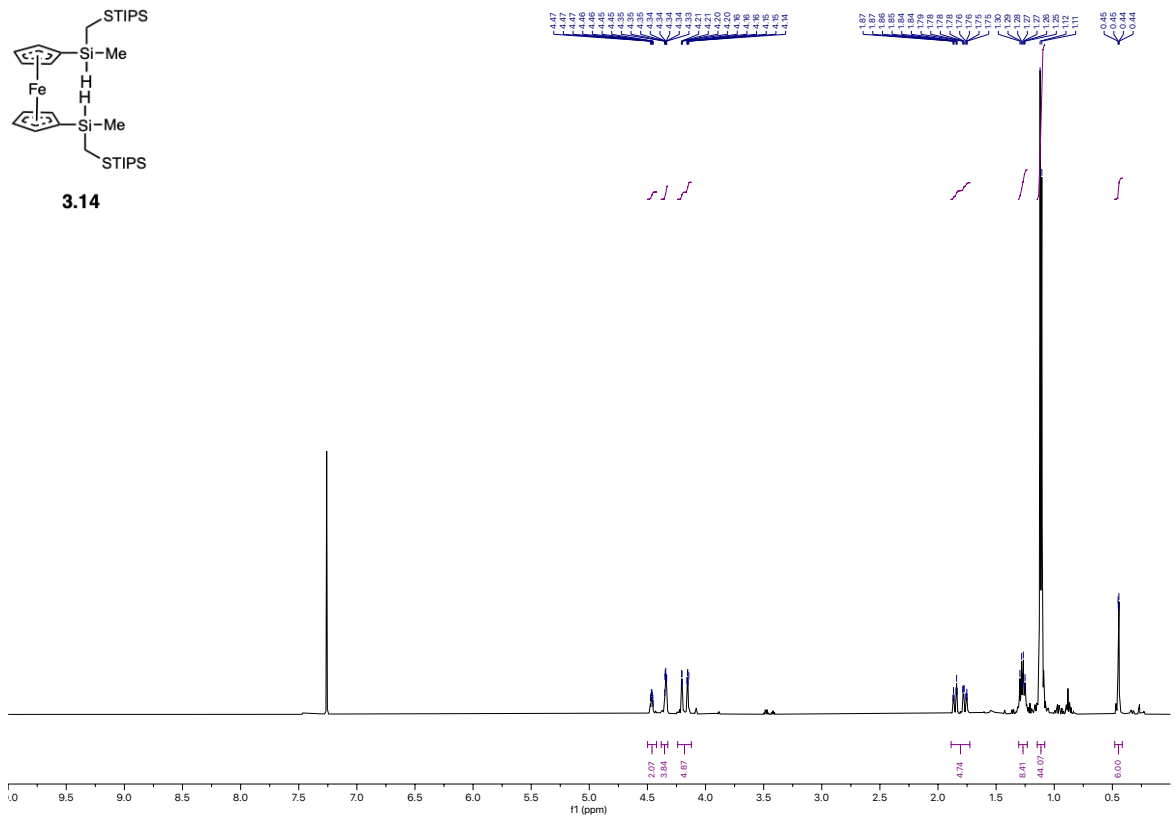
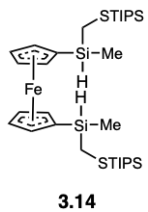
in hexanes, 2.53 ml, 2 eq) was added and stirred for 1 hour at 0 °C. **3.10** (5.82 mmol, 2 eq) was then added, and the reaction was removed from the ice bath and allowed to stir at room temperature for 2.5 hours. The reaction was then quenched with NH₄Cl, the ether layer was dried with Na₂SO₄ and then filtered, and concentrated. The crude product was purified by silica gel flash chromatography (0-2% EtOAc/Hexanes) to yield a pale yellow liquid (80%). ¹H NMR (500 MHz, CDCl₃) δ 4.46 (td, 2H), 4.34 (ddd, 4H), 4.24 – 4.12 (m, 5H), 1.89 – 1.73 (m, 5H), 1.31 – 1.23 (m, 6H), 1.11 (d, 36H), 0.45 (dd, 6H).



3.19

To a flame dried flask, equipped with a stir bar, was added a solution of **4.6** (90.79 mmol, 1 eq) in THF (363 ml). KSAc (90.79 mmol, 1 eq) was added and the reaction was allowed to reflux for 3 hours. The reaction was then cooled to room temperature, filtered, concentrated, and purified by silica gel flash chromatography (0-100% Ether/Pentanes) yield a pale yellow liquid (60%). ¹H NMR (500 MHz, CDCl₃) δ 3.85 (q, 2H), 2.34 (s, 3H), 2.19 (t, 2H), 0.23 (t, 3H).





3.9. References

- ¹ Waldrop, M. M. *Nature*. **2016**, 530, 145.
- ² Markov, I. L. *Nature*. **2014**, 512 (7513), 147–154.
- ³ Choi, H.; Mody, C. C. M. *Soc. Stud. Sci.* **2009**, 39 (1), 11–50.
- ⁴ Stulen, R. H.; Sweeney, D. W. *IEEE J. Quantum Electron.* **1999**, 35 (5), 694–699
- ⁵ Tao, N. J. *Nat. Nanotechnol.* **2006**, 1 (3), 173–181.
- ⁶ Moth-Poulsen, K.; Bjørnholm, T. *Nat. Nanotechnol.* **2009**, 4 (9), 551–556.
- ⁷ Aradhya, S. V.; Venkataraman, L. *Nat. Nanotechnol.* **2013**, 8 (6), 399.
- ⁸ Ward, D. R.; Scott, G. D.; Keane, Z. K.; Halas, N. J.; Natelson, D. *J. Phys. Condens. Matter.* **2008**, 20 (37), 374118.
- ⁹ Sun, L.; Diaz-Fernandez, Y. A.; Gschneidner, T. A.; Westerlund, F.; Lara-Avila, S.; Moth-Poulsen, K. *Chem. Soc. Rev.* **2014**, 43 (43), 7378–7411.
- ¹⁰ Xu, B.; Tao, N. J. *Science*. **2003**, 301 (5637), 1221–1223.
- ¹¹ Su, T. A.; Widawsky, J. R.; Li, H.; Klausen, R. S.; Leighton, J. L.; Steigerwald, M. L.; Venkataraman, L.; Nuckolls, C. *J. Am. Chem. Soc.* **2013**, 135 (49), 18331–18334.
- ¹² Kim, N. T.; Li, H.; Venkataraman, L.; Leighton, J. L. *J. Am. Chem. Soc.* **2016**, 138, 11505–11508.
- ¹³ Li, H.; Kim, N. T.; Su, T. A.; Steigerwald, M. L.; Nuckolls, C.; Darancet, P.; Leighton, J. L.; Venkataraman, L. *J. Am. Chem. Soc.* **2016**, 138, 16159–16164.
- ¹⁴ Li, H.; Su, T. A.; Zhang, V.; Steigerwald, M. L.; Nuckolls, C.; Venkataraman, L. *J. Am. Chem. Soc.* **2015**, 137 (15), 5028–5033.
- ¹⁵ Nozawa, T.; Nagata, M.; Ichinohe, M.; Sekiguchi, A. *J. Am. Chem. Soc.* **2011**, 133, 5773–5775.
- ¹⁶ Ishikawa, M.; Naka, A.; Yoshizawa, K. *Dalton Trans.* **2016**, 45(8), 3210–3235.
- ¹⁷ Kumada, M.; Kondo, T.; Mimura, K.; Ishikawa, M. *J. Organomet. Chem.* **1972**, 43, 293.
- ¹⁸ Li, H.; Kim, N. T.; Su, T. A.; Steigerwald, M. L.; Nuckolls, C.; Darancet, P.; Leighton, J. L.; Venkataraman, L. *J. Am. Chem. Soc.* **2016**, 138, 16159–16164.
- ¹⁹ Schmidbaur, H.; Ebenhöch, J.H. *Zeitschrift für Naturforschung B.* **1986**, 41(12), 1527–1534.
- ²⁰ Pestunovich, V. A.; Kirpichenko, S. V.; Lazareva, N. F.; Albanov, A. I.; Voronkov, M. G. *J. Organomet. Chem.* **2007**, 692, 11, 2160 – 2167.